UNIVERSITY OF CALIFORNIA SAN DIEGO

Ecology and conservation of manta and devil rays

A dissertation submitted in partial satisfaction of the requirements for the degree
Doctor of Philosophy

in

Marine Biology

by

Joshua David Stewart

Committee in charge:

Professor Brice Semmens, Chair
Professor Octavio Aburto
Professor Lisa Ballance
Professor Ronald Burton
Professor Carolyn Kurle

2018

The Dissertation of Joshua David Stewart is approved, and it is acceptable in quality and form for publication on microfilm and electronically:

_____

_____

_____

_____

_____
Chair

University of California San Diego

2018

DEDICATION

To my mother, Marcy, for all of the years under the blue whale at the museum, the unequaled love and encouragement. Your spirit will be with me forever.

EPIGRAPH

"We can say that Muad'Dib learned rapidly because his first training was in how to learn. And the first lesson of all was the basic trust that he could learn."

-Frank Herbert, *Dune*

TABLE OF CONTENTS

LIST OF TABLES

LIST OF FIGURES

ACKNOWLEDGEMENTS

I would like to express my deepest gratitude to all of my committee members: Brice Semmens, Octavio Aburto, Ronald Burton, Carolyn Kurle, and Lisa Ballance. Each and every one of them provided me with invaluable mentoring, insights, and career advice. Against their better judgment, they invited me into their laboratories, trusted me with sensitive equipment, and asked themselves, "How much damage could he really do?" They have constantly shaped my thinking and made me a better scientist, and I cannot thank them enough for their patience and encouragement. I am eternally grateful to Brice for first planting the idea of graduate school in my head and recruiting me to his lab despite my skepticism of moving across the country to this place called San Diego where everyone was suspiciously happy. I owe a huge debt of gratitude to Octavio for his enthusiasm in our first meeting, his willingness to facilitate and support my research in Mexico, and his ability to help me make my work more impactful and relevant to management and conservation.

This dissertation would not have been possible without a number of inspiring collaborations. I thank my many coauthors for their tireless efforts, insightful discussions, and camaraderie: Calvin Beale, Daniel Fernando, Abraham Sianipar, Mauricio Hoyos-Padilla, Karey Kumli, Robert Rubin, Jose Avila, Kerstin Forsberg, Chris Rohner, Gonzo Araujo, Joshua Rambahiniarison, and Alessandro Ponzo. In particular, I would like to thank Robert Rubin for his undying enthusiasm, love of animals and the ocean, amazing discussions over fine wine, and most of all for his friendship. I am extremely grateful for all of the assistance I received from students and volunteers, especially Iliana Fonseca, Aldo Zavala, Antonio Ruiz, and Taylor Smith.

I would like to thank all of my colleagues at The Manta Trust for their collaborations outside of this dissertation, for making the research we do relevant to policy and management, and for their commitment to protecting these incredible animals. I would especially like to thank Guy Stevens, who first connected me with manta rays and instilled in me a lasting curiosity, wonder, and passion for mantas. I also extend a special thanks to my 'family' at the Our World Underwater Scholarship Society. During my year as a scholar, I discovered my love of manta rays, my passion for research and conservation, and met my PhD supervisor. Without the many incredible opportunities the scholarship afforded me, I really don't know where I would be today. Further, I'd like to thank Charles Beeker and Dr. Claudia Johnson for supporting my first forays into marine science, training me to interact with the underwater world, and encouraging me to pursue graduate school.

Thank you to the SIO Graduate Department and the SIO Business Office for their excellent administrative support as I have navigated the Ph.D. process. Especially, Gilbert Bretado, Maureen McGreevy, Maureen McCormack, Marty Tullar, and James Pollock.

To the Semmens lab, including but not limited to, Lynn Waterhouse, Brian Stock, Noah Ben-Aderet, Lyall Bellquist, Christy Semmens, and others over the years: thank you for the fun, the games, the love and support. I can't imagine a better group of people to eat lunch with every day. Sorry for all the dog hair. I have been so fortunate to have an incredible group of friends (both at Scripps and elsewhere) throughout my time in graduate school. In no particular order they include: Lynn Waterhouse & Dan Popa, Brian Stock & Sarah Lerch, Danny & Katie Sedivec, Alfredo Giron, Arturo Ramirez, Andrew Johnson, and Noah Ben-Aderet. You guys are the best.

Thanks to three fellowships during my time at Scripps, I had the freedom to explore topics that excited my sense of exploration and curiosity. I was able to take risks and come into my own as a scientist, and for that I will be forever grateful. The National Science Foundation Graduate Research Fellowship (DGE-1144086) is what initially secured my acceptance to graduate school, and supported me for the first three years while I got my research off the ground. A Switzer Fellowship from the Robert & Patricia Switzer Foundation supported my research and provided exceptional leadership and policy communications training. The Nancy Foster Scholarship (NA15NOS4290068) from NOAA's Office of National Marine Sanctuaries not only supported me as a student, but allowed me to put my research to work in protecting the marine natural resources of the United States of America, facilitated unparalleled collaborative opportunities with the National Marine Sanctuary network, and helped me grow as a science communicator. I am especially grateful to Kate Thompson, Marlies Tumolo, Seaberry Nachbar, Claire Fackler, and Steve Gittings for their mentorship, support, and their incredible positive attitudes.

I cannot even begin to express how fortunate I am to have such a loving, caring, and supportive family. Thank you for everything, Mom, Dad and Jeremy. From the very first discussion about what I want to be when I grow up, my dad, Marion, said, "Do what you love, and the rest will follow." Thanks, dad, for the decades of unwavering support. I'm doing what I love and I've never been happier. Making your dad proud is a great feeling, but it's a close second to making your older brother proud. Thanks, Jeremy, for always being excited about what I'm doing. Most of all, thanks to my mom, Marcy, who was my number one fan right up to her untimely passing. I don't know how many hours we spent together in the museum of natural history staring at the wild sea creatures that I quickly fell in love with. Your love and support

were unparalleled. You built my confidence, taught me the value of joy, and fostered a deep sensitivity in me. I love you now and always.

Finally, to my wife, Madeline, there are no words I can write here to adequately express my gratitude for everything that you've done for me. You stuck with me even when I was away playing with fishes for weeks or months on end. You moved with me across the country to a place you had never even visited. You support me with patience and love every day as I pursue my passion. And most of all, you've had to listen to me talk about manta rays every day for the past seven years. In no particular order: I'm sorry. Thank you. I love you more than anything.

MATERIAL PUBLISHED IN THE DISSERTATION

Chapter 1, in full, is a reprint of the material as it appears in Biological Conservation 2016. Stewart, J.D., Beale, C.D., Fernando, D., Sianipar, A.B., Burton, R., Semmens, B.X., Aburto-Oropeza, O. The dissertation author was the primary investigator and author of this material.

Chapter 2, in full, is a reprint of the material as it appears in Zoology 2016. Stewart, J.D., Hoyos-Padilla, O.M., Kumli, K., Rubin, R.D. The dissertation author was the primary investigator and author of this material.

Chapter 3, in full, is a reprint of the material as it appears in Marine Ecology Progress Series 2017. Stewart, J.D., Rohner, C.A., Araujo, G., Avila, J., Fernando, D., Forsberg, K., Ponzo, A., Rambahiniarison, J.M., Kurle, C.A., Semmens, B.X. The dissertation author was the primary investigator and author of this material.

VITA

2010 Bachelor of Arts, Indiana University

2015 Master of Science, University of California San Diego

2018 Doctor of Philosophy, University of California San Diego

PUBLICATIONS

Stewart, J.D., Barroso, A., Butler, R.H., Munns, R.J. "Caught at the surface: myctophids make easy prey for dolphins and devil rays." Ecology vol. 99, 2017.

Stewart, J.D., Rohner, C.A., Araujo, G., Avila, J., Fernando, D., Forsberg, K., Ponzo, A., Rambahiniarison, J.M., Kurle, C.M., Semmens, B.X. "Trophic overlap in mobulid rays: insights from stable isotope analysis." Marine Ecology Progress Series vol. 580, 2017.

Rohner, C.A., Burgess, K., Rambahiniarison, J., Stewart, J.D., Ponzo, A., Richardson, A. "Mobulid rays feed on euphausiids in the Bohol Sea." Royal Society Open Science vol. 4, 2017.

O'Malley, M., Heinrichs, S., Hilton, P., Townsend, K., Stewart, J.D. "Characterization of the Trade in Manta and Devil Ray Gill Plates in China and Southeast Asia Through Trader Surveys." Aquatic Conservation vol. 27, 2017.

Stewart, J.D., Beale, C.D., Fernando, D., Burton, R., Aburto-Oropeza, O., Semmens, B.X. "Spatial Ecology and Conservation of *Manta birostris* in the Indo-Pacific." Biological Conservation vol. 200, 2016.

Stewart, J.D., Hoyos-Padilla, O.M., Kumli, K., Rubin, R.D. "Deep-Water Feeding and Behavioral Plasticity in *Manta birostris* Revealed by Archival Tags and Submersible Observations." Zoology vol. 119, 2016.

Stewart, J.D., Stevens, G.W.M, Marshall, G.J., Abernathy, K. "Are mantas self aware or simply social? A response to Ari & D'Agostino 2016." Journal of Ethology vol. 35, 2016.

FIELDS OF STUDY

Major Field: Marine Biology (Marine Ecology)

Studies in Animal Movement
Studies in Population Ecology
Studies in Quantitative Ecology
Professor Brice Semmens

Studies in Conservation Biology
Studies in Marine Ecology
Professor Octavio Aburto & Professor Brice Semmens

Studies in Population Genetics
Professor Ronald Burton

Studies in Stable Isotope Ecology
Professor Carolyn Kurle & Professor Brice Semmens

ABSTRACT OF THE DISSERTATION

Ecology and conservation of manta and devil rays

by

Joshua David Stewart

Doctor of Philosophy in Marine Biology

University of California San Diego, 2018

Professor Brice Semmens, Chair

Manta and devil rays (collectively mobulids) are planktivorous pelagic rays that have received little scientific attention in comparison to many other marine megafauna species. Major knowledge gaps remain in the biology and ecology of mobulid rays, often hindering effective management of these species. In the past decade, substantial declines in mobulid populations have been recorded in response to targeted fisheries and bycatch of these species in both commercial and artisanal fisheries. This dissertation seeks to fill several critical knowledge gaps in the spatial ecology and foraging behavior of mobulid rays in the Indo-Pacific. Chapter 1 uses a

combination of satellite archival tagging, stable isotope analysis, and high-throughput genetic sequencing to examine the horizontal movements and population structure of oceanic manta rays (*Manta birostris*) in the Indo-Pacific. We find that oceanic manta populations exhibit philopatry within relatively restricted home ranges, and demonstrate little connectivity between both neighboring and distant populations. These findings suggest that management and conservation action can be applied effectively at local scales in addition to the international agreements that are typically relied upon for marine megafauna species. Chapter 2 examines the diving behavior of oceanic manta rays at a remote archipelago off of Mexico's Pacific coast using satellite archival tagging and opportunistic submersible observations. We found evidence of multiple feeding modes with different vertical distributions, seasonal changes in vertical habitat use, deep-water foraging behavior, and association with both the thermocline and the deep scattering layer. Taken together, these findings suggest a high degree of behavioral plasticity in oceanic manta rays that may explain their ability to remain resident by shifting their prey targets vertically rather than over large horizontal distances. Chapter 3 uses stable isotope analysis and Bayesian mixing models to assess the trophic overlap in five species of sympatric mobulid rays at three sites across the Indo-Pacific. We find that the degree of trophic overlap is inversely related to regional primary productivity characteristics, with greater overlap in lower-productivity regions. We posit that this is a result of prey density thresholds required by mobulids to make foraging energetically profitable. The trophic relationships we observe help explain the patterns of multispecies mobulid bycatch in regions such as Sri Lanka and the Philippines, and interspecies seasonal and spatial differences in bycatch risk of mobulid rays in Peru. This dissertation contributes substantially to our understanding of mobulid ray spatial ecology and foraging

dynamics, and appropriate management and conservation approaches for these threatened species.

CHAPTER 1:

Spatial ecology and conservation of *Manta birostris* in the Indo-Pacific

JOSHUA D. STEWART, CALVIN S. BEALE, DANIEL FERNANDO, ABRAHAM B. SIANIPAR, RONALD S. BURTON, BRICE X. SEMMENS, OCTAVIO ABURTO-OROPEZA

Biological Conservation 200 (2016) 178–183

Contents lists available at ScienceDirect

Biological Conservation

journal homepage: www.elsevier.com/locate/bioc

Spatial ecology and conservation of *Manta birostris* in the Indo-Pacific

Joshua D. Stewart [a,b,*], Calvin S. Beale [c], Daniel Fernando [d,b,e], Abraham B. Sianipar [f], Ronald S. Burton [a], Brice X. Semmens [a], Octavio Aburto-Oropeza [a]

[a] Scripps Institution of Oceanography, University of California, San Diego, 9500 Gilman Dr., La Jolla, CA 92093, USA
[b] The Manta Trust, Catemwood House, Corscombe, Dorchester, Dorset DT2 0NT, UK
[c] Misool Manta Project, Jalan Gunung Umsini No. 51, RT 03/RW 03 Kampung Baru, Sorong, Papua Barat 98413, Indonesia
[d] Department of Biology and Environmental Science, Linnaeus University, 39182 Kalmar, Sweden
[e] Blue Resources, 86 Barnes Place, Colombo 00700, Sri Lanka
[f] Conservation International, Jalan Pejaten Barat No. 16A, Kemang, Jakarta 12550, Indonesia

ARTICLE INFO

Article history:
Received 22 February 2016
Received in revised form 29 April 2016
Accepted 22 May 2016
Available online 20 June 2016

Keywords:
ddRAD sequencing
Marine conservation
Mobulid
Pop-off satellite archival tagging
Stable isotope analysis

ABSTRACT

Information on the movements and population connectivity of the oceanic manta ray (*Manta birostris*) is scarce. The species has been anecdotally classified as a highly migratory species based on the pelagic habitats it often occupies, and migratory behavior exhibited by similar species. As a result, in the absence of ecological data, population declines in oceanic manta have been addressed primarily with international-scale management and conservation efforts. Using a combination of satellite telemetry, stable isotope and genetic analyses we demonstrate that, contrary to previous assumptions, the species appears to exhibit restricted movements and fine-scale population structure. *M. birostris* tagged at four sites in the Indo-Pacific exhibited no long-range migratory movements and had non-overlapping geographic ranges. Using genetic and isotopic analysis, we demonstrate that the observed movements and population structure persist on multi-year and generational time scales. These data provide the first insights into the long-term movements and population structure of oceanic manta rays, and suggest that bottom-up, local or regional approaches to managing oceanic mantas could prove more effective than existing, international-scale management strategies. This case study highlights the importance of matching the scales at which management and relevant ecological processes occur to facilitate the effective conservation of threatened species.

1. Introduction

Oceanic manta rays (*Manta birostris*) are an iconic and poorly studied species of marine megafauna. Despite decades of interest from the public and a high value in the recreational dive industry (O'Malley et al., 2013), manta rays have only recently received scientific attention (Couturier et al., 2012). Most ecological studies focus on the smaller, coastally associated reef manta ray (*Manta alfredi*), and demonstrate patterns of residency with few long-distance movements (Dewar et al., 2008; Deakos et al., 2011; Jaine et al., 2014; Braun et al., 2015). Oceanic manta rays tend to occupy more pelagic, offshore habitats than their coastal sister species (Kashiwagi et al., 2011), and they are presumed to be highly migratory based primarily on the behaviors exhibited by species similar in habitat preference, foraging strategies and size (Skomal et al., 2009; Hueter et al., 2013; Thorrold et al., 2014).

Oceanic mantas, along with closely related mobula rays (*Mobula* spp.), are caught frequently as bycatch in pelagic fisheries, and have been increasingly targeted over the last decade as demand for their gill plates grows in Asian markets (Couturier et al., 2012). Low fecundity and small population sizes make mantas highly susceptible to fisheries impacts (Dulvy et al., 2014). Targeted fisheries and bycatch are driving family-wide declines of mobulids (Ward-Paige et al., 2013; Croll et al., 2015) and long-term monitoring efforts have recorded local declines in manta and mobula sighting frequency (White et al., 2015).

As with other migratory species, conservation efforts for oceanic manta rays primarily focus on international agreements such as the Convention on International Trade in Endangered Species (CITES) and the Convention on the Conservation of Migratory Species (CMS) in an attempt to restrict the main economic drivers of manta fisheries and prevent targeted capture. However, the effectiveness of international approaches to managing migratory marine species is questionable. For example, a recent meta-analysis of global elasmobranch catches concluded that populations continue to be overexploited by countries that

* Corresponding author at: Scripps Institution of Oceanography, University of California, San Diego, 9500 Gilman Dr., La Jolla, CA 92093, USA.
E-mail addresses: j8stewart@ucsd.edu (J.D. Stewart), calvin@misoolecoresort.com (C.S. Beale), daniel@mantatrust.org (D. Fernando), abraham.sianipar@gmail.com (A.B. Sianipar), rburton@ucsd.edu (R.S. Burton), bsemmens@ucsd.edu (B.X. Semmens), maburto@ucsd.edu (O. Aburto-Oropeza).

http://dx.doi.org/10.1016/j.biocon.2016.05.016
0006-3207/

have signed international agreements to curb elasmobranch fisheries (Davidson et al., 2015). In recent years, local and national level management strategies have also been implemented to protect both reef and oceanic manta rays, including national fisheries bans in several countries and local spatial protections such as marine protected areas or sanctuaries focused on mantas. Local management approaches such as these can have substantial benefits to large, threatened elasmobranchs (Graham et al., 2016).

Given the lack of data on the ecology and stock structure of oceanic manta rays, it is unclear at which spatial scale management efforts for the species should be focused (e.g. international, national, or local). The few published tagging studies on the species have so far identified few long-distance movements (Graham et al., 2012; Hearn et al., 2014), and stock structure and population connectivity remain entirely unexplored. Additional information on the spatial ecology and population structure of the species is necessary to evaluate current management plans and develop new strategies to improve their efficacy in halting or reversing ongoing population declines.

Here we examine the movements and connectivity of *M. birostris* populations at four sites in the Indo-Pacific separated by 600 to 13,000 km in an attempt to identify the most relevant ecological and management unit to inform conservation decisions. We use a combination of satellite telemetry, stable isotope and genetic analysis to examine the movements and connectivity of populations on a range of spatial and temporal scales from daily movements to generational connectivity. We selected sites that had varying productivity regimes, oceanographic patterns, and sighting frequencies of oceanic mantas to make this work as broadly applicable to the species as possible, given the paucity of published data.

2. Methods

Our study sites included: (1) A productive coastal upwelling region in Bahia de Banderas (Mexico Nearshore) where mantas are found in large numbers from February through May each year. (2) The pelagic Revillagigedo Islands (Mexico Offshore), 400 km southwest of Baja California and 600 km west of the Mexico Nearshore site, where mantas can be found reliably from October through June. (3) The Raja Ampat region of eastern Indonesia, a complex archipelago habitat where shifting monsoon winds lead to substantial variability in productivity between summer and winter months (Schalk, 1987), and peak oceanic manta sightings occur in November and April each year. (4) Sri Lanka, where monsoon winds drive shifting productivity regimes in both coastal and pelagic systems (Charles et al., 2012), and artisanal fishermen frequently catch oceanic manta rays in pelagic habitats between May and September. While not exhaustive, these four sites are representative of the majority of habitats where the species is found (Kashiwagi et al., 2011).

We deployed pop-up satellite archival tags (PSAT) and a single towed satellite tag (SPLASH) (Wildlife Computers (WC), Washington USA; Desert Star (DS), California, USA) approximately evenly on males and females (Supplementary Table S1). We analyzed WC archival tag data using WC GPE3 software, which uses a Hidden Markov Model and incorporates environmental variables, bathymetry and movement speed to create probability surfaces of tag locations. We overlaid raw SPLASH tag GPS and Argos satellite positions in Indonesia, which have an accuracy ranging from finer than 100 m to 1500 m. We decoded raw DS archival tag positions using DS SeaTrack software.

We collected white muscle tissue samples from all study sites for both stable isotope and genetic analyses. We freeze-dried samples for stable isotope analysis and analyzed $\delta^{13}C$ and $\delta^{15}N$ values to compare isotope signatures between populations. We did not extract lipids from our samples as they had C:N ratios below 3.5 (Post et al., 2007) (mean 3.24 SD 0.25). To identify differences between populations, we used a model selection approach on multiple population grouping scenarios. We then fit the same linear model to each grouping scenario and used Akaike Information Criterion (AIC) values to identify the best-fit model, representing the grouping scenario best supported by the data.

We used double-digest Restriction Associated DNA (ddRAD) sequencing methods to assess population structure using a subset of individuals from each population. We used the program Stacks (Catchen et al., 2013) to clean, process and analyze raw ddRAD data and calculate population metrics. We filtered out low-F_{ST} Single Nucleotide Polymorphisms (SNPs) to better observe population structure, and performed null controls to ensure that filtering methods were not biasing results (Fig. S1). We used the program Structure 2.3 (Pritchard et al., 2000) to identify population clusters among samples. All methods are discussed in further detail in Supplementary information.

3. Results

We deployed PSATs (n = 21) on oceanic manta rays in Raja Ampat, Indonesia (n = 9) and Pacific Mexico (n = 12), and one towed SPLASH tag on an oceanic manta in Raja Ampat. We deployed tags continuously over two years in Indonesia, and in discrete intervals over approximately 20 months when manta aggregations were present and logistical constraints allowed in Mexico. We recovered data from 18 tags (Table S1). Satellite telemetry revealed restricted home ranges, residency, and an absence of large-scale migratory behavior. Tagged mantas in both regions remained within the respective countries' EEZs for the entire tagging periods (Fig. 1). We observed complete separation during the tagging periods between mantas tagged at the Mexico Nearshore site (n = 5 tags) and the Mexico Offshore site (n = 4 tags), with no recorded movements between sites by mantas tagged at either location. PSAT deployments in Mexico lasted a mean of 175 days (SD 28) for Wildlife Computers tags and 7 and 28 days for the two Desert Star tags that reported. Tags deployed in Mexico popped off a maximum of 92.4 km (offshore; mean 51 SD 36.4) and 81.1 km (nearshore; mean 47.2 SD 24.5) from their deployment sites. PSAT deployments in Indonesia lasted a mean of 165 days (SD 32), and the single SPLASH tag deployment lasted 64 days. Tags deployed in Indonesia popped off a maximum of 259.2 km (mean 158.6 SD 91.9) from their deployment sites. We interpreted the 95% probability polygon for all tags from a given deployment location to be a metric for those animals' combined geographic range (Pedersen et al., 2011). The 95% polygon areas were similar across regions: 79,293 km^2 (Indonesia), 70,926 km^2 (Mexico Offshore), and 66,680 km^2 (Mexico Nearshore), which on average is roughly equivalent to a circle with a radius of 150 km.

We analyzed stable isotope ratios of white muscle tissue samples from 74 mantas across the four study sites (Mexico Nearshore, n = 15; Mexico Offshore, n = 12; Indonesia, n = 8; Sri Lanka, n = 39). Results from stable isotope analyses showed differences in $\delta^{15}N$ values between eastern Pacific populations and western Pacific/Indian Ocean populations that are consistent with patterns observed in different regional denitrification regimes, with enriched $\delta^{15}N$ values in more productive eastern Pacific waters and depleted $\delta^{15}N$ values in oligotrophic waters of the western Pacific and Indian ocean (Seminoff et al., 2012) (Fig. 2). We also observed differences in $\delta^{13}C$ values between the two populations in Mexico that are typically observed between coastal and offshore environments (Hobson, 1999), with more enriched $\delta^{13}C$ values in coastal manta samples and depleted $\delta^{13}C$ values in offshore manta samples. This suggests that mantas tagged at the mainland site are foraging in nearshore environments, while those tagged at the offshore site are foraging in more pelagic environments, which is consistent with the movement patterns observed in tagging data. Isotopic differences between mantas sampled in Sri Lanka and Indonesia were less well defined, likely due to the similarity of baseline isotopic signatures in these two regions (Heikoop et al., 2000). Our model selection approach grouped Indonesian and Sri Lankan populations but kept Mexican populations distinct in the best-fit model by an AIC margin of 17.56 (Supplementary information), supporting the observed isotopic differences

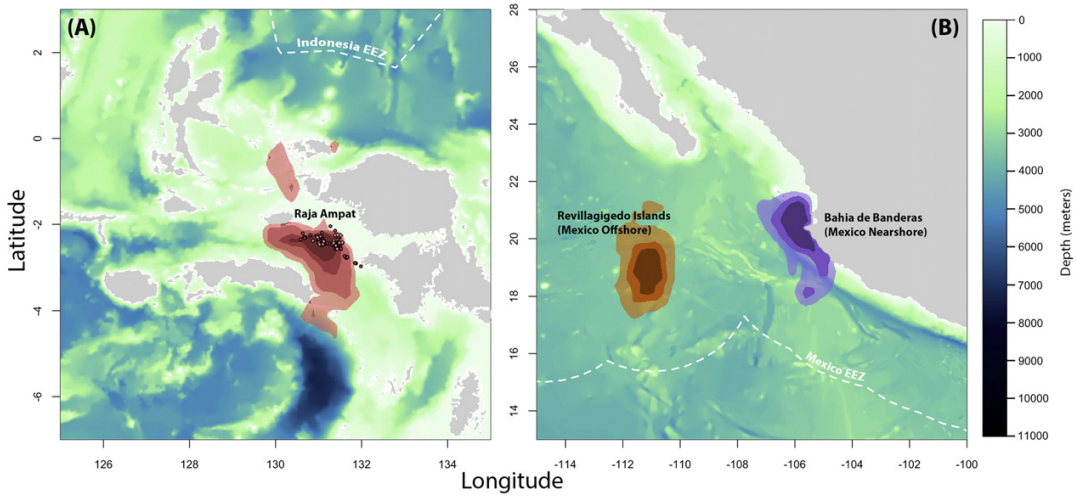

Fig. 1. Tag locations from mantas tagged in (A) Raja Ampat, Indonesia and (B) Pacific Mexico. Polygons represent probability density surfaces for all tags from a given deployment location. Light to dark shades represent 95%, 75%, and 50% probability contours. The 95% contour represents the smallest area where tagged animals were expected to spend 95% of their time. Filled circles (dark red) and diamonds (light red) in (A) represent GPS and Argos satellite locations, respectively, recorded by the single deployed SPLASH tag. Maps and probability density surfaces were created using R.

outlined above. Based on an estimated weight of 1500 kg for an individual of 5 m disc width (Notarbartolo-Di-Sciara, 1988) we calculated a 100% tissue turnover time of 665 days using published body mass-tissue incorporation rates for teleosts and elasmobranchs (Weidel et al., 2011; Kim et al., 2012). This suggests that isotope values reported here represent multi-year averages, and that the separation between populations observed in satellite telemetry results remains true on multi-year time scales.

We included a subset of tissue samples in genetic analyses (Mexico Nearshore, n = 12; Mexico Offshore, n = 10; Indonesia, n = 8; Sri Lanka, n = 12). Genetic results were consistent with satellite telemetry and stable isotope analysis. We recovered 25,040 Single Nucleotide Polymorphisms (SNPs) from double digest Restriction-site Associated DNA (ddRAD) sequencing and included 3108 SNPs in the final population structure analysis (See Supplementary Information). While our sample size per location was relatively low, high-throughput sequencing methods such as ddRAD provide many thousands of SNPs across which to estimate population structure. As a result, the large number of loci reduces the probability of miss-assigning an individual to a population based on allele frequencies, despite small sample sizes that may confound population structure analyses using traditional sequencing methods (Nikolic et al., 2009). Analysis with Structure 2.3 provided the greatest support for 3 populations, which demonstrate structure between Coastal Mexico, Offshore Mexico and Sri Lanka (Fig. 3). We did not include tissue samples from Indonesia due to low DNA yields (see Supplementary information).

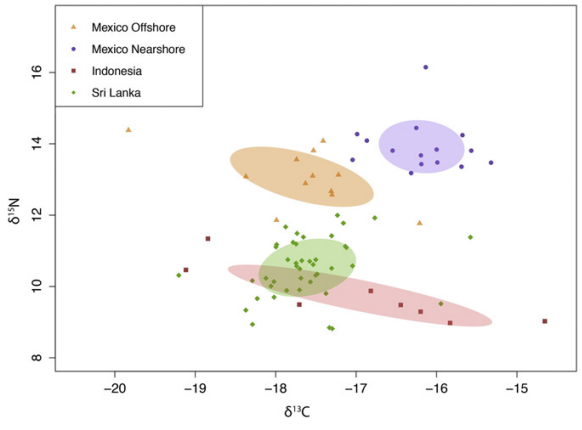

Fig. 2. Isotope signatures of manta populations across the Indo-Pacific. Shaded polygons represent sample-size corrected standard ellipses for each population, calculated using the package 'SIBER' in R. Differences in $\delta^{15}N$ values between populations from Mexico and those from Indonesia and Sri Lanka correspond to higher baseline $\delta^{15}N$ values in the highly productive Tropical Eastern Pacific as compared with the more oligotrophic waters of the Western Pacific and Indian Oceans. The shift in $\delta^{13}C$ values between the two populations in Mexico corresponds to differences in baseline $\delta^{13}C$ values between the coastal and offshore habitats occupied by the two populations.

4. Discussion

Using three separate methodologies that provide data at multiple spatial and temporal scales, we provide the first long-term information on the population structure and spatial ecology of the world's largest ray. The consistent agreement between satellite tagging, stable isotope and genetic results strongly suggest that oceanic manta rays in these regions form well-structured subpopulations and exhibit a high degree of residency.

These findings do not preclude occasional long-distance movements by the species. The large body size of oceanic manta rays makes the species physiologically capable of swimming long distances. For example, one individual was recorded traveling from mainland Ecuador to the Galapagos Islands, over 1400 km straight-line distance (Hearn et al., 2014). Additionally, long-distance movements may account for the occasional sightings of oceanic manta rays in regions outside their typical distribution (Duffy and Abbott, 2003; Couturier et al., 2015). However, the stable isotope and genetic data we present in this study demonstrate that such cases of long-distance movements are likely rare and do not generate substantial gene flow or interpopulation exchange of individuals. This is in contrast to other large filter-feeding elasmobranchs that exhibit low genetic differentiation and must therefore maintain higher rates of interpopulation exchange (Hoelzel et al., 2006; Schmidt et al., 2009). In the case of Hearn et al., 2014, eight out of nine tagged oceanic mantas remained within a restricted geographic range, and Graham et al., 2012 recorded no long-distance movements by oceanic mantas tagged in the Gulf of Mexico. Many of the locations

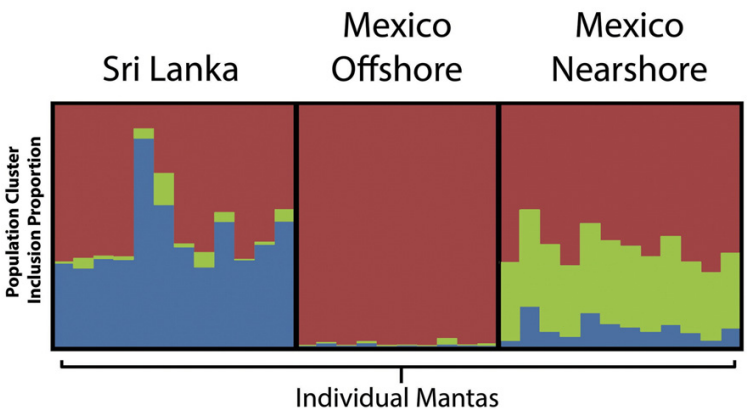

Fig. 3. Estimated genetic structure of oceanic manta populations in Pacific Mexico and Sri Lanka. Each individual included in the genetic analysis is represented by a vertical line, which is partitioned into colored segments representing the estimated membership of an individual in three model-defined population clusters (not necessarily related to geographic populations). Three population clusters (K = 3) received the highest likelihood score in three replicates of Structure analyses for a range of K = 1 to K = 5. We did not include Indonesian samples in the final population structure interpretation due to low DNA yield.

where *M. birostris* is found regularly, including all of the field sites in this study, are seasonal aggregation sites with peaks in manta occurrence that last for several weeks or months, and long periods with few or no sightings (Luiz et al., 2009; Girondot et al., 2014). Despite our satellite tag deployments covering both peak sighting periods and subsequent low seasons, all tagged mantas remained close to their respective tag deployment location. Our findings suggest that these seasonal cycles do not include long-distance movements, but instead may simply represent transitions from coastal aggregation sites to nearby offshore habitats where there is far less survey effort and therefore fewer sightings. Consequently, the available data on *M. birostris* suggest that the most relevant management unit for the species exists at the local or regional scale.

Since the genus was split into two species (Marshall et al., 2009), *M. alfredi* has been considered a predominantly coastal, resident species while *M. birostris* has been considered a pelagic migrant (Couturier et al., 2012). However, recent studies have blurred the proposed ecological characteristics that define the movements and habitat selection of the two species (Kashiwagi et al., 2011). For example, while reef manta rays are predominantly resident, they also undertake occasional long-distance movements of several hundred kilometers (Germanov and Marshall, 2014; Jaine et al., 2014; Braun et al., 2015). Further, reef manta rays access both coastal habitats and offshore, pelagic habitats where they are presumably foraging (Braun et al., 2014; Jaine et al., 2014). Similarly, oceanic manta rays are predominantly resident based on our findings, but also make occasional long-distance movements (Hearn et al., 2014), and feed both in coastal (JDS unpubl.) and deeper, offshore habitats (Stewart et al., in press). Given these similarities in the two species' spatial ecology and habitat use, it remains unclear what factors originally drove speciation and continue to maintain a species boundary. Past introgression (Kashiwagi et al., 2012) and recent evidence of hybridization (Walter et al., 2014) suggest that this boundary may only be weakly maintained, perhaps in part due to the overlap in the two species' ecology.

Our tagging data were collected over several years, while the life span of these animals may exceed 40 years (Couturier et al., 2012). While the stable isotope and genetic results suggest that occasional long-distance movements do not contribute substantially to mixing between populations, further studies are necessary to quantify rates of interpopulation exchange, a useful parameter in identifying the extinction risk of local populations (Hanski, 1999). It is also important to note that we did not deploy tags in Sri Lanka, and we were not able to obtain genetic results from Indonesia. Consequently, our two sites in Mexico were the only populations in this study where we obtained results from all three methods. However, these two sites are also the most geographically proximate, and all three methods indicate population structure and spatial segregation between the two populations. Future genetic studies incorporating samples from a broader range of sites would contribute greatly to our understanding of the species' global population structure and gene flow.

Tag-recorded diving behavior and submersible observations at the same offshore Mexican islands in this study (Stewart et al., in press) indicate that mantas exhibit a high degree of behavioral plasticity and change their vertical habitat use seasonally in order to exploit zooplankton aggregations that remain relatively constant in abundance, but not vertical location, throughout the year (Blackburn et al., 1970). Along with a year-round food source, suitable juvenile habitat overlapping with or adjacent to adult habitat would eliminate the main incentives for long-range migratory behavior. Researchers rarely observe juvenile oceanic manta rays in the wild at seamounts or islands, where the majority of in-water encounters occur. However, gill-net fisheries land high numbers of juveniles at our study site in Sri Lanka, primarily in offshore pelagic habitats, and juvenile oceanic manta rays are sometimes encountered in oceanic habitats far from shore in Mexico (R. Rubin, Pers. Comm.). This suggests that oceanic manta rays may exhibit age- or size-based habitat segregation, remaining within the same geographic region but exploiting different habitats. Alternatively, adult and juvenile oceanic mantas may use similar offshore pelagic habitats but juveniles may avoid cleaning stations and other near-shore habitats in an effort to reduce predation until they reach a sufficient size, paralleling the use of nursery habitats common in other elasmobranchs (Heupel et al., 2007).

While the movements of highly mobile marine species across international boundaries often necessitates management by international agencies, agreements or conventions, these large-scale efforts at management often fall short of preventing the overharvest of vulnerable marine species (Fonteneau, 2007; Ferretti et al., 2010; Rocha et al., 2014). On the other hand, species with poorly connected subpopulations and smaller geographic ranges have a higher local extinction risk than species that form well-connected metapopulations (Hanski, 1999), presenting a different set of management challenges. However, managing non-mobile species can be more straightforward for socioeconomic reasons (e.g. fewer stakeholder groups, proximity of consumers to resource)(Ostrom, 1999) and practical management considerations (e.g. jurisdictional considerations, smaller enforcement area). Nonetheless, in cases where adequate management action is not taken, non-mobile species often suffer more dramatic local population impacts than mobile species (McCauley et al., 2015).

Although our observations are based on samples from only four populations, their ecological and oceanographic characteristics span much of the range that oceanic mantas are known to inhabit. Therefore, the apparent insularity of the study populations has substantial implications for the species' conservation and management. Our results indicate that fisheries for manta rays are drawing on vulnerable, local populations, increasing the rate of population decline and the risk of local extinctions. In light of these findings, at least one major population decline of oceanic manta rays can be interpreted as a virtual extirpation of the species. A fishery for mantas in southern Baja California, Mexico in the 1980s and '90s led to the near disappearance of the species in what was perhaps the best-known location for diver interactions with mantas (R. Rubin, G. Notarbartolo di Sciara, Pers. Comm.). Even after twelve years of continuous protection by the Mexican government, there are no signs of recovery in the Gulf of California's manta population, which is consistent with the insularity of the two populations in Pacific Mexico studied here.

The restricted geographic ranges revealed by tagging data suggest that oceanic manta rays can benefit from local management initiatives, and that reducing or eliminating local fisheries will play a critical role in preventing population declines. The effectiveness of local-scale management is exemplified by the community-driven Raja Ampat Shark and Ray Sanctuary in Indonesia. The sanctuary covers a substantial portion of the geographic range of mantas we tagged in Indonesia, and has a strong track record of self-enforcement and community engagement. In Mexico, local-scale management action could include expanding the Revillagigedo Islands Biosphere Reserve to cover the pelagic habitat between the islands and increasing the existing 12-mile buffer zone around each island to further protect the manta population throughout its geographic range. Furthermore, the spatial ecology of oceanic manta ray populations should be incorporated into marine protected area planning, especially in the case of so-called 'mega-MPAs' that could cover the entire geographic range of a population, to increase the value of these large designations to the species. Local management actions such as these are far less challenging to implement than the international management efforts that have thus far dominated manta ray conservation (Ostrom, 1999).

In some cases even populations of oceanic manta rays with relatively restricted ranges can straddle international borders, for example in Peruvian and Ecuadorian waters (Hearn et al., 2014). Under such circumstances international efforts to coordinate management action remain a valuable conservation tool and should not be abandoned. However, our study suggests that local and national management efforts may operate at scales most relevant to oceanic manta ray populations, and such efforts have been underutilized in addressing population declines of this vulnerable species. This study highlights the importance of identifying ecological units and understanding the relevant scales at which ecological processes occur in threatened species in order to design and implement effective conservation strategies.

Acknowledgements

The PADI Foundation (Grant No. 7842), The New England Aquarium MCAF, Save Our Seas Foundation (Grant No. 242), Carl F. Bucherer, Misool Baseftin, Conservation International, SEA Aquarium (Singapore), The Punta Mita Foundation, Wolcott Henry, Monique Bar, David Connell, Eric Krauss, Mary O'Malley, Lupo Dion, CIMEC and the Gulf of California Marine Program provided financial support. Roger Hill, Todd Lindstrom and Molly Burke provided technical support. This study was made possible by the Mexican National Commission for Protected Areas, the Indonesian Ministry of Marine Affairs and Fisheries, and the communities of Raja Ampat, Indonesia, and Yelapa and Puerto Vallarta, Mexico.

This material is based in part upon work supported by the National Science Foundation Graduate Research Fellowship under Grant No. DGE-1144086 to J.D.S. Any opinions, findings, and conclusions or recommendations expressed in this material are those of the authors and do not necessarily reflect the views of the National Science Foundation.

Appendix A. Supplementary data

Supplementary data to this article can be found online at http://dx.doi.org/10.1016/j.biocon.2016.05.016.

References

Blackburn, M., Laurs, R.M., Owen, R.W., Zeiyzschel, B., 1970. Seasonal and areal changes in standing stocks of phytoplankton, zooplankton and micronekton in the eastern tropical Pacific. Mar. Biol. 7, 14–31.
Braun, C.D., Skomal, G.B., Thorrold, S.R., Berumen, M.L., 2014. Diving behavior of the reef manta ray links coral reefs with adjacent deep pelagic habitats. PLoS One 9, 1–8.
Braun, C.D., Skomal, G.B., Thorrold, S.R., Berumen, M.L., 2015. Movements of the reef manta ray (*Manta alfredi*) in the Red Sea using satellite and acoustic telemetry. Mar. Biol.
Catchen, J., Hohenlohe, P.A., Bassham, S., Amores, A., Cresko, W.A., 2013. Stacks: an analysis tool set for population genomics. Mol. Ecol. 22, 3124–3140.
Charles, A., Branch, T.A., Alagiyawadu, A., Baldwin, R., Marsac, F., 2012. Seasonal distribution, movements and taxonomic status of blue whales (*Balaenoptera musculus*) in the northern Indian Ocean. J. Cetacean Res. Manag. 12, 203–218.
Couturier, L.I.E., Marshall, A.D., Jaine, F.R.A., Kashiwagi, T., Pierce, S.J., Townsend, K.A., Weeks, S.J., Bennett, M.B., Richardson, A.J., 2012. Biology, ecology and conservation of the Mobulidae. J. Fish Biol. 80, 1075–1119.
Couturier, L., Jaine, F., Kashiwagi, T., 2015. First photographic records of the giant manta ray *Manta birostris* off eastern Australia. PeerJ 3, e742.
Croll, D.A., Dewar, H., Dulvy, N.K., Fernando, D., Francis, M.P., Galvan-Magana, F., Hall, M., Heinrichs, S., Marshall, A., McCauley, D., Newton, K.M., Notarbartolo-Di-Sciara, G., O'Malley, M., O'Sullivan, J., Poortvliet, M., Roman, M., Stevens, G., Tershy, B.R., White, W.T., 2015. Vulnerabilities and fisheries impacts: the uncertain future of manta and devil rays. Aquat. Conserv. Mar. Freshwat. Ecosyst.
Davidson, L.N.K., Krawchuk, M.A., Dulvy, N.K., 2015. Why have global shark and ray landings declined: improved management or overfishing? Fish Fish.
Deakos, M.H., Baker, J.D., Bejder, L., 2011. Characteristics of a manta ray *Manta alfredi* population off Maui, Hawaii, and implications for management. Mar. Ecol. Prog. Ser. 429, 245–260.
Dewar, H., Mous, P., Domeier, M., Muljadi, A., Pet, J., Whitty, J., 2008. Movements and site fidelity of the giant manta ray, *Manta birostris*, in the Komodo Marine Park, Indonesia. Mar. Biol. 155, 121–133.
Duffy, C.A.J., Abbott, D., 2003. Sightings of mobulid rays from northern New Zealand, with confirmation of the occurrence of *Manta birostris* in New Zealand waters. N. Z. J. Mar. Freshw. Res. 37, 715–721.
Dulvy, N.K., Pardo, S.A., Simpfendorfer, C.A., Carlson, J.K., 2014. Diagnosing the dangerous demography of manta rays using life history theory. PeerJ 2, e400.
Ferretti, F., Worm, B., Britten, G.L., Heithaus, M.R., Lotze, H.K., 2010. Patterns and ecosystem consequences of shark declines in the ocean. Ecol. Lett. 13, 1055–1071.
Fonteneau, A., 2007. SCRS 2006 : towards clear and firm ICCAT reports on atlantic bluefin tuna stocks? An open letter to the bluefin group and to the SCRS. Collect. Vol. Sci. Pap. ICCAT 60, 1027–1034.
Germanov, E.S., Marshall, A.D., 2014. Running the gauntlet: regional movement patterns of *Manta alfredi* through a complex of parks and fisheries. PLoS One 9, e110071.
Girondot, M., Bédel, S., Delmoitiez, L., Russo, M., Chevalier, J., Guéry, L., Ben Hassine, S., Féon, H., Jribi, I., 2014. Spatio-temporal distribution of *Manta birostris* in French Guiana waters. J. Mar. Biol. Assoc. U. K. 95, 153–160.
Graham, R.T., Witt, M.J., Castellanos, D.W., Remolina, F., Maxwell, S., Godley, B.J., Hawkes, L.A., 2012. Satellite tracking of manta rays highlights challenges to their conservation. PLoS One 7, 3–8.
Graham, F., Rynne, P., Estevanez, M., Luo, J., Ault, J.S., Hammerschlag, N., 2016. Use of marine protected areas and exclusive economic zones in the subtropical western North Atlantic Ocean by large highly mobile sharks. Divers. Distrib. (n/a–n/a).
Hanski, I., 1999. Metapopulation Ecology. Oxford University Press.
Hearn, A.R., Acuna, D., Ketchum, J.T., Penaherrera, C., Green, J., Marshall, A., Guerrero, M., Shillinger, G., 2014. Elasmobranchs of the Galapagos Marine Reserve. In: Denkinger, J., Vinueza, L. (Eds.), Galapagos Mar. Reserv. A Dyn. Soc. Syst., pp. 23–59
Heikoop, J., Dunn, J.J., Risk, M.J., Tomascik, T., Schwarcz, H.P., Sandeman, I.M., Sammarco, P.W., 2000. d15N and d13C of coral tissue show significant inter-reef variation. Coral Reefs 19, 189–193.
Heupel, M.R., Carlson, J.K., Simpfendorfer, C.A., 2007. Shark nursery areas: concepts, definition, characterization and assumptions. Mar. Ecol. Prog. Ser. 337, 287–297.
Hobson, K.A., 1999. Tracing origins and migration of wildlife using stable isotopes: a review. Oecologia 120, 314–326.
Hoelzel, A.R., Shivji, M.S., Magnussen, J., Francis, M.P., 2006. Low worldwide genetic diversity in the basking shark (*Cetorhinus maximus*). Biol. Lett. 2, 639–642.
Hueter, R.E., Tyminski, J.P., de la Parra, R., 2013. Horizontal movements, migration patterns, and population structure of whale sharks in the Gulf of Mexico and northwestern Caribbean sea. PLoS One 8, e71883.
Jaine, F.R.A., Rohner, C.A., Weeks, S.J., Couturier, L.I.E., Bennett, M.B., Townsend, K.A., Richardson, A.J., 2014. Movements and habitat use of reef manta rays off eastern Australia: offshore excursions, deep diving and eddy affinity revealed by satellite telemetry. Mar. Ecol. Prog. Ser. 510, 73–86.
Kashiwagi, T., Marshall, A.D., Bennett, M.B., Ovenden, J.R., 2011. Habitat segregation and mosaic sympatry of the two species of manta ray in the Indian and Pacific Oceans: *Manta alfredi* and *M. birostris*—CORRIGENDUM. Mar. Biodivers. Rec. 4.

Kashiwagi, T., Marshall, A.D., Bennett, M.B., Ovenden, J.R., 2012. The genetic signature of recent speciation in manta rays (*Manta alfredi* and *M. birostris*). Mol. Phylogenet. Evol. 64, 212–218.
Kim, S.L., del Rio, C.M., Casper, D., Koch, P.L., 2012. Isotopic incorporation rates for shark tissues from a long-term captive feeding study. J. Exp. Biol. 215, 2495–2500.
Luiz, O.J., Balboni, A.P., Kodja, G., Andrade, M., Marum, H., 2009. Seasonal occurrences of *Manta birostris* (Chondrichthyes: Mobulidae) in southeastern Brazil. Ichthyol. Res. 56, 96–99.
Marshall, A.D., Compagno, L.J.V., Bennett, M.B., 2009. Redescription of the genus Manta with resurrection of *Manta alfredi*. Zootaxa 28, 1–28.
McCauley, D.J., Pinsky, M.L., Palumbi, S.R., Estes, J.A., Joyce, F.H., Warner, R.R., 2015. Marine defaunation: animal loss in the global ocean. Science 347 (1255641–1255641).
Nikolic, N., Fève, K., Chevalet, C., Høyheim, B., Riquet, J., 2009. A set of 37 microsatellite DNA markers for genetic diversity and structure analysis of Atlantic salmon *Salmo salar* populations. J. Fish Biol. 74, 458–466.
Notarbartolo-Di-Sciara, G., 1988. Natural history of the rays of the genus Mobula in the Gulf of California. Fish. Bull.
O'Malley, M.P., Lee-Brooks, K., Medd, H.B., 2013. The global economic impact of manta ray watching tourism. PLoS One 8.
Ostrom, E., 1999. Revisiting the commons: local lessons, global challenges. Science 284, 278–282.
Pedersen, M.W., Patterson, T.A., Thygesen, U.H., Madsen, H., 2011. Estimating animal behavior and residency from movement data. Oikos 120, 1281–1290.
Post, D.M., Layman, C.A., Arrington, D.A., Takimoto, G., Quattrochi, J., Montaña, C.G., 2007. Getting to the fat of the matter: models, methods and assumptions for dealing with lipids in stable isotope analyses. Oecologia 152, 179–189.
Pritchard, J.K., Stephens, M., Donnelly, P., 2000. Inference of population structure using multilocus genotype data. Genetics 155, 945–959.
Rocha, R.C., Clapham, P.J., Ivashchenko, Y.V., 2014. Emptying the oceans: a summary of industrial whaling catches in the 20th century. Mar. Fish. Rev. 76, 37–48.
Schalk, P.H., 1987. Monsoon-related changes in zooplankton biomass in the eastern Banda Sea and Aru Basin. Biol. Oceanogr. 5, 1–12.
Schmidt, J.V., Schmidt, C.L., Ozer, F., Ernst, R.E., Feldheim, K.A., Ashley, M.V., Levine, M., 2009. Low genetic differentiation across three major ocean populations of the whale shark, *Rhincodon typus*. PLoS One 4.
Seminoff, J.A., Benson, S.R., Arthur, K.E., Eguchi, T., Dutton, P.H., Tapilatu, R.F., Popp, B.N., 2012. Stable isotope tracking of endangered sea turtles: validation with satellite telemetry and δ15N analysis of amino acids. PLoS One 7.
Skomal, G.B., Zeeman, S.I., Chisholm, J.H., Summers, E.L., Walsh, H.J., McMahon, K.W., Thorrold, S.R., 2009. Transequatorial migrations by basking sharks in the western Atlantic Ocean. Curr. Biol. 19, 1019–1022.
Stewart, J.D., Hoyos-Padilla, E.M., Kumli, K.R. & Rubin, R.D. Deep-water feeding and behavioral plasticity in *Manta birostris* revealed by archival tags and submersible observations. Zoology, http://dx.doi.org/10.1016/j.zool.2016.05.010 (in press).
Thorrold, S.R., Afonso, P., Fontes, J., Braun, C.D., Santos, R.S., Skomal, G.B., Berumen, M.L., 2014. Extreme diving behaviour in devil rays links surface waters and the deep ocean. Nat. Commun. 5, 4274.
Walter, R.P., Kessel, S.T., Alhasan, N., Fisk, A.T., Heath, D.D., Chekchak, T., Klaus, R., Younis, M., Hill, G., Jones, B., Braun, C.D., Berumen, M.L., DiBattista, J.D., Priest, M.A., Hussey, N.E., 2014. First record of living *Manta alfredi* × *Manta birostris* hybrid. Mar. Biodivers. 44, 1–2.
Ward-Paige, C.A., Davis, B., Worm, B., 2013. Global population trends and human use patterns of Manta and Mobula rays. PLoS One 8, e74835.
Weidel, B.C., Carpenter, S.R., Kitchell, J.F., Vander Zanden, M.J., 2011. Rates and components of carbon turnover in fish muscle: insights from bioenergetics models and a whole-lake 13C addition. Can. J. Fish. Aquat. Sci. 68, 387–399.
White, E.R., Myers, M.C., Flemming, J.M., Baum, J.K., 2015. Shifting elasmobranch community assemblage at Cocos Island—an isolated marine protected area. Conserv. Biol.

Spatial Ecology and Conservation of *Manta birostris* in the Indo-Pacific

Supplementary Information

By

Joshua D. Stewart[1,2*], Calvin S. Beale[3], Daniel Fernando[4,2,5], Abraham B. Sianipar[6], Ronald S. Burton[1], Brice X. Semmens[1], Octavio Aburto-Oropeza[1]

[1]Scripps Institution of Oceanography, University of California, San Diego,9500 Gilman Dr., La Jolla, CA 92093, USA

[2]The Manta Trust, Catemwood House, Corscombe, Dorchester, Dorset, DT2 0NT, UK

[3]Misool Manta Project, Jalan Gunung Umsini No. 51, RT 03 / RW 03 Kampung Baru, Sorong, Papua Barat 98413, Indonesia

[4] Department of Biology and Environmental Science, Linnaeus University, 39182 Kalmar, Sweden

[5]Blue Resources, 86 Barnes Place, Colombo 00700, Sri Lanka

[6]Conservation International, Jalan Pejaten Barat No. 16A, Kemang, Jakarta 12550, Indonesia

*Corresponding Author: j8stewart@ucsd.edu

Supplementary Table S1: Tag Deployments. We deployed Wildlife Computers (WC) and Desert Star (DS) archival and towed satellite tags on oceanic manta rays (*Manta birostris*) on mainland Pacific Mexico (Mexico NS), offshore islands in Pacific Mexico (Mexico OS) and West Papua Indonesia. Diver-estimated disc width (Size) is reported in meters. Four of 22 tags did not report back, indicated by (-). Deployment length is listed in days, along with the Latitude and Longitude coordinates of tag deployments and pop-off locations. Deploy-Pop Dist is the distance in kilometers between the tag deployment and pop off locations.

Tag ID	Manufacturer & Model	Region	Sex	Size (m)	Deploy Date	Deploy Length (d)	Deploy Lon	Deploy Lat	Pop Lon	Pop Lat	Deploy-Pop Dist (km)
132235	WC MiniPAT	Mexico (NS)	F	4.5	24-Jul-13	193	-105.591	20.480	-106.040	20.445	47.045
133515	WC MiniPAT	Mexico (NS)	M	4.0	8-Aug-14	178	-105.475	20.497	-105.637	20.718	29.835
133516	WC MiniPAT	Mexico (NS)	M	4.0	8-Aug-14	113	-105.475	20.497	-105.542	19.970	59.081
139046	DS SeaTag-MOD	Mexico (NS)	M	4.5	8-Aug-14	-	-	-	-	-	-
139047	DS SeaTag-MOD	Mexico (NS)	M	4.5	8-Aug-14	-	-	-	-	-	-
148429	DS SeaTag-MOD	Mexico (NS)	F	5.0	27-Feb-15	28	-105.475	20.497	-105.383	19.774	81.056
148428	DS SeaTag-MOD	Mexico (NS)	F	4.5	27-Feb-15	7	-105.475	20.497	-105.604	20.380	18.727
132234	WC MiniPAT	Mexico (OS)	F	4.5	7-Apr-14	-	-	-	-	-	-
134937	WC MiniPAT	Mexico (OS)	F	4.5	7-Apr-14	181	-110.814	19.331	-110.838	19.284	5.837
134938	WC MiniPAT	Mexico (OS)	F	4.5	7-Apr-14	184	-110.814	19.331	-111.113	18.821	64.937
134939	WC MiniPAT	Mexico (OS)	M	4.5	7-Apr-14	189	-110.814	19.331	-111.053	18.533	92.349
134940	WC MiniPAT	Mexico (OS)	M	4.0	8-Apr-14	186	-110.907	18.779	-111.270	18.317	64.100
122097	WC PAT MK10	Indonesia	M	4.5	26-Sep-12	162	130.648	-2.259	130.435	-0.865	157.007
122098	WC PAT MK10	Indonesia	M	3.5	10-Nov-12	159	130.648	-2.259	130.923	0.084	262.644
122099	WC PAT MK10	Indonesia	F	3.5	8-Jan-13	-	-	-	-	-	-
122098b	WC MiniPAT	Indonesia	F	5.0	8-May-14	181	130.648	-2.259	131.545	-2.569	105.572
130966	WC MiniPAT	Indonesia	M	4.0	27-May-14	180	130.648	-2.259	131.496	-0.170	251.002
130967	WC MiniPAT	Indonesia	F	5.0	21-Sep-13	186	130.648	-2.259	131.969	-0.342	259.171
130968	WC MiniPAT	Indonesia	M	3.5	25-Oct-13	177	130.648	-2.259	131.100	-0.450	207.599
130969	WC MiniPAT	Indonesia	F	5.0	8-May-14	184	130.648	-2.259	131.559	-2.183	101.710
130970	WC MiniPAT	Indonesia	F	3.5	13-Oct-13	90	130.648	-2.259	130.725	-2.238	8.905
130971	WC SPLASH	Indonesia	F	4.0	7-May-14	64	130.648	-2.259	131.276	-2.044	73.805

Supplementary Table S2: F_{ST} values between Indo-Pacific *Manta birostris* populations and *Manta alfredi* samples from Indonesia. Stacks was unable to calculate F_{ST} values for the Indonesia population of *M. birostris* due to low coverage.

	Mexico Offshore	**Sri Lanka**	**Indonesia**	***Manta alfredi***
Mexico Mainland	0.00253435	0.00368851	-	0.0205798
Mexico Offshore		0.00273346	-	0.0258658
Sri Lanka			-	0.0238001
Indonesia				-

Supplementary Figure S1: 90th percentile F_{ST} Structure plots from true data (A) and null control data (B)

(A)

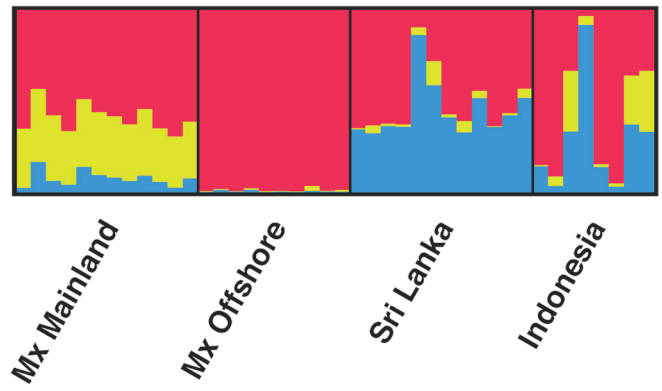

(B)

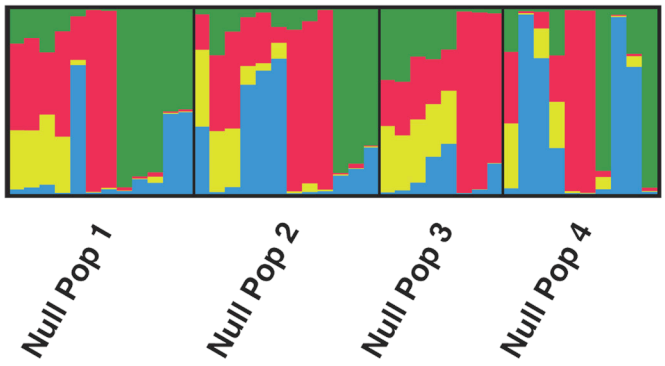

Supplementary Figure S2: Isotopic differences between round ray white muscle tissue stored in 95% ethanol (red; n=7) and 70% isopropanol (black; n=6). We observed a significant difference in $\delta^{13}C$ values, but not in $\delta^{15}N$ values.

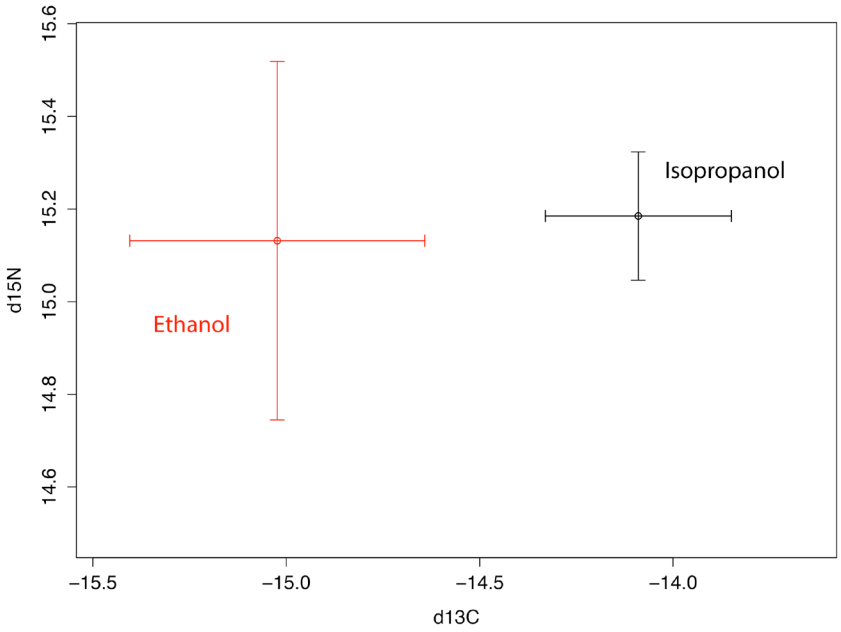

Supplementary Methods and Results

Satellite Telemetry

We tagged 22 oceanic manta rays with a combination of Wildlife Computers and Desert Star pop-off archival satellite tags and Wildlife Computers SPLASH tags (Supplementary Table S1). We programmed pop-off archival satellite tags to have deployment lengths of 6 months (Supplementary Table S1), after which point they detached from the animal and transmitted partial archived geolocation data as battery life allowed. We used a 2-meter Hawaiian sling-style spear pole to deploy tags, which were attached to the animals using a 6cm titanium dart (Wildlife Computers). In the case of archival satellite tags, we used a 10cm stainless steel tether between the application dart and the tag, while in the case of the single SPLASH tag deployed we used a 60cm tether to allow the tag to break the surface while being towed in order to obtain GPS positions and communicate with satellites.

We analyzed PAT Mk10 and MiniPAT light-based geolocation data using Wildlife Computers' Global Position Estimator v3 (GPE3) software. GPE3 uses a Hidden Markov Model that incorporates raw light-based geolocation data, tag-recorded sea surface temperature data, remotely-sensed satellite sea-surface temperature, seafloor bathymetry, and maximum recorded tag depth to estimate daily locations, and a movement prior to constrain maximum daily travel distance. We estimated an average cruising speed for mantas of approximately 1 m/s by converting an open-mouth swimming speed of 0.68 m/s reported for feeding manta rays in the Gulf of Mexico[1] and

converting it to a closed-mouth swimming speed using open- versus closed-mouth swimming speeds reported for basking sharks[2]. We also calculated movement speeds from GPS locations recorded by the single Wildlife Computers SPLASH tag. The mean movement speed between successive locations was 0.42 m/s, however GPE3 was not able to converge with movement speeds this slow. Consequently, we used the less conservative 1 m/s for all GPE3 analyses. We averaged daily probability surfaces for all tags from a given tagging location using the package 'raster' in R. We resampled the 0.25° GPE3 grid at a resolution of 0.0083° using bilinear interpolation ('raster' function 'resample') and plotted 50^{th}, 75^{th}, 90^{th} and 95^{th} percentile polygons from the merged probability surface. We decoded raw Desert Star SeaTag-MOD data using the Desert Star SeaTrack software. However, very few location estimates were recovered from the tag deployments, and consequently we only included the deployment and pop-off locations in further analyses.

Tissue Sample Collection and Storage

We used a 2-meter Hawaiian sling-style spear pole with custom Pneudart marine biopsy tips to collect tissue samples from free-swimming *M. birostris* individuals. In the case of Sri Lanka, we collected tissue samples from landed individuals at two fishing ports in the southwest of the country. While there is no consensus on the effect of ethanol on $\delta^{13}C$ and $\delta^{15}N$ stable isotope values[3,4] in general, most preservation studies on fish muscle and fin tissue indicate that there are negligible effects on $\delta^{15}N$ values, and the shift in $\delta^{13}C$ values after long-term storage in ethanol is low and, importantly, consistent[3,5–8]. Consequently, as remote, tropical sampling locations generally did not allow for preferred preservation methods such as freezing, we stored tissue samples in 95-100% ethanol, except in the case of Indonesia where samples may have been inadvertently stored in store-bought isopropyl alcohol.

ddRAD Sequencing

We extracted DNA from 25mg of white muscle tissue using a Qiagen DNeasy Blood & Tissue Kit. We determined the quantity of DNA in each extracted sample using a PicoGreen assay (Life Technologies). We then diluted samples to a concentration of 10ng/uL using molecular grade water. We performed double digest Restriction Associated DNA (ddRAD) library preparation following the Peterson et al.[9] protocol. We performed a double digest of genomic DNA for each sample using XhoI and MseI restriction enzymes incubated at 37 °C for one hour. We cleaned digested DNA fragments using an AMPure purification kit (Agencourt). We performed two washes in 80% ethanol and eluted into 20uL of elution buffer (Qiagen). We then performed a second DNA quantification on 1uL of sample using a PicoGreen assay. We ligated XhoI inline barcodes and MseI indices to cleaned, digested DNA. We used 24 barcodes and 2 indices to provide 48 unique tag combinations. In addition to the 42 *M. birostris* samples presented in this study, we included six *Manta alfredi* samples as a reference for genetic variation. We separated the samples into two groups by MseI index and then pooled 25uL of each sample and reduced the total volume to 30 uL using a QIAQuick PCR Purification kit (Qiagen). We ran the pooled sample on a 2% agarose gel to separate fragments by length, and removed a band between 300-400 base pairs. We purified the size-selected fragments using a MinElute Gel Purification Kit (Qiagen) and eluted in

20uL elution buffer. We then amplified the samples using a PCR reaction as described in Peterson et al[9]. After amplification, we performed a second gel purification step, this time selecting fragments from 350-450 base pairs in length to account for the added length of PCR primers. We did a final quantification of DNA concentration using a PicoGreen assay. Samples were sequenced at the University of California Irvine Genomics High-Throughput Facility on an Illumina HiSeq 2500 using version 3 chemistry for paired end 100 cycles. Outputs were de-multiplexed by the sequencing facility into paired end reads for each individual.

We separated the single-end and paired-end reads of each sample and used Stacks[10] v1.21 program process_radtags to clean the raw data [flag -c], discard low quality reads [-q], and recover ambiguous barcodes and tags [-r]. After processing, we concatenated single and paired end files to produce a single data file per individual. We then used the program denovo_map.pl to identify and catalog SNPs with a minimum stack depth of 3 identical reads per locus [-m 3], a maximum of 4 mismatches between loci for an individual [-M 4], and a maximum of 2 mismatches between loci when constructing the catalog [-n 2]. Finally, we ran the Populations program separately to generate F_{ST} values and create outputs formatted for Structure[11]. For the Populations program, we required 50% of individuals in a population to have data at a locus [-r 0.5] and for the locus to be present in at least two populations [-p 2] in order to process it. We set a minimum stack depth per locus [-m] to 5 and set the minor allele frequency [-a] to 0.1. We completed this workflow once including the *M. alfredi* samples and then repeated the process and further analysis using *M birostris* samples only. Following the approach described in Puebla et al.[12], we selected SNPs in the 90th percentile of F_{ST} values across all populations to account for extremely slow mutation rates in elasmobranchs[13] and the recent (less than 1 mya[14] and possibly as recently as 30,000 ya[15]) divergence of the two manta species that may otherwise obscure population structure, illustrated by low inter-species F_{ST} values (Supplementary Table S2). The mean F_{ST} value of 90th percentile SNPs was 0.07 (range: 0.029 – 0.326). 430 of these SNPs had an F_{ST} value over 0.1. We then ran both the complete SNP dataset and the 90th percentile dataset through Structure using an admixture model, a burn-in of 20,000 and a model run of 80,000 iterations, and a range of putative populations from one to five. We performed three replicates of this analysis and selected the most likely number of populations using Structure Harvester[16]. We combined replicates using the cluster-matching program CLUMPP[17] and plotted results using Distruct[18]. To determine if filtering for high F_{ST} SNPs was biasing our results towards additional populations, we ran a null control. We randomized individual membership in populations and re-ran Stacks denovo_map.pl and populations with this null population map. We then performed the same 90th percentile F_{ST} SNP filtering on the null control samples and analyzed the results in Structure following the same method outlined above.

We recovered 25,040 SNPs from ddRAD analysis and included 3,108 in the final population structure analysis. The mean stack depth per individual was 22.95 (SD 9.27). With all 25,040 SNPs included, Structure identified a single population (K=1) as having the greatest likelihood. With 3,108 SNPs (90th percentile F_{ST}) included, Structure identified three populations (K=3) as having the greatest likelihood. The Structure analysis of the null control data identified four populations (K=4) as having the greatest likelihood, but the identified populations did not have any geographic relevance

(Supplementary Figure S1). This suggests that the 90th percentile F_{ST} filtering for the true population data did not bias the results towards additional structure. The samples from Indonesia had extremely low coverage, with a max of 9% and min of 0% of SNPs in the catalog from any individual (mean 4.75%, SD 4.33%). By contrast, coverage in other populations was 70.75% (SD 11.1%; Mexico Mainland), 68.9% (SD 7.22%; Mexico Offshore), and 55.75% (SD 15.43%; Sri Lanka). Samples from Indonesia may have inadvertently been stored in store-bought rubbing alcohol (70% isopropanol), which would explain the low DNA yield. However we were unable to confirm whether samples were stored in 70% isopropanol or 95% ethanol. Consequently, we excluded these samples from the interpretation of genetic analyses. Stacks v1.21 also outputs F_{IS} scores, an inbreeding coefficient, for each population. These were: Sri Lanka 0.0933; Nearshore Mexico 0.0983; Offshore Mexico 0.0711. We used the equation $\chi^2 = NF_{IS}^2$ from Hedrick (2011), where N is the sample size for each population, to calculate a χ^2 value of significance (df = 1) for each population's inbreeding coefficient. In all cases inbreeding coefficients were not significant ($p > 0.75$).

Stable Isotope Analysis

For stable isotope sample preparation, we rinsed samples in deionized water and then freeze-dried approximately 10mg (wet) of white muscle tissue from each individual for 24-48 hours using a FreeZone 2.5 freeze drier (Labconco). We pulverized dried muscle tissue using a Wig-L-Bug dental amalgamator. We ground samples for 45 seconds or until they were entirely powdered and well mixed. We then weighed out between 0.5 and 1mg of powdered tissue and packaged it in a 5x9mm tin capsule (Costech). We sent samples to the UC Santa Cruz Stable Isotope Laboratory (UCSC-SIL) and the Scripps Institution of Oceanography Stable Isotope Laboratory (SIO-SIL). UCSC-SIL analyzed samples using an NC2500 Elemental Analyzer (CE Instruments) interfaced to a Delta Plus XP isotope ratio mass spectrometer (ThermoFinnigan). SIO-SIL analyzed samples using a Costech 4010 Elemental Analyzer interfaced to a Delta Plus XP isotope ratio mass spectrometer.

To determine if tissue biopsies from mantas sampled in Indonesia would have significantly different isotope ratios if they were in fact stored in isopropanol, we performed a validation experiment using white muscle from a single round stingray (*Urolophus halleri*). We removed approximately 2g of white muscle tissue from one individual that was sacrificed for a separate study. We separated the muscle tissue into 13 samples, 7 of which we preserved in 95% ethanol, and 6 of which we preserved in store-bought isopropyl alcohol. After 60 days we removed the samples from their preservatives and prepared and analyzed them for $\delta^{13}C$ and $\delta^{15}N$ values using the method noted above (Supplementary Figure S2). We performed a t-test on $\delta^{13}C$ and $\delta^{15}N$ values between the two sample preservation methods. We found a significant difference in $\delta^{13}C$ values ($p=0.0008$), with a difference of 0.93 per mil between sample means. We did not detect any significant difference in $\delta^{15}N$ values between the two groups ($p=0.761$). If some or all of the samples from Indonesia were stored in isopropanol, we could expect an increase in $\delta^{13}C$ values as compared with samples stored in ethanol. However, even accounting for this possible shift, we would not expect the observed differences between populations to change. Indonesian and Sri Lankan samples are overlapping in $\delta^{13}C$ with or without a

shift from storage procedures, and the $\delta^{15}N$ differences between Indonesian samples to those collected in Mexico would not change.

To identify isotopic differences between populations, we used a model selection approach on multiple population grouping scenarios. We created the following population groupings: All Different (same as observed data); Indonesia and Sri Lanka populations combined; Mexico populations combined; Indonesia and Sri Lanka populations combined *and* Mexico populations combined; and all populations combined. We created design matrices for the population scenarios, using a dummy variable 'N' (0 or 1) to distinguish between nitrogen isotope values (N=1) and carbon isotope values (N=0). We then fit the same linear model to each grouping scenario using the equation Isotopes~N+Population with function 'lm' in R. We used AIC to identify the best-fit model, representing the grouping scenario best supported by the data. We used the package SIBER in R to calculate standard ellipses corrected for small sample sizes using the standard.ellipse() function and SEAc outputs.

Supplementary Literature Cited

1. Paig-Tran, E. W. M., Kleinteich, T. & Summers, A. P. The filter pads and filtration mechanisms of the devil rays: Variation at macro and microscopic scales. *J. Morphol.* **274,** 1026–1043 (2013).
2. Sims, D. W. Filter-feeding and cruising swimming speeds of basking sharks compared with optimal models: They filter-feed slower than predicted for their size. *J. Exp. Mar. Bio. Ecol.* **249,** 65–76 (2000).
3. Sarakinos, H. C., Johnson, M. L. & Zanden, M. J. Vander. A synthesis of tissue-preservation effects on carbon and nitrogen stable isotope signatures. *Can. J. Zool.* **80,** 381–387 (2002).
4. Barrow, L. M., Bjorndal, K. A. & Reich, K. J. Effects of Preservation Method on Stable Carbon and Nitrogen Isotope Values. *Physiol. Biochem. Zool.* **81,** 688–693 (2008).
5. Kelly, B., Dempson, J. B. & Power, M. The effects of preservation on fish tissue stable isotope signatures. *J. Fish Biol.* **69,** 1595–1611 (2006).
6. Kaehler, S. & Pakhomov, E. a. Effects of storage and preservation on the d13C and d15N signatures of selected marine organisms. *Mar. Ecol. Prog. Ser.* **219,** 299–304 (2001).
7. Vizza, C., Sanderson, B. L., Burrows, D. G. & Coe, H. J. The effects of ethanol preservation on fish fin stable isotopes: Does variation in C:N ratio and body size matter? *Trans. Am. Fish. Soc.* **142,** 1469–1476 (2013).
8. Stallings, C. D. *et al.* Effects of preservation methods of muscle tissue from upper-trophic level reef fishes on stable isotope values (δ13C and δ15N). *PeerJ* 1–16 (2015). doi:10.7717/peerj.874
9. Peterson, B. K., Weber, J. N., Kay, E. H., Fisher, H. S. & Hoekstra, H. E. Double digest RADseq: an inexpensive method for de novo SNP discovery and genotyping in model and non-model species. *PLoS One* **7,** e37135 (2012).
10. Catchen, J., Hohenlohe, P. A., Bassham, S., Amores, A. & Cresko, W. A. Stacks:

an analysis tool set for population genomics. *Mol. Ecol.* **22,** 3124–40 (2013).

11. Pritchard, J. K., Stephens, M. & Donnelly, P. Inference of population structure using multilocus genotype data. *Genetics* **155,** 945–959 (2000).
12. Puebla, O., Bermingham, E. & McMillan, W. O. Genomic atolls of differentiation in coral reef fishes (Hypoplectrus spp., Serranidae). *Mol. Ecol.* **23,** 5291–5303 (2014).
13. Dudgeon, C. L. *et al.* A review of the application of molecular genetics for fisheries management and conservation of sharks and rays. *J. Fish Biol.* **80,** 1789–1843 (2012).
14. Kashiwagi, T., Marshall, A. D., Bennett, M. B. & Ovenden, J. R. The genetic signature of recent speciation in manta rays (Manta alfredi and M. birostris). *Mol. Phylogenet. Evol.* **64,** 212–218 (2012).
15. Poortvliet, M. *et al.* A dated molecular phylogeny of manta and devil rays (Mobulidae) based on mitogenome and nuclear sequences. *Mol. Phylogenet. Evol.* **83,** 72–85 (2015).
16. Earl, D. A. & VonHoldt, B. M. Structure Harvester: a website and program for visualizing Structure output and implementing the Evanno method. *Conserv. Genet. Resour.* **4,** 359–361 (2012).
17. Jakobsson, M. & Rosenberg, N. A. CLUMPP: a cluster matching and permutation program for dealing with label switching and multimodality in analysis of population structure. *Bioinformatics* **23,** 1801–6 (2007).
18. Rosenberg, N. A. distruct: a program for the graphical display of population structure. *Mol. Ecol. Notes* **4,** 137–138 (2003).
19. Hedrick, P. W. *Genetics of Populations*. (Jones & Bartlett Learning, 2011).

Chapter 1, in full, is a reprint of the material as it appears in Biological Conservation 2016. Stewart, J.D., Beale, C.D., Fernando, D., Sianipar, A.B., Burton, R., Semmens, B.X., Aburto-Oropeza, O. The dissertation author was the primary investigator and author of this material.

CHAPTER 2:

Deep-water feeding and behavioral plasticity in *Manta birostris* revealed by archival tags and submersible observations

JOSHUA D. STEWART, EDGAR MAURICIO HOYOS-PADILLA, KATHERINE R. KUMLI, ROBERT D. RUBIN

Zoology 119 (2016) 406–413

Contents lists available at ScienceDirect

Zoology

journal homepage: www.elsevier.com/locate/zool

Deep-water feeding and behavioral plasticity in *Manta birostris* revealed by archival tags and submersible observations

Joshua D. Stewart[a,b,*], Edgar Mauricio Hoyos-Padilla[c,d], Katherine R. Kumli[e], Robert D. Rubin[e,f]

[a] *Scripps Institution of Oceanography, University of California, San Diego, 9500 Gilman Dr., La Jolla, CA 92093, USA*
[b] *The Manta Trust, Catemwood House, Corscombe, Dorchester, Dorset, DT2 0NT, UK*
[c] *Pelagios Kakunja A.C., Sinaloa 1540, Las Garzas, 23070, La Paz, Baja California Sur, Mexico*
[d] *Fins Attached, 19675 Still Glen Drive, Colorado Springs, CO 80908, USA*
[e] *Pacific Manta Research Group, University of California Davis Bodega Marine Laboratory, 2099 Westshore Rd., Bodega Bay, CA 94923, USA*
[f] *Santa Rosa Junior College, 1501 Mendocino Ave, Santa Rosa, CA 95401, USA*

ARTICLE INFO

Article history:
Received 14 January 2016
Received in revised form 7 March 2016
Accepted 24 May 2016
Available online 31 May 2016

Keywords:
Manta birostris
Mobulidae
Foraging ecology
Deep scattering layer
Diving behavior

ABSTRACT

Foraging drives many fundamental aspects of ecology, and an understanding of foraging behavior aids in the conservation of threatened species by identifying critical habitats and spatial patterns relevant to management. The world's largest ray, the oceanic manta (*Manta birostris*) is poorly studied and threatened globally by targeted fisheries and incidental capture. Very little information is available on the natural history, ecology and behavior of the species, complicating management efforts. This study provides the first data on the diving behavior of the species based on data returned from six tagged individuals, and an opportunistic observation from a submersible of a manta foraging at depth. Pop-off archival satellite tags deployed on mantas at the Revillagigedo Archipelago, Mexico recorded seasonal shifts in diving behavior, likely related to changes in the location and availability of zooplankton prey. Across seasons, mantas spent a large proportion of their time centered around the upper limit of the thermocline, where zooplankton often aggregate. Tag data reveal a gradual activity shift from surface waters to 100–150 m across the tagging period, possibly indicating a change in foraging behavior from targeting surface-associated zooplankton to vertical migrators. The depth ranges accessed by mantas in this study carry variable bycatch risks from different fishing gear types. Consequently, region-specific data on diving behavior can help inform local management strategies that reduce or mitigate bycatch of this vulnerable species.

1. Introduction

Foraging behavior is a fundamentally important aspect of animal ecology. How, when and where species feed drives competition (Menge, 1972), reproductive success (Suryan et al., 2000), spatial ecology and distribution (Friedlaender et al., 2006), and can also influence evolutionary patterns such as speciation through niche separation (Pastene et al., 2007; Poortvliet et al., 2015). Understanding the foraging ecology of threatened species will aid in their conservation and management as feeding behavior often determines critical habitat use and spatial patterns that are important in preventing or mitigating targeted or incidental capture and other human impacts (James et al., 2006).

The oceanic manta ray (*Manta birostris*), distributed circumglobally in tropical and subtropical warm seas, is the largest and most highly derived member of the devil ray family (Mobulidae) (Compagno, 1999; McEachran and Aschliman, 2004). Compared to its smaller congener, the reef manta ray (*Manta alfredi*), it inhabits colder, pelagic, upwelled regions in association with seamounts and oceanic islands, and is the least well-known member of the genus (Marshall et al., 2009; Kashiwagi et al., 2011). Oceanic manta rays, and in some areas reef mantas, are threatened globally by fisheries. The species is landed in targeted fisheries in countries such as Indonesia, Philippines, Mozambique, Peru, and previously Mexico; taken as non-discarded bycatch in Sri Lanka, India, and a variety of other small-scale artisanal fisheries; and caught frequently but discarded in purse seine tuna fisheries globally, with a high presumed post-release mortality rate (Croll et al., 2015). While

* Corresponding author at: Scripps Institution of Oceanography, University of California, San Diego, 9500 Gilman Dr., La Jolla, CA 92093, USA.
E-mail address: j8stewart@ucsd.edu (J.D. Stewart).

http://dx.doi.org/10.1016/j.zool.2016.05.010
0944-2006/

reliable fisheries landing data or population trends are unavailable, the demographic characteristics of mantas make them highly susceptible to fisheries impacts (Dulvy et al., 2014). Large-scale studies suggest family-wide declines for mobulid rays globally (Ward-Paige et al., 2013), and several studies indicate severe declines in local manta populations based on catch rates or sighting frequency (Lewis et al., 2015; White et al., 2015). Improving our understanding of the ecology and critical habitat use of manta rays will help facilitate effective management. Major knowledge gaps exist in our understanding of population connectivity and stock structure in oceanic manta rays, which impacts the scale at which management action is implemented; and the habitat use and diving behavior of the species, which may determine individuals' susceptibility to incidental capture in various fishing methods such as gill nets and purse seines.

Most studies of manta rays have focused on descriptive morphology and natural history observations in near-surface environments. As a result of the recent division of the genus into two distinct species (Marshall et al., 2009), many previous research findings attributed to oceanic mantas are now correctly recognized as describing aspects of the biology of the reef manta ray. As such, fundamental biological and ecological information for oceanic mantas is rare. Graham et al. (2012) reported on the horizontal movements of tagged oceanic mantas in the Gulf of Mexico, although tagged individuals may have belonged to a third, undescribed Caribbean species (*Manta* sp. cf. *birostris*; Marshall et al., 2009). While many planktivores are highly mobile and often undertake long-distance migrations related to foraging (Corkeron and Connor, 1999; Skomal et al., 2009), neither manta species has been shown to follow this trend, with recent data suggesting patterns of residency in both species (Deakos et al., 2011; Braun et al., 2014; Stewart et al., 2016). However, there are several recorded long-distance movements in both species of manta of over 400 km, which may be relevant to aspects of the species' life history or critical habitat use (Rubin et al., 2008; Germanov and Marshall, 2014; Hearn et al., 2014).

A more robust body of literature is available for the reef manta ray than the oceanic manta, and the diving and foraging patterns of other mobulids may provide insight into the most likely strategies exhibited by oceanic manta rays. Feeding on near-surface aggregations of zooplankton is commonly observed in a variety of mobulids (Notarbartolo di Sciara, 1988; Jaine et al., 2012; Paig-Tran et al., 2013). Some species also presumably forage in deep-water habitats, including prolific dives by *Mobula tarapacana* to access dense aggregations of bathypelagic fishes (Thorrold et al., 2014) and movements between shallow reef habitats and deep, offshore pelagic habitats by *Manta alfredi* (Braun et al., 2014). Additional studies suggest that deep nighttime dives made by reef manta rays may provide access to vertically migrating zooplankton entering the epipelagic zone (Anderson et al., 2011; Braun et al., 2014).

Here we report on the diving and foraging behavior of oceanic manta rays at the Revillagigedo Archipelago, a remote, pelagic archipelago in Pacific Mexico. We observed a coupling of surface and deep-water feeding areas and seasonal variation in diving behavior related to variation in thermocline depth. In addition we provide video evidence of daytime foraging at depth, in dense aggregations of zooplankton in close proximity to the sea floor. These data provide the first insights into diving patterns and habitat use of oceanic manta rays in pelagic environments.

2. Materials and methods

2.1. Archival tag deployments

We deployed miniPAT tags (Wildlife Computers, Redmond, WA, USA) on oceanic manta rays at San Benedicto Island (The Boiler) on April 7th, 2014 (female: $n = 3$; male: $n = 1$) and at Socorro Island (Cabo Pearce) on April 8th, 2014 (male: $n = 1$). We programmed miniPAT tags to detach and begin transmitting archived data after 180 days. Previously, we had deployed PAT Mk-10 tags (Wildlife Computers) on oceanic mantas at Roca Partida and San Benedicto (The Boiler) on November 12th and 13th, 2003, respectively ($n = 2$, sexes unknown). We programmed those Mk-10 tags to detach and begin transmitting after 60 and 150 days. Both tag models collect data on temperature, depth and light level at 5-second (miniPAT) and 5-minute (Mk-10) intervals, and subsequently transmit temperature and depth data histograms binned into preset intervals, as well as partial time-series data at coarse intervals via satellite after the tags detach. We programmed miniPATs to bin depth and temperature data in 6-hour intervals starting at midnight in Baja California Sur (GMT-6). We considered the combined 18:00–00:00 and 00:00–06:00 bins to represent nighttime hours, and the combined 06:00–12:00 and 12:00–18:00 bins to represent daytime hours. We programmed Mk-10 tags to bin data in 12-hour intervals starting at 00:00 and 12:00. We used PERMANOVAs (on 2014 data only; 'adonis' function in the R package 'vegan') to compare nighttime and daytime diving behavior between months. We considered the effect of month, night/day, and the interaction of these two terms on both depth and temperature distributions using the equation:

$$\text{Response variable} \sim \text{month} + \text{time of day} + \text{month} : \text{time of day}$$

where the response variable was either depth or temperature. We ordinated the binned depth and temperature data for plotting purposes using a non-parametric multidimensional scaling ('metaMDS' function in the R package 'vegan').

MiniPAT tags also collect, and report via satellite, data on the temperature and depth of the mixed layer. Archived temperature and depth samples are used to keep a running estimate of the mixed layer temperature. Subsequent samples are considered to be taken from within the mixed layer if the temperature reading is +/– 0.5 °C from the current estimate, and the depth is less than 200 m. The tag will automatically update its estimate of the mixed layer temperature if it encounters the surface, or if it detects water that is well mixed within 50 m of the surface. The surface is defined as any depth reading between 0 and 5 m. The water is considered well mixed if a change of depth of greater than 15 m is observed with a corresponding change in temperature of less than 0.05 °C (Wildlife Computers, pers. comm.). For example, if the tag records a sea surface temperature (SST) of 18 °C, this is initially set as the mixed layer temperature. If the tag then encounters a water temperature of 16 °C at 5 m depth, which extends to 20 m depth or greater, the mixed layer temperature is reset to 16 °C. The transmitted data include the range of SST readings observed, the range of the estimated mixed layer temperatures, the time spent within mixed layers, and the deepest depth recorded within the layer, over the 6-hour period. We only considered mixed layer depth records where the maximum diving depth of the tag exceeded the mixed layer depth for the same 6-hour period, and we interpreted the base of the mixed layer as the top of the thermocline. We sorted mixed layer depth records into bins with the same bounds as the diving histograms in order to directly compare histograms of the two datasets. We converted frequency histograms of mixed layer depths into percentages and overlaid them on diving histograms at a 0.1 x scale to create an inset (see Fig. 1). Not every 6-hour diving histogram period had a corresponding mixed layer depth due to gaps in satellite-transmitted data. We selected all of the diving histogram data that had a mixed layer depth from the same time period and the same tag, and determined the percentage of time spent in the depth bin containing the base of the mixed layer. We conducted all analyses using R version 3.2.3 (R Core Team, 2015).

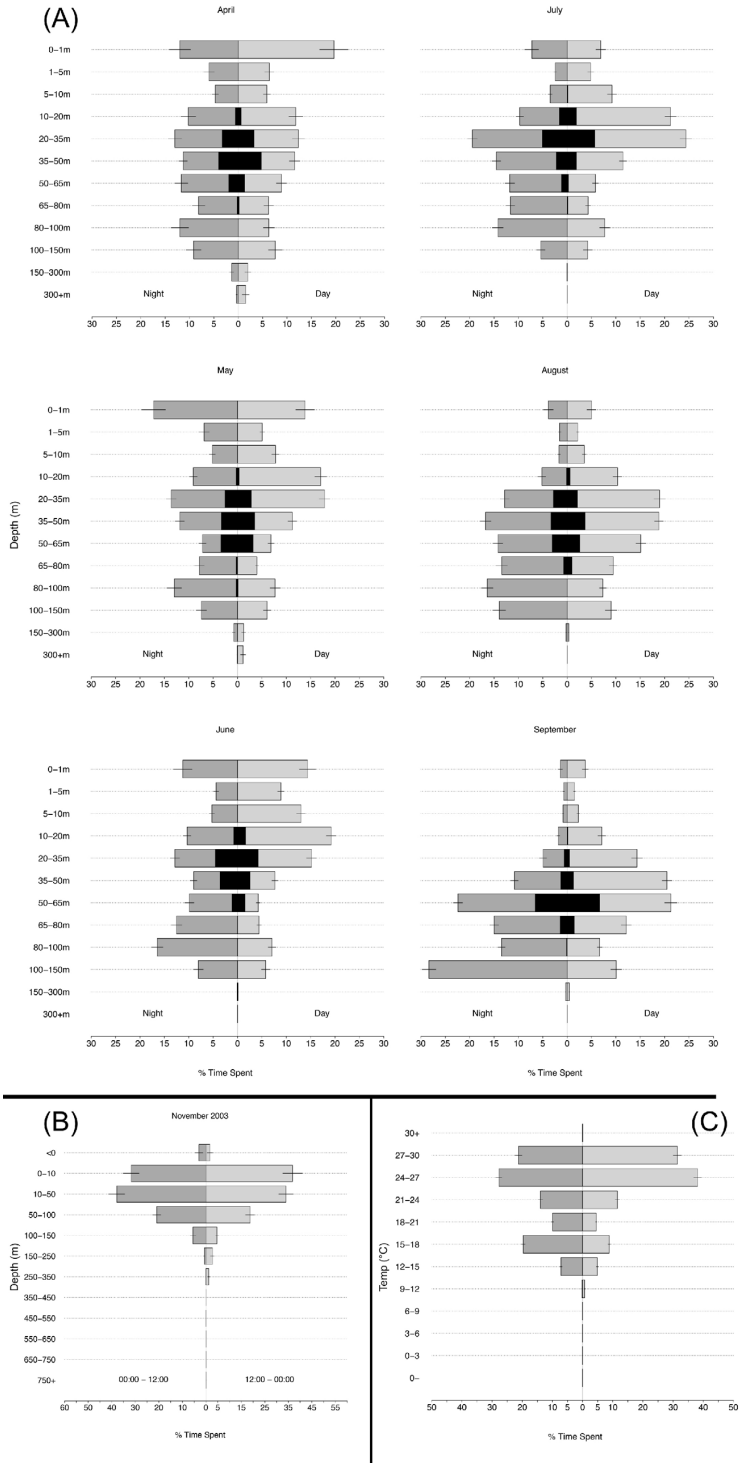

Fig. 1. (A) Depth distributions from four oceanic manta rays (combined) separated into nighttime and daytime periods, recorded by miniPAT tags deployed from April to September 2014 at the Revillagigedo Archipelago. Histogram bars represent mean values across all individuals in a given month, and error bars represent standard error. Inset black bars represent frequency histograms of mixed layer depth, separated into the same depth bins as diving data for ease of comparison. Mixed layer frequency histograms were converted to percentages and plotted as inset histograms at a 0.1× scale. For example, black bars at 5% represent 50% of mixed layer depth records in that binned depth range. (B) Depth distributions from two oceanic manta rays (combined) recorded by PAT Mk-10 tags deployed in November 2003 at the Revillagigedo Archipelago. (C) Temperature histograms recorded by miniPAT tags averaged across the entire tagging period (April to September 2014).

We reported horizontal movements recorded by miniPAT tags in Stewart et al. (2016).

Tagging methods were carried out in accordance with protocol S12116 approved by the University of California, San Diego Institutional Animal Care and Use Committee.

2.2. Submersible observations

During the *Televisa–Por el Planeta* expedition, project scientists made submersible dives around the islands of Roca Partida, San Benedicto and Socorro from March 6 to March 30, 2014 to survey the benthic assemblages of the Revillagigedo Archipelago. Over the 25 days, 34 submersible dives were conducted at Socorro Island (Bahia UNAM, $n = 1$; Cabo Pearce, $n = 11$; and Punta Tosca, $n = 10$), San Benedicto Island (The Canyon, $n = 10$), and Roca Partida ($n = 2$). During each dive, researchers recorded high-definition video to facilitate benthic and pelagic species identification and analysis of bottom fauna and substrate composition.

3. Results

3.1. Archival tagging

Both of the PAT Mk-10 tags deployed in 2003, and four of the five miniPAT tags deployed in 2014 (female: $n = 2$; male: $n = 2$) reported and transmitted data. The PAT Mk-10 tags both detached after 11 days, while the four miniPAT tags detached after 181, 184, 186 and 189 days. The distribution of depths accessed by animals tagged in 2014 varied across months, with a general trend of a greater proportion of time spent deeper as the tagging period progressed from April to September (Fig. 1A). PAT Mk-10 deployments are summarized in Fig. 1B. Both depth and temperature utilization were significantly different between night and day and between months, and the interaction of those effects was also statistically significant ($p < 0.001$ in all cases). After the depth and temperature data are ordinated, the months of April–June and August–September form distinctive clusters, with no overlap between those groups on the ordination axis 1 (NMDS1; supplementary Figs. S1 and S2 in the online Appendix. This multidimensional separation is highlighted by the differences in diving behavior between the months of April–June and August–September, with April–June showing a greater proportion of time spent at the surface, and August-September showing a greater proportion of time spent in deeper water (Fig. 1A). July appears to be an intermediate month, overlapping with both the April–June cluster and August–September cluster in NMDS1 for diving data (supplementary Fig. S1, but clustering with August–September on the temperature data ordination (supplementary Fig. S2. For both depth and temperature data, the ordinated centroids of night and day bins are well separated both within months and for all months combined (supplementary Figs. S1 and S2).

There were 741 out of 1,367 diving histograms that had an associated mixed layer depth record from the same time, date and tag. Tagged mantas spent, on average, 11.33–21.64 percent of their time in the depth bins containing the base of the mixed layer (also interpreted as the start of the thermocline) during daytime hours, and 9.65–21.24 percent during nighttime hours per month. These data are reported by month in Table 1.

The tag deployments in November 2003 summarized diving data into very different histogram bins than the 2014 tag deployments and recorded data during 12-hour periods that covered daytime and nighttime hours approximately evenly (midnight to noon and noon to midnight). The November 2003 diving data indicate that mantas spent on average over 90% of their time in the top 100 m of the water column. Furthermore, the proportion of time spent in the 0–10 m, 10–50 m, and 50–100 m bins in 2003 are more similar to the months of April–June than to July–September 2014, although we emphasize that these data sources are not directly comparable due to the differences in temporal and depth binning.

Table 1
Percentage of time spent by tagged mantas in the same depth bin as the base of the mixed layer, which we considered a proxy for the location of the thermocline.

Month	% Time (Day)	SD (Day)	% Time (Night)	SD (Night)
April	13.01	8.13	15.29	8.95
May	11.33	6.87	9.65	6.66
June	11.51	6.78	10.46	6.66
July	19.60	10.34	18.25	8.59
August	19.80	8.34	16.80	9.51
September	21.64	10.12	21.24	8.95

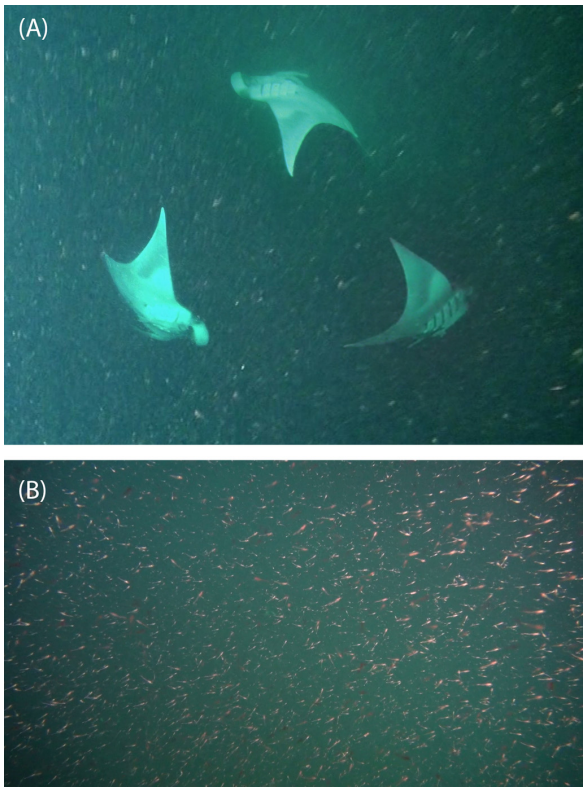

Fig. 2. (A) An oceanic manta ray performs barrel rolls to forage on zooplankton prey in an epipelagic scattering layer. Photo illustration created from three video frame grabs. Footage was captured from a submersible at 11:22 a.m. in 130–140 m depth. The full video is available as supplementary content in the online Appendix. (B) Close-up of prey in aggregation at the time of feeding, made up of mysid shrimp, calanoid copepods, euphausiids and other zooplankton. Video was taken on the *Televisa-Por el Planeta* expedition.

3.2. Submersible observations

On March 29th, 2014 at 11:22 a.m., E.M. Hoyos-Padilla recorded an oceanic manta ray foraging on a thick layer of zooplankton at 130–140 m depth (Fig. 2 and supplementary Video 1 in the online Appendix off of Cabo Pearce (Socorro Island) (Fig. 3). The manta had its cephalic fins fully extended, its mouth open, and its oral cavity expanded. Furthermore, it was making continuous somersaults through the zooplankton layer at depth, consistent with feeding strategies observed in both members of the Manta genus (Couturier

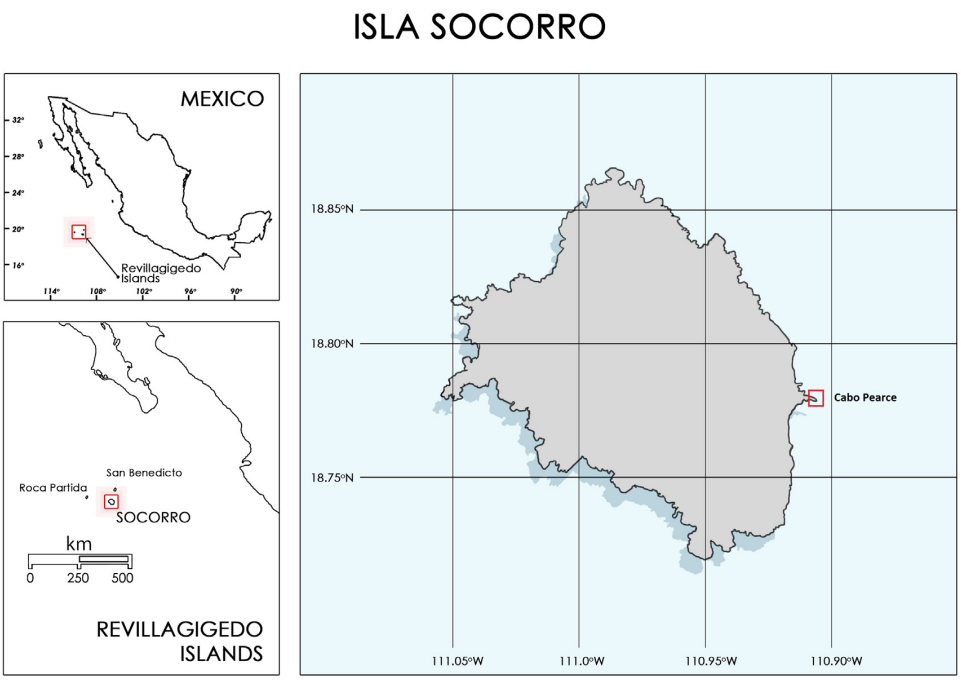

Fig. 3. A map of the Revillagigedo Archipelago with a detail on Cabo Pearce, on the island of Socorro, where the deep-water foraging was observed from a submersible and one PSAT was deployed. Additional tags were deployed at San Benedicto and Roca Partida.

et al., 2012). We identified mysid shrimp (Mysidae), euphausiids (Euphausiacea), and copepods (Calanoida) in the zooplankton layer, as well as a variety of other unidentifiable zooplanktors. We note that visual identification was challenging from the video, especially in differentiating between mysids and euphausiids. The zooplankton layer was approximately 10 m above the sea floor (supplementary Video 2 in the online Appendix.

4. Discussion

Based on our results, oceanic manta rays demonstrate a high degree of plasticity in the depths they access throughout the year, and we posit that this is driven primarily by shifts in prey location and foraging behaviors. The most consistent pattern across the six months of diving data in 2014 was the close relationship between mixed layer depths and the depth ranges most frequently accessed by mantas. As the tag-recorded mixed layer depths shift from month to month, the most commonly accessed depths closely match these changes (Fig. 1). Zooplankton density is often greatest at the thermocline, which begins at the base of the mixed layer (Sameoto, 1984, 1986). This aggregation of zooplankton within the thermocline can be made up of zooplankton that remains within the thermocline day and night, or vertical migrators that enter the thermocline only at night (Sameoto, 1986). We speculate that oceanic mantas are foraging on zooplankton within the thermocline throughout the year, both during the day and night, and may be using the thermocline as a cue to identify regions of high zooplankton density where foraging efficiency can be maximized (Pelletier et al., 2012).

In April and May, nighttime depth utilization closely resembled daytime behavior, while from June through September tagged individuals accessed deeper waters at night. While studies reporting on the seasonal density and distribution of zooplankton in this region are sparse in the literature, the available data (Blackburn et al., 1970) indicate that the input of vertical migrators into the top 200 m of the water column is minimal in April and May, but increases from June to September and throughout the rest of the year. This could explain the shift to deeper nighttime diving from June onwards in our tag data, as mantas increasingly access portions of the deep scattering layer at its shallow extreme. Despite the differences in histogram bins between 2003 and 2014 tag deployments, based on the similarity of the November 2003 diving data to those of the months of April through June in 2014, it is possible that the deeper diving behavior of mantas is restricted to the summer months, while individuals spend more time in near-surface waters from November through June. However, this inference carries the obvious limitation that these two sets of tags were deployed more than ten years apart, and inter-annual variability in local and regional oceanography may be responsible for the change in depth distribution from September (2014) to November (2003) rather than seasonal patterns in diving behavior.

During April and May, tagged mantas spent over 15% of their time on average (night and day combined) in the top meter of the water column. This time spent immediately at the surface could be attributed to either surface feeding (Notarbartolo di Sciara, 1988; Paig-Tran et al., 2013) or basking behavior (Notarbartolo di Sciara, 1987; Canese et al., 2011; Thorrold et al., 2014) both frequently observed in mobulids. *M. tarapacana* accessing depths of up to 1,800 m and temperatures lower than 5 °C frequently basked for extended periods at the surface before and after deep dives, presumably to recover body temperatures after long periods in cold water (Thorrold et al., 2014). Our diving data, on the other hand, show that tagged mantas spent more time at the surface in months with less deep diving behavior, and less time at the surface in months with more deep diving behavior. If mantas were basking at the surface after exposure to colder water temperatures, we would expect basking and deep dives to occur concurrently. Further, mantas spent a large portion of their time at the surface in

these months both during the night and day, whereas *M. tarapacana* only exhibited basking behavior during daytime hours. It is possible that oceanic mantas in this study did not require active thermoregulation in the form of basking because they rarely accessed waters colder than 15 °C. Instead, we posit that the surface time represents foraging behavior on surface zooplankton, which is often observed at the Revillagigedo Archipelago (Rubin et al., unpublished data). The shift throughout the tagging period away from surface activity and towards deeper diving suggests that mantas may have switched from surface feeding to foraging on the deep scattering layer as the nighttime influx of vertical migrators became more regular or the density of zooplankton increased. If our interpretations of the observed diving behavior are correct, the mantas tagged in this study exhibited three distinct foraging patterns that shifted across seasons: foraging (i) at the surface; (ii) in the thermocline; and (iii) on vertical migrators at depths over 100 m. This demonstrates a high degree of behavioral plasticity to account for the shifts in location and/or abundance of prey resources.

The major limitation of the present study and all other attempts to infer behavior from tag-recorded diving data is the lack of direct behavioral observations. Without direct observations, we are limited to interpreting diving data in relation to covariates that we expect to be meaningful, such as zooplankton location and density. These interpretations are further hindered by the paucity of zooplankton time-series data in the region and lack of zooplankton data collected during the tagging period, both of which are unsurprising given the remoteness of the study site and difficulty in conducting fieldwork there. Our observations could be supported by future research examining the isotopic signatures of putative sources (e.g. surface zooplankton, deep scattering layer zooplankton, etc.) and the relative contribution of these sources to manta tissue isotopic signatures at the islands (e.g. Couturier et al., 2013; McCauley et al., 2014).

Given the absence of direct observations during the tagging period, the opportunistic submersible observation described here is of significant value. While oceanic manta rays, and a variety of other mobulid rays, have been observed feeding on zooplankton in surface and near-surface waters (Notarbartolo di Sciara, 1988; Paig-Tran et al., 2013) and presumably recorded feeding in bathypelagic zones (Thorrold et al., 2014), this is the first direct observation of a mobulid ray foraging at depth. During the submersible observation, the manta ray made continuous barrel rolls, apparently circling repeatedly through the densest area of zooplankton. The morphological adaptations of mobulid gill plates that facilitate cross-flow filtration allow them to retain a variety of particle sizes, even those smaller than the filter pores (Paig-Tran et al., 2013). This mechanism may enable mantas to efficiently feed on mixed zooplankton assemblages such as the one we observed, where prey items range in size from larger mysids and euphausiids to much smaller calanoid copepods. While barrel-rolling behavior is observed frequently in near-surface waters, our observation confirms that this foraging strategy is also exhibited at depth. Diving to depths of 100–150 m, which would include the observed manta feeding at 130–140 m, made up on average only 5–10% of daytime water column use during the tagging period. This suggests that either (i) the observed behavior represented opportunistic or infrequent foraging; or (ii) this type of behavior is more frequent in March and earlier months when no tag data were collected. We do not believe this was an observation of foraging on zooplankton within the thermocline, as the mixed layer depth rarely exceeded 80 m and never 100 m. Thus, this represents a fourth feeding strategy: daytime foraging on epipelagic scattering layers or aggregations of zooplankton.

Tag-recorded diving data, an opportunistic observation from a submersible, and personal observations by the authors of mantas surface-feeding suggest that manta rays are accessing prey resources in a variety of different habitats at the islands by employing several foraging strategies. The horizontal movement data from tags deployed in 2014, along with stable isotope and genetic analyses, indicate that oceanic manta rays at the Revillagigedo Archipelago exhibit philopatry and remain resident to a restricted geographic region surrounding the archipelago (Stewart et al., 2016). This is in contrast to other large marine vertebrates, including planktivores, that inhabit similar oceanic habitats and often undertake extensive migrations between breeding and foraging grounds (Corkeron and Connor, 1999; Hueter et al., 2013; Thorrold et al., 2014). In the Tropical Eastern Pacific near the Revillagigedo Archipelago, the standing stock of zooplankton in the upper 200 m remains largely consistent throughout the year (Blackburn et al., 1970), potentially providing a year-round food source and contributing to the observed philopatry by making long-distance movements to access prey unnecessary. However, accessing this year-round food supply may require frequent changes in diving behavior and habitat use in order to target resources that shift seasonally in vertical distribution. These shifts in diving behavior and vertical habitat use may also be related to horizontal, onshore–offshore movements across the study period. However, due to the substantial uncertainty in light-based geolocation from this type of archival tag (in many cases estimated locations have an error radius of 50–100 km), it was not possible for us to separate nearshore and pelagic diving patterns. However, acoustic tagging data from the islands (Rubin, unpublished data) demonstrate that mantas generally leave the near-shore habitats during late afternoon and nighttime hours, presumably entering more offshore, pelagic habitats. This may explain the differences between daytime and nighttime diving patterns in some months, as mantas may need to move into deeper waters to access vertically migrating zooplankton at night. Recent improvements to tagging technology, such as the addition of Fastloc GPS that has an accuracy on the scale of tens of meters (Dujon et al., 2014), could help determine the horizontal component of seasonal shifts in diving behavior in future studies.

Oceanic manta rays are threatened by both targeted fisheries and incidental bycatch, and the conservative reproductive strategy of the species makes populations extremely susceptible to fisheries-induced declines (Dulvy et al., 2014; White et al., 2015). Understanding spatial and temporal changes in habitat use can help prevent bycatch of the species, as the various fishing gears and strategies that incidentally capture mantas target different depth ranges. For example, the population of mantas studied here would be far more susceptible to surface-set gill nets, one of the primary gear types associated with manta and mobula bycatch (Couturier et al., 2012), between April and June than between July and September. Similarly, bycatch of mantas in midwater trawls from 50 to 150 m, observed in the Peruvian Merluza fishery (S. Rojas Perea, pers. comm.), would be much more likely to occur during months in which mantas are more frequently accessing those depths. Consequently, region-specific data on diving behavior can help inform local management strategies designed to reduce or mitigate bycatch of this vulnerable species. At the Revillagigedo Archipelago, the high density of recreational dive boats present from November through June may present additional threats to the manta population. Many dive operators use down-lines to provide easy descents to dive sites, and mantas occasionally become entangled in these lines as well as lines connected to divers' surface marker buoys, causing severe injuries (E.M. Hoyos-Padilla, pers. obs.). Our data indicate that mantas spend a large proportion of their time near the surface, where they are likely most susceptible to entanglement in these down lines, from April to June, and perhaps starting again in November. Personal observations by the authors further indicate that mantas are present in near-surface waters from November through June. Additional tag-

ging data across the entire year would help determine the relative threat of entanglements to mantas in different seasons.

Marine science is increasingly dominated by data collected by remote instrumentation, from global-level environmental data to individual-level movement data such as those presented here. As these data become removed from direct observations, it can be challenging to interpret them in an ecological or behavioral context. Tagging data in marine systems, in particular, have the limitation of showing us where an animal goes, but not what it is doing. Direct observations of behavior that is unusual or that takes place in hard-to-reach environments aid in the interpretation of remotely-sensed data and allow us to, in effect, ground-truth our assumptions about how marine species are using various habitats. Improvements and breakthroughs in technology such as accelerometers and photographic and video imaging built into animal-mounted tags can improve our understanding of marine ecology and individual behaviors. In the case of oceanic manta rays, future work employing both novel and existing technology, such as short-deployment animal-mounted cameras, will provide a better understanding of habitat use, foraging and natural history of the species.

Acknowledgements

This study was funded by grants from The New England Aquarium Marine Conservation Action Fund, sponsorship from Carl F. Bucherer Watchmakers, and donations from David Connell, Mary O'Malley and Lupo Dion. The submersible expedition was funded by Televisa, Aeromexico and Grupo Nacional Provincial (Documentary: *Por el Planeta*). Research activities were made possible by the Gulf of California Marine Program and the Mexican National Commission for Protected Areas. Both expeditions were greatly facilitated through assistance by the personnel of the Secretaria del Medio Ambiente y Recursos Naturales (SEMARNAT), the Comision de Areas Naturales Protegidas (CONANP), and the Mexican Navy (SEMAR) under the scientific permits issued by CONANP (F00.DRPBCPN.-000211/13), SEMARNAT (FAUT 0265) and SAGARPA (Oficio No. DGOPA.06668.150612.1691). J.D.S. was supported in part by a NOAA ONMS Nancy Foster Scholarship (NA15NOS4290068). This material is based in part upon work supported by the National Science Foundation Graduate Research Fellowship under Grant No. DGE-1144086 to J.D.S. Any opinions, findings, and conclusions or recommendations expressed in this material are those of the authors and do not necessarily reflect the views of the National Science Foundation.

Appendix A. Supplementary data

Supplementary data associated with this article can be found, in the online version, at http://dx.doi.org/10.1016/j.zool.2016.05.010.

References

Anderson, R.C., Adam, M.S., Goes, J.I., 2011. From monsoons to mantas: seasonal distribution of *Manta alfredi* in the Maldives. Fish. Oceanogr. 20, 104–113.

Blackburn, M., Laurs, R.M., Owen, R.W., Zeiyzschel, B., 1970. Seasonal and areal changes in standing stocks of phytoplankton: zooplankton and micronekton in the eastern tropical Pacific. Mar. Biol. 7, 14–31.

Braun, C.D., Skomal, G.B., Thorrold, S.R., Berumen, M.L., 2014. Diving behavior of the reef manta ray links coral reefs with adjacent deep pelagic habitats. PLoS One 9, e88170.

Canese, S., Cardinali, A., Romeo, T., Giusti, M., Salvati, E., Angiolillo, M., Greco, S., 2011. Diving behavior of the giant devil ray in the Mediterranean Sea. Endanger. Species Res. 14, 171–176.

Compagno, L., 1999. Systematics and body form. In: Hamlett, W.C. (Ed.), Sharks, Skates and Rays: The Biology of Elasmobranch Fishes. Johns Hopkins University Press, Baltimore, pp. 1–42.

Corkeron, P.J., Connor, R.C., 1999. Why do baleen whales migrate? Mar. Mammal Sci. 15, 1228–1245.

Couturier, L.I.E., Marshall, A.D., Jaine, F.R.A., Kashiwagi, T., Pierce, S.J., Townsend, K.A., Weeks, S.J., Bennett, M.B., Richardson, A.J., 2012. Biology, ecology and conservation of the Mobulidae. J. Fish Biol. 80, 1075–1119.

Couturier, L.I.E., Rohner, C.A., Richardson, A.J., Marshall, A.D., Jaine, F.R.A., Bennett, M.B., Townsend, K.A., Weeks, S.J., Nichols, P.D., 2013. Stable isotope and signature fatty acid analyses suggest reef manta rays feed on demersal zooplankton. PLoS One 8, e77152.

Croll, D.A., Dewar, H., Dulvy, N.K., Fernando, D., Francis, M.P., Galvan-Magana, F., Hall, M., Heinrichs, S., Marshall, A., McCauley, D., Newton, K.M., Notarbartolo-Di-Sciara, G., O'Malley, M., O'Sullivan, J., Poortvliet, M., Roman, M., Stevens, G., Tershy, B.R., White, W.T., 2015. Vulnerabilities and fisheries impacts: the uncertain future of manta and devil rays. Aquat. Conserv. Mar. Freshw. Ecosyst., http://dx.doi.org/10.1002/aqc.2591.

Deakos, M.H., Baker, J.D., Bejder, L., 2011. Characteristics of a manta ray *Manta alfredi* population off Maui, Hawaii, and implications for management. Mar. Ecol. Prog. Ser. 429, 245–260.

Dujon, A.M., Lindstrom, R.T., Hays, G.C., 2014. The accuracy of Fastloc-GPS locations and implications for animal tracking. Methods Ecol. Evol. 5, 1162–1169.

Dulvy, N.K., Pardo, S.A., Simpfendorfer, C.A., Carlson, J.K., 2014. Diagnosing the dangerous demography of manta rays using life history theory. PeerJ 2, e400.

Friedlaender, A.S., Halpin, P.N., Qian, S.S., Lawson, G.L., Wiebe, P.H., Thiele, D., Read, A.J., 2006. Whale distribution in relation to prey abundance and oceanographic processes in shelf waters of the Western Antarctic Peninsula. Mar. Ecol. Prog. Ser. 317, 297–310.

Germanov, E.S., Marshall, A.D., 2014. Running the gauntlet: regional movement patterns of *Manta alfredi* through a complex of parks and fisheries. PLoS One 9, e110071.

Graham, R.T., Witt, M.J., Castellanos, D.W., Remolina, F., Maxwell, S., Godley, B.J., Hawkes, L.A., 2012. Satellite tracking of manta rays highlights challenges to their conservation. PLoS One 7, e36834.

Hearn, A.R., Acuna, D., Ketchum, J.T., Penaherrera, C., Green, J., Marshall, A., Guerrero, M., Shillinger, G., 2014. Elasmobranchs of the Galapagos Marine Reserve. In: Denkinger, J., Vinueza, L. (Eds.), The Galapagos Marine Reserve: A Dynamic Social-Ecological System. Springer, New York, pp. 23–59.

Hueter, R.E., Tyminski, J.P., de la Parra, R., 2013. Horizontal movements, migration patterns, and population structure of whale sharks in the Gulf of Mexico and northwestern Caribbean Sea. PLoS One 8, e71883.

Jaine, F.R., Couturier, L.I.E., Weeks, S.J., Townsend, K.A., Bennett, M.B., Fiora, K., Richardson, A.J., 2012. When giants turn up: sighting trends, environmental influences and habitat use of the manta ray *Manta alfredi* at a coral reef. PLoS One 7, e46170.

James, M.C., Sherrill-Mix, S.A., Martin, K., Myers, R.A., 2006. Canadian waters provide critical foraging habitat for leatherback sea turtles. Biol. Conserv. 133, 347–357.

Kashiwagi, T., Marshall, A.D., Bennett, M.B., Ovenden, J.R., 2011. Habitat segregation and mosaic sympatry of the two species of manta ray in the Indian and Pacific Oceans: *Manta alfredi* and *M. birostris* –CORRIGENDUM. Mar. Biodivers. Rec. 4, e86, http://dx.doi.org/10.1017/S1755267211000881.

Lewis, S.A., Nanen, S., Dharmadi, F., O'Malley, M.P., Campbell, S.J., Yusuf, M., Sianipar, A., 2015. Assessing Indonesian manta and devil ray populations through historical landings and fishing community interviews. PeerJ PrePrints 3, e1642.

Marshall, A.D., Compagno, L.J.V., Bennett, M.B., 2009. Redescription of the genus *Manta* with resurrection of *Manta alfredi*. Zootaxa 28, 1–28.

McCauley, D.J., DeSalles, P.A., Young, H.S., Papastamatiou, Y.P., Caselle, J.E., Deakos, M.H., Gardner, J.P.A., Garton, D.W., Collen, J.D., Micheli, F., 2014. Reliance of mobile species on sensitive habitats: a case study of manta rays (*Manta alfredi*) and lagoons. Mar. Biol. 161, 1987–1998.

McEachran, J., Aschliman, N., 2004. Phylogeny of Batoidea. In: Carrier, J., Musick, J., Heithaus, M. (Eds.), Biology of Sharks and Their Relatives. CRC Press, New York, pp. 79–113.

Menge, B.A., 1972. Competition for food between two intertidal starfish species and its effect on body size and feeding. Ecology 53, 635–644.

Notarbartolo di Sciara, G., 1987. A revisionary study of the genus *Mobula* Rafinesque, 1810 (Chondrichthyes: Mobulidae) with the description of a new species. Zool. J. Linn. Soc. 91, 1–91.

Notarbartolo di Sciara, G., 1988. Natural history of the rays of the genus *Mobula* in the Gulf of California. Fish. Bull. 86, 45–66.

Paig-Tran, E.W.M., Kleinteich, T., Summers, A.P., 2013. The filter pads and filtration mechanisms of the devil rays: variation at macro and microscopic scales. J. Morphol. 274, 1026–1043.

Pastene, L.A., Goto, M., Kanda, N., Zerbini, A.N., Kerem, D., Watanabe, K., Bessho, Y., Hasegawa, M., Nielsen, R., Larsen, F., Palsbøll, P.J., 2007. Radiation and speciation of pelagic organisms during periods of global warming: the case of the common minke whale, *Balaenoptera acutorostrata*. Mol. Ecol. 16, 1481–1495.

Pelletier, L., Kato, A., Chiaradia, A., Ropert-Coudert, Y., 2012. Can thermoclines be a cue to prey distribution for marine top predators? A case study with little penguins. PLoS One 7, 4–8.

Poortvliet, M., Olsen, J.L., Croll, D.A., Bernardi, G., Newton, K., Kollias, S., O'Sullivan, J., Fernando, D., Stevens, G., Galván Magaña, F., Seret, B., Wintner, S., Hoarau, G., 2015. A dated molecular phylogeny of manta and devil rays (Mobulidae) based on mitogenome and nuclear sequences. Mol. Phylogenet. Evol. 83, 72–85.

R Core Team, 2015. R: A Language and Environment for Statistical Computing. R Foundation for Statistical Computing, Vienna, Austria https://r-project.org.

Rubin, R., Kumli, K., Chilcott, G., 2008. Dive characteristics and movement patterns of acoustic and satellite-tagged manta rays (*Manta birostris*) in the Revillagigedos Islands of Mexico. In: Joint Meeting of Ichthyologists and Herpetologists, Montreal, Canada, Abstract 0318, http://www.asih.org/meetingabstracts2008.

Sameoto, D.D., 1984. Vertical distribution of zooplankton biomass and species in northeastern Baffin Bay related to temperature and salinity. Polar Biol. 2, 213–224.

Sameoto, D.D., 1986. Influence of the biological and physical environment on the vertical distribution of mesozooplankton and micronekton in the eastern tropical Pacific. Mar. Biol. 93, 263–279.

Skomal, G.B., Zeeman, S.I., Chisholm, J.H., Summers, E.L., Walsh, H.J., McMahon, K.W., Thorrold, S.R., 2009. Transequatorial migrations by basking sharks in the western Atlantic Ocean. Curr. Biol. 19, 1019–1022.

Stewart, J.D., Beale, C.S., Fernando, D., Sianipar, A.B., Burton, R.S., Semmens, B.X., Aburto-Oropeza, O., 2016. Spatial ecology and conservation of *Manta birostris* in the Indo-Pacific. Biol. Conserv. 200, 178–183.

Suryan, R.M., Irons, D.B., Benson, J., 2000. Prey switching and variable foraging strategies of black-legged kittiwakes and the effect on reproductive success. Condor 102, 374–384.

Thorrold, S.R., Afonso, P., Fontes, J., Braun, C.D., Santos, R.S., Skomal, G.B., Berumen, M.L., 2014. Extreme diving behaviour in devil rays links surface waters and the deep ocean. Nat. Commun. 5, 4274, http://dx.doi.org/10.1038/ncomms5274.

Ward-Paige, C.A., Davis, B., Worm, B., 2013. Global population trends and human use patterns of *Manta* and *Mobula* rays. PLoS One 8, e74835.

White, E.R., Myers, M.C., Flemming, J.M., Baum, J.K., 2015. Shifting elasmobranch community assemblage at Cocos Island – an isolated marine protected area. Conserv. Biol. 29, 1186–1197.

Chapter 2, in full, is a reprint of the material as it appears in Zoology 2016. Stewart, J.D., Hoyos-Padilla, O.M., Kumli, K., Rubin, R.D. The dissertation author was the primary investigator and author of this material.

CHAPTER 3:

Trophic overlap in mobulid rays: insights from stable isotope analysis

JOSHUA D. STEWART, CHRISTOPH A. ROHNER, GONZALO ARAUJO, JOSE AVILA, DANIEL FERNANDO, KERSTIN FORSBERG, ALESSANDRO PONZO, JOSHUA M. RAMBAHINIARISON, CAROLYN M. KURLE, BRICE X. SEMMENS

Vol. 580: 131–151, 2017
https://doi.org/10.3354/meps12304

MARINE ECOLOGY PROGRESS SERIES
Mar Ecol Prog Ser

Published September 29

Trophic overlap in mobulid rays: insights from stable isotope analysis

Joshua D. Stewart[1,2,*], Christoph A. Rohner[3], Gonzalo Araujo[4], Jose Avila[5], Daniel Fernando[2,6,7], Kerstin Forsberg[5], Alessandro Ponzo[4], Joshua M. Rambahiniarison[4], Carolyn M. Kurle[8], Brice X. Semmens[1]

[1]Scripps Institution of Oceanography, University of California San Diego, La Jolla, CA 92093, USA
[2]The Manta Trust, Dorset DT2 0NT, UK
[3]Marine Megafauna Foundation, Praia do Tofo, Inhambane, Mozambique
[4]Large Marine Vertebrates Research Institute Philippines, Jagna, Bohol 6308, Philippines
[5]Planeta Oceano, Lima 15074, Peru
[6]Department of Biology and Environmental Science, Linnaeus University, Kalmar 39182, Sweden
[7]Blue Resources Trust, Colombo 00700, Sri Lanka
[8]Division of Biological Sciences, University of California San Diego, La Jolla, CA 92093, USA

ABSTRACT: Mobulid rays, a group of closely related filter-feeders, are threatened globally by bycatch and targeted fisheries. Their habitat use and feeding ecology are not well studied, and most efforts have focused on temporally limited stomach content analysis or inferences from tagging data. Previous studies demonstrate a variety of different diving behaviors across species, which researchers have interpreted as evidence of disparate foraging strategies. However, few studies have examined feeding habitats and diets of multiple mobulid species from a single location, and it is unclear if the proposed differences in diving and inferred foraging behavior are examples of variability between species or regional adaptations to food availability. Here, we use stable isotope data from mobulids landed in fisheries to examine the feeding ecology of 5 species at 3 sites in the Indo-Pacific. We use Bayesian mixing models and analyses of isotopic niche areas to demonstrate dietary overlap between sympatric mobulid species at all of our study sites. We show the degree of overlap may be inversely related to productivity, which is contrary to prevailing theories of niche overlap. We use isotope data from 2 tissues to examine diet stability of *Manta birostris* and *Mobula tarapacana* in the Philippines. Finally, we observe a significant but weak relationship between body size and isotope values across species. Our findings highlight challenges to bycatch mitigation measures for mobulid species and may explain the multi-species mobulid bycatch that occurs in a variety of fisheries around the world.

KEY WORDS: Niche overlap · Mixing model · Feeding ecology · Bycatch risk

INTRODUCTION

Mobulid rays are a group of closely related, highly derived filter-feeders that, in many cases, have overlapping habitats and geographic distributions (Couturier et al. 2012). Periods of cladogenesis within the Mobulidae coincide with periods of global warming, and speciation within the family has occurred as recently as within the last million years (Kashiwagi et al. 2012, Poortvliet et al. 2015). Hypotheses for the drivers of these speciation events include fragmentation of productive upwelling environments and reduced food availability during extended periods of global warming, and physical barriers to dispersal and connectivity during ice ages (Poortvliet et al. 2015). The most recently diverged mobulid species

*Corresponding author: j8stewart@ucsd.edu

shows evidence of hybridization (Walter et al. 2014), suggesting that differences in behavior and habitat use, as opposed to geographic isolation, may be the primary factors driving and maintaining speciation (Kashiwagi et al. 2011, 2012).

Over the past decade, demand for mobulid gill plates in Asian medicine has led to targeted fisheries and increased bycatch retention of mobulid rays (Couturier et al. 2012). While these growing targeted fisheries have catalyzed focused conservation and scientific attention for mobulids (Ward-Paige et al. 2013, White et al. 2015, Lewis et al. doi:10.7287/peerj.preprints.1334v1), bycatch of these species likely impacted populations long before large-scale targeted fisheries began. Mobulid rays are vulnerable to incidental capture in gill nets, purse seines, trawls, and even long lines (Croll et al. 2016). Moreover, their low annual reproductive output and conservative demographic characteristics make them highly susceptible to fisheries-induced population declines (Dulvy et al. 2014, Pardo et al. 2016), even when catch rates are low. Understanding horizontal and vertical habitat use, which are likely driven by foraging in many cases, can help determine when mobulid rays are most vulnerable to incidental capture in fisheries and can aid in the development of bycatch mitigation measures (Stewart et al. 2016b).

Several studies have examined the horizontal and vertical movements of mobulid rays using satellite telemetry (Canese et al. 2011, Croll et al. 2012, Braun et al. 2014, Jaine et al. 2014, Thorrold et al. 2014, Stewart et al. 2016b), and others have used direct observations to identify feeding patterns and prey sources (Notarbartolo di Sciara 1988). The results of these studies demonstrate differences in habitat use (e.g. Croll et al. 2012, Thorrold et al. 2014), vertical movements (e.g. Canese et al. 2011, Croll et al. 2012, Braun et al. 2014, Jaine et al. 2014, Thorrold et al. 2014, Stewart et al. 2016b), and in some cases prey sources between mobulid species (Notarbartolo di Sciara 1988). However, few studies have examined the feeding ecology of multiple mobulid species in a given region or within a single species at multiple locations (see Notarbartolo di Sciara 1988, Sampson et al. 2010). Consequently, it remains unclear whether the observed differences in foraging behavior and habitat use are consistent between species or simply a result of regional variations in resource availability. Armstrong et al. (2016) demonstrated that mantas require zooplankton to reach threshold densities before feeding becomes energetically profitable, and therefore regional patterns in prey availability could conceivably have a greater influence on mobulid feeding behavior than morphological and behavioral differences between species.

Researchers are increasingly using stable isotope analysis as a tool for inferring the trophic ecology of animals, providing insight into trophic niche separation (Cherel et al. 2007, Plass-Johnson et al. 2013), trophic overlap (Foley et al. 2014, Jackson et al. 2016), diet composition (Semmens et al. 2009), and diet shifts (Ben-David et al. 1997, MacNeil et al. 2005). Stable isotopes of carbon ($\delta^{13}C$) and nitrogen ($\delta^{15}N$) are 2 of the most commonly used isotopes in ecological studies, as they can provide information on feeding locations and prey types due to predictable changes in $\delta^{13}C$ across habitats (France 1995) and increases in $\delta^{15}N$ at higher trophic levels (Owens 1987). Importantly, the use of stable isotopes to infer trophic dynamics requires a number of experimentally validated parameters, including fractionation and tissue incorporation rates (Gannes et al. 1997), which can be challenging to obtain for species that are not easily studied in a laboratory setting. Further, factors such as diet composition, body condition, organism size, and metabolic rate can influence isotopic incorporation, and few studies have explicitly examined these effects (Gannes et al. 1997, Newsome et al. 2010). While acknowledging these limitations, isotope analysis is particularly useful in marine species, as it can provide a large temporal window into the diet of animals that are otherwise challenging to observe in the wild for long periods (e.g. MacNeil et al. 2005, Cherel et al. 2007). In most regions, mobulid rays are present sporadically and unreliably at sites accessible by researchers, making direct observations challenging (Couturier et al. 2012). With the exception of coastally associated reef manta rays (e.g. Anderson et al. 2011, Jaine et al. 2012) and occasional opportunistic observations (e.g. Stewart et al. 2016b), direct observations of feeding behavior in mobulids are rare and largely restricted to surface feeding and daylight hours, complicating efforts to characterize the trophic ecology of this family. These characteristics make stable isotope analysis a powerful tool for studying the trophic ecology of mobulid rays.

In this study, we examine the trophic ecology and isotopic niche separation of 5 species of mobulid rays using stable isotope analysis. We use a Bayesian mixing model to assess the diet contribution of prey sources identified and sampled from stomach contents at 1 study site, and we compare the isotopic niche areas and isotopic niche separation between species and across regions. We use samples collected from fisheries landings at 3 sites throughout the Indo-

Pacific to examine how resource partitioning may change across regions with varying productivity and resource availability.

MATERIALS AND METHODS

Study sites and sample collection

Our study sites included (1) the coast of northern Peru, (2) Sri Lanka, and (3) the Bohol Sea in the Philippines (Fig. 1). We analyzed muscle samples from 5 species of mobulid rays (4 species per site) from Peru (n = 46), the Philippines (n = 192), and Sri Lanka (n = 102) and liver samples from 2 species in the Philippines (n = 30) (Table 1).

Peru

In Peru, we collected skeletal muscle samples of *Manta birostris* (n = 3), *Mobula japanica* (n = 20), *Mobula munkiana* (n = 18), and *Mobula thurstoni* (n = 5) at landing sites throughout the Tumbes region, in the north of the country, from August 2012 through May 2013. Fishers typically caught mobulid rays within approximately 10 to 30 km of shore (over the continental shelf) as non-discarded bycatch in purse seines and gill nets targeting tuna. Rays were landed either whole, gutted, or in many cases only as pectoral fins. We only included samples in this study from individuals that could be confidently identified from images recorded at the time of tissue collection (Stevens 2014). Where possible, we recorded disc width of landed individuals (Table 1).

Sri Lanka

In Sri Lanka, we collected skeletal muscle samples from *M. birostris* (n = 37), *M. japanica* (n = 27), *Mobula tarapacana* (n=27), and *M. thurstoni* (n = 11) landed at fish markets in Negombo, in the west of the country, and Mirissa, in the south, from November 2010 through August 2013. In most cases, fishers reported catching the mobulids within 20 km of shore on the edge of the continental shelf, while other samples were collected from mobulids caught on long-range expeditions within and outside the exclusive economic zone and off the continental shelf. Rays were landed gutted, and we recorded disc width of individuals where possible (Table 1).

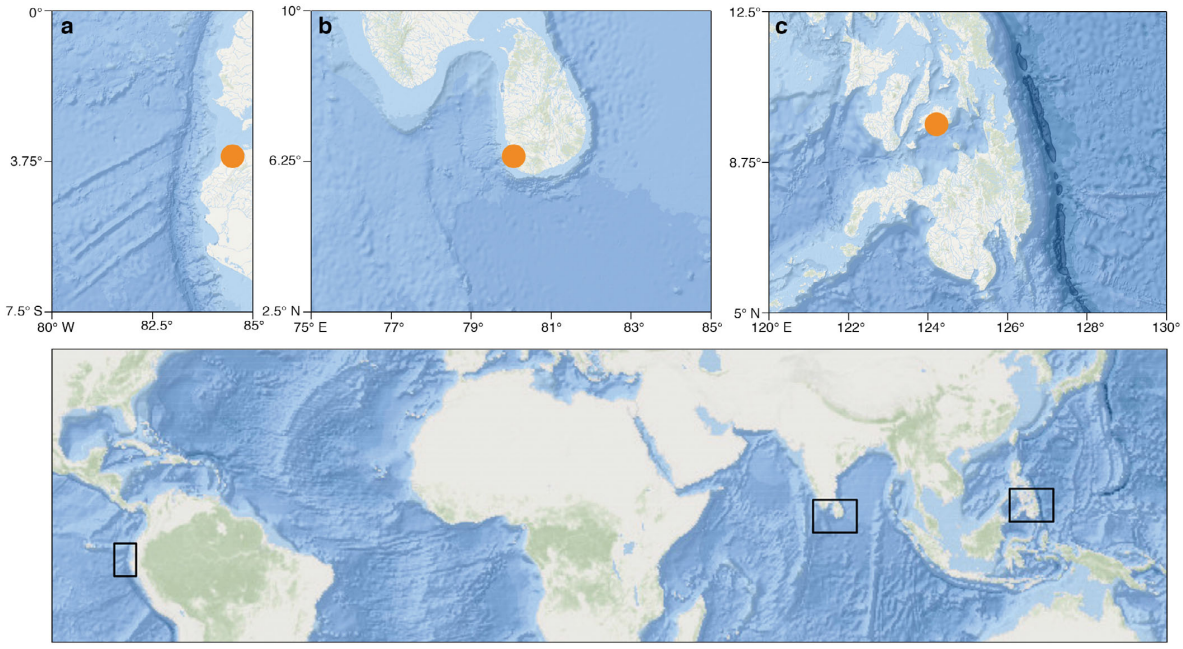

Fig. 1. Study sites. Bounding boxes for chl *a* satellite data are displayed in the lower map, while bathymetric maps of the study sites are displayed within those bounding boxes for (a) Peru, (b) Sri Lanka, and (c) Philippines. Orange circles indicate the locations of primary tissue sample collection sites for each region

Table 1. Summary information for tissues collected from mobulids, including mass conversions and tissue turnover rates, and their prey. All values are means ± SD. All mobulid tissues were skeletal muscle unless otherwise noted. Liver tissues were high in lipids, which leads to lower $\delta^{13}C$ values; therefore, we lipid extracted (LE) the liver tissues and report $\delta^{13}C$ values for intact (bulk) and LE liver tissues (see 'Materials and methods')

Region/species	No. of samples	Disc width (cm)	Converted mass (mean, kg)	Tissue turnover (mean, d)	$\delta^{15}N$ (‰)	$\delta^{13}C$ (‰)	LE $\delta^{13}C$ (‰)	Bulk C:N	LE C:N
Peru									
Manta birostris	3	365.3 ± 265.9	601.5	550.8	10.4 ± 1.3	−16.7 ± 1.0	–	3.1 ± 0.1	–
Mobula japanica	20	172.0 ± 61.2	42.9	324.9	10.9 ± 1.0	−17.4 ± 0.4	–	3.1 ± 0.1	–
Mobula munkiana	18	143.4 ± 40.5	25.3	292.4	12.5 ± 0.2	−17.1 ± 0.2	–	3.2 ± 0.1	–
Mobula thurstoni	5	90.4 ± 8.5	8.0	231.9	9.9 ± 0.9	−17.6 ± 0.3	–	3.2 ± 0.1	–
Philippines									
M. birostris	42	438.5 ± 55.4	1024.8	612.8	9.6 ± 0.4	−16.5 ± 0.7	–	3.2 ± 0.2	–
M. birostris liver	15	–	–	245.1	9.1 ± 0.4	−22.9 ± 0.7	−19.8 ± 1.3	17.9 ± 4.8	7.9 ± 1.5
M. japanica	42	192.2 ± 24.3	62.7	350.5	9.9 ± 0.4	−16.2 ± 0.4	–	3.1 ± 0.1	–
Mobula tarapacana	35	237.9 ± 49.6	171.8	428.7	9.8 ± 0.6	−16.1 ± 0.6	–	3.1 ± 0.1	–
M. tarapacana liver	15	–	–	171.5	10.1 ± 0.6	−21.9 ± 0.7	−19.5 ± 0.9	14.5 ± 4.0	7.3 ± 1.2
M. thurstoni	73	147.4 ± 24.1	31.0	304.4	9.5 ± 0.4	−16.2 ± 0.5	–	3.1 ± 0.1	–
Sri Lanka									
M. birostris	37	253.9 ± 54.6	208.0	445.4	10.6 ± 0.8	−17.6 ± 0.4	–	3.2 ± 0.1	–
M. japanica	27	207.0 ± 21.9	80.6	368.5	10.7 ± 0.5	−17.8 ± 0.5	–	3.2 ± 0.1	–
M. tarapacana	27	205.0 ± 44.2	111.4	393.1	10.9 ± 0.8	−17.4 ± 0.6	–	3.2 ± 0.1	–
M. thurstoni	11	126.3 ± 19.9	20.2	279.3	10.4 ± 0.3	−18.0 ± 0.4	–	3.2 ± 0.1	–
Philippines stomach contents									
Euphausiids	40	–	–	–	7.6 ± 0.5	−18.3 ± 0.4	–	3.7 ± 0.2	–
Copepods[a]	3	–	–	–	6.9 ± 0.4	−19.8 ± 0.8	–	3.9 ± 0.5	–
Chaetognaths[a]	3	–	–	–	8.4 ± 0.4	−18.8 ± 0.5	–	3.3 ± 0.2	–
Pteropods	1	–	–	–	5.24	−12.2	–	8.2	–
Pteropods[a]	6	–	–	–	6.2 ± 0.1	−14.6 ± 2.5	–	4.3 ± 0.9	–
Myctophids	11	–	–	–	9.0 ± 0.8	−17.9 ± 0.9	–	3.3 ± 0.4	–
Sardinella spp.	6	–	–	–	9.7 ± 0.4	−17.8 ± 0.8	–	4.1 ± 0.6	–
Cubiceps spp.	3	–	–	–	8.4 ± 0.3	−17.3 ± 0.3	–	3.5 ± 0.1	–

[a]Samples collected in a zooplankton tow

Philippines

In the Philippines, we analyzed samples collected from *M. birostris* (n = 42), *M. japanica* (n = 42), *M. tarapacana* (n = 35), and *M. thurstoni* (n = 73) at a landing site in Jagna, on the island of Bohol, from December 2012 through May 2014. Mobulids were landed primarily during the dry season from mid-November to mid-June. Fishers captured mobulids in the central and eastern Bohol Sea, typically between 5 and 50 km from shore at night and in the top 30 m of the water column over depths greater than 1000 m. We collected skeletal muscle tissue and recorded disc width where possible (Table 1). We collected stomach contents from a subset of individuals across all species, and we collected liver samples from a subset of *M. tarapacana* (n = 15) and *M. birostris* (n = 15). In some cases, prey sources were present in a number of different stomach content samples but in quantities that were too small to prepare for stable isotope analysis (e.g. copepods, chaetognaths, and pteropods; see Rohner et al. 2017 for a detailed analysis of stomach contents). While these prey sources did not make up a substantial portion of the diet during the period when stomach contents were collected, their relative importance may change throughout the year. Because isotope analysis allows for dietary insights over a longer tissue integration period, we chose to include these sources in our analyses. To obtain adequate material for isotope analysis, we performed 1 plankton tow in Pintuyan, Southern Leyte, during February 2016. We only included copepods, chaetognaths, and pteropods from the plankton tow in isotope analyses; no other species or groups that were not present in stomach contents were included.

We visually sorted prey collected in mobulid stomach contents and plankton tows to the species level except for copepods, which we pooled across species to obtain enough material for isotope analysis. We further sorted prey species using microscopy (details reported in Rohner et al. 2017). In 2 cases, fish samples collected from *M. tarapacana* stomachs could not be visually identified. We extracted DNA from these samples at Scripps Institution of Oceanography using a Qiagen DNeasy kit and sequenced 16S genes for genetic identification. We matched these sequences to existing barcodes using the basic local alignment search tool database (Madden 2002), which identified them as *Sardinella* sp. and *Cubiceps* sp. Myctophids were typically found whole and intact in *M. birostris* stomach contents, and we subsampled these to include a portion of skin, connective tissue, and muscle, which we homogenized and included as a single sample per fish. In all cases, only 1 fish was present per stomach content sample (n = 11). The remains of the partially digested *Sardinella* sp. and *Cubiceps* sp. from the *M. tarapacana* stomach contents were homogenized for analysis after removing degraded tissue. We found multiple specimens of *Sardinella* sp. (n = 6) and *Cubiceps* sp. (n = 3) per stomach content sample, and we analyzed each individual fish as a separate prey sample. Euphausiids, copepods, and chaetognaths were each pooled (within species) to obtain sufficient tissue for isotope analysis. We took 1 pooled subsample of euphausiids per stomach content sample (n = 40 samples). We separated partially digested from intact euphausiids within each stomach content sample and only included intact euphausiids in our subsamples for isotope analysis. We took multiple pooled subsamples of copepods (n = 3 samples) and chaetognaths (n = 3 samples) from 1 plankton tow. In the case of pteropods, 1 individual constituted 1 sample, and we obtained specimens from 1 stomach content sample (n = 1 individual) and 1 plankton tow (n = 6 individuals) (Table 1). While additional samples of prey species collected by plankton tows across a longer period of time would have been ideal, logistical constraints restricted our available samples to a single plankton tow to supplement stomach contents in the present study.

Sample storage

As remote tropical sampling locations generally did not allow for preferred preservation methods such as freezing, we stored tissue, stomach content, and plankton tow samples in 95% ethanol. While there is no consensus on the effect of ethanol on $\delta^{13}C$ and $\delta^{15}N$ stable isotope values (Sarakinos et al. 2002, Barrow et al. 2008, Burgess & Bennett 2017), most preservation studies on fish muscle and fin tissue indicate there are negligible effects of ethanol on $\delta^{15}N$ values, and the shift in $\delta^{13}C$ values after long-term storage in ethanol is low (typically a mean increase of 0.5 to 1.5‰) (Kaehler & Pakhomov 2001, Sarakinos et al. 2002, Kelly et al. 2006, Vizza et al. 2013, Stallings et al. 2015). Additionally, Burgess & Bennett (2017) suggest that storage of elasmobranch tissues in ethanol mimics the effects of urea extraction, perhaps by acting as a solvent. In Peru, samples were stored in 96% ethanol + 0.1 mM EDTA, as they were initially intended for genetic analysis. To our knowledge, there are no studies that examine the effects of ethanol and EDTA preservation on isotope values. Sample preservation studies have examined the impacts of DMSO storage on isotope values (Lesage et al. 2010), and in at least 1 case, a DMSO + EDTA solution was used (Hobson et al. 1997). The mean effect of DMSO and DMSO + EDTA storage on isotope values was similar for both $\delta^{13}C$ (−4.74 vs. −5.1) and $\delta^{15}N$ (−0.7 vs −0.9), suggesting that EDTA does not have a substantial additional impact on isotope values. Importantly, where EDTA was added to a DMSO buffer, the variance of isotope values did not change as compared to frozen samples (Hobson et al. 1997), which would impact estimates of isotopic niche area in the present study. The storage and preservation of samples in ethanol (or ethanol + EDTA) makes them challenging or impossible to compare with other isotopic values in the literature for the same species or potential source items that were preserved differently. However, these storage methods should not affect the estimation of isotopic niche area or within-region comparison of sources and consumers given the consistent preservation methodology utilized across samples. We did not compare isotope values among samples that were preserved only in ethanol with those preserved in ethanol + EDTA.

Isotope analysis

For stable isotope sample preparation, we soaked samples in deionized water for 5 min and then rinsed them to remove debris and residual ethanol from storage. We then freeze-dried approximately 10 mg (wet) of tissue from each individual for 24 h using a FreeZone 2.5 freeze drier (Labconco). In the case of

liver samples, we freeze-dried 30 mg (wet) of tissue from each individual for 72 h.

The high lipid content of elasmobranch livers can result in lower $\delta^{13}C$ values (Logan & Lutcavage 2010, Kim & Koch 2012). We therefore lipid-extracted liver samples using petroleum ether (Dobush et al. 1985), following the protocol outlined in Kim & Koch (2012). As lipid extraction with petroleum ether appears to affect $\delta^{15}N$ values (Parng et al. 2014), we subsampled liver prior to lipid extraction and used non-lipid-extracted samples for $\delta^{15}N$ values and lipid-extracted samples for $\delta^{13}C$ values. We did not lipid-extract muscle tissue, as their carbon to nitrogen (C:N) ratios fell below the C:N threshold of 3.5 suggested by Post et al. (2007), indicating these tissues had sufficiently low lipid content that would not affect $\delta^{13}C$ values (see Table 1). We did not lipid-extract prey samples because their C:N values (3.8 ± 0.7, mean ± SD) indicated they were not lipid-rich as defined by Newsome et al. (2010), and the tissue quantity of many prey samples (especially copepods and chaetognaths) was so low that lipid extraction was not practical. However, to assess the possible impacts of the lipid content of prey samples on our mixing models, we did apply mathematical lipid normalization equations (see 'Materials and methods: Statistics and mixing models'). We homogenized pteropods whole without acid-washing or removing carbonate shell components, which may have artificially increased $\delta^{13}C$ values for pteropods in our results (Mateo et al. 2008).

We homogenized dried mobulid muscle tissue and prey fish samples using a Wig-L-Bug dental amalgamator and mobulid liver and zooplankton prey samples manually using a mortar and pestle. We then packaged between 0.5 and 1.0 mg of powdered tissue in 5 × 9 mm tin capsules (Costech). Samples were analyzed at the University of California Santa Cruz Stable Isotope Laboratory using an NC2500 elemental analyzer (CE Instruments) interfaced to a Delta Plus XP isotope ratio mass spectrometer (Thermo-Finnigan) with an acetanilide standard.

We estimated tissue-specific stable isotope turnover times for skeletal muscle by calculating the average mass of each species based on species-specific disc width to mass conversions from Notarbartolo di Sciara (1988) and using the body mass tissue incorporation rates for carbon and nitrogen in teleosts and elasmobranchs described in Kim et al. (2012b). No disc width to mass conversion is available for *M. birostris*, so we used the conversion formula for *M. tarapacana*, which is the second-largest mobulid species in the present study. MacNeil et al. (2006) estimated the incorporation rates of nitrogen in liver tissue to be approximately 40% of the incorporation rates of nitrogen for muscle tissue in a controlled feeding experiment using freshwater stingrays, and we therefore applied this scaling factor to our muscle tissue nitrogen incorporation rates for *M. birostris* and *M. tarapacana* to arrive at approximate nitrogen incorporation rates for liver.

Statistics and mixing models

We performed all statistical analyses using the R software program (R Core Team 2016). We used the Stable Isotope Bayesian Ellipses in R (SIBER) package (Jackson et al. 2011) to create standard ellipses representing relative isotopic niche widths in bivariate $\delta^{13}C$ and $\delta^{15}N$ space, where the standard ellipse represents bivariate standard deviation. We generated Bayesian credible intervals of the standard ellipse area of each species as well as for the overall mobulid assemblage (all species combined) within each region. We computed the pairwise overlaps between mobulid species within each region and used the mean proportional overlap among species as a metric for community overlap. Bayesian estimation of standard ellipses allows for an unbiased estimate of relative isotopic niche area even at small sample sizes, in contrast with metrics such as convex hulls, which are positively correlated with sample size (Jackson et al. 2011). Therefore, our median estimates of isotopic niche metrics should not be impacted by small sample sizes, although uncertainty and therefore credible interval width should be greater. We excluded *M. birostris* in Peru from isotopic niche area comparisons, as the extremely large credible intervals resulting from small sample size (n = 3) made comparisons uninformative. However, we did include *M. birostris* in the mean proportional isotopic niche overlap calculations for Peru to keep the total number of species constant at each site to allow for comparisons across regions. For all SIBER analyses, we used 2 chains of 10 000 iterations with a burn-in of 1000 and thinning of 10.

To determine the contribution of prey sources to mobulids' diets in the Philippines, we used MixSIAR, a Bayesian stable isotope mixing model (Stock & Semmens 2016). We included 7 prey sources in the model: euphausiids, copepods, chaetognaths, myctophids, *Sardinella*, *Cubiceps*, and pteropods. We subsequently made 2 combinations of 3 groups *a posteriori* by summing their model output posterior distributions based on their functional role, because 7 sources would likely be confounded with only 2 trac-

ers ($\delta^{15}N$ and $\delta^{13}C$) (B. X. Semmens et al. unpubl.). The grouping scenarios were (1) zooplankton (chaetognaths, copepods, euphausiids), fish (myctophids, *Sardinella*, *Cubiceps*), and pteropods; and (2) epipelagic (chaetognaths, copepods, *Sardinella*), mesopelagic (euphausiids, myctophids, *Cubiceps*), and pteropods. We kept pteropods separate from the aggregated groupings due to the dissimilarity of their isotopic signature and possible influences of carbonate shells on the measured isotope values. We did not combine these groups *a priori* (before inclusion in the model) because the combined source groups were not bivariate normally distributed, which is an expectation of the mixing model (B. X. Semmens et al. unpubl.).

Dietary lipids in prey sources may be routed directly to consumer tissues (Newsome et al. 2010, Parng et al. 2014), making it more appropriate to leave prey samples with lipids intact. However, to account for uncertainty in the importance of dietary lipid content, as well as possible influences of carbonate shells in our pteropod samples, we ran 2 versions of our mixing models. The first included bulk prey samples and bulk consumer samples, while the second used correction factors to account for lipid content and carbonate shells. For the second mixing model, we applied muscle tissue-specific fish C:N correction factors for $\delta^{13}C$ (Logan et al. 2008) to our myctophid, *Sardinella*, and *Cubiceps* sources and euphausiid species-specific C:N correction factors for $\delta^{13}C$ to our chaetognath, copepod, euphausiid, and pteropod sources, because euphausiids were the only marine invertebrates for which correction factors were available (Logan et al. 2008). After accounting for lipid content, we applied a correction factor of −6‰ $\delta^{13}C$ to pteropod samples, representing the mean difference in whole versus acid-washed marine gastropods reported in (Mateo et al. 2008). We ran each version of the mixing model (bulk and lipid/carbonate corrected) with both informative and uninformative priors as specified below.

Trophic discrimination factors, or the differences in prey and consumer isotope values that result from metabolic processes, are an important aspect of mixing models, but the determination of appropriate trophic discrimination factors has remained a hotly contested debate in the literature (Gannes et al. 1997, Caut et al. 2008, Hussey et al. 2010b). Determining discrimination factors generally requires laboratory experiments or controlled feeding studies, which are not practical or readily available for many species, including mobulids. Couturier et al. (2013) proposed discrimination factors of 2.4‰ for nitrogen and 1.3‰ for carbon based on stable isotope values of wild reef manta rays and their putative prey sources. These values fall within the range of other published elasmobranch discrimination factors, although laboratory experiments demonstrate considerable variation, even within species (Hussey et al. 2010a, Kim et al. 2012a, Malpica-Cruz et al. 2012). One advantage of Bayesian mixing models is their ability to incorporate uncertainty in parameter estimates and propagate this uncertainty throughout the model (Moore & Semmens 2008). We used mean values of 2.4‰ for nitrogen and 1.3‰ for carbon (Couturier et al. 2013) but used a standard deviation of 1‰ for both isotopes in our mixing models to account for the variability in laboratory-derived trophic discrimination factors, the uncertainty of the discrimination factors proposed for wild reef manta rays, and possible differences between mobulid species. Specifically, we selected a standard deviation of 1‰, as it adequately covers the range of $\delta^{15}N$ and $\delta^{13}C$ trophic discrimination factors reported in laboratory experiments with elasmobranchs (Hussey et al. 2010a, Kim et al. 2012a, Malpica-Cruz et al. 2012).

In addition to trophic discrimination factors, Bayesian mixing models require prior distributions for proportional diet contribution of all prey sources. We ran 2 different iterations of our mixing model. The first model used priors that are uninformative on the simplex, where all possible sets of diet proportions are given equal weight in the prior distributions (B. X. Semmens et al. unpubl.). Priors are specified using a Dirichlet distribution, where an uninformative prior has a probability $\alpha_i = 1/(\text{n sources})$ for each source i. The second model used semi-informative priors, which we based on the presence and abundance of the 7 prey sources in stomach content samples from each species. An informative prior could be specified as $\alpha_{i,j}$ = n records of prey species i in stomach contents of consumer species j. However, in some cases, 1 or 2 prey sources dominated stomach content samples or may have been the only prey sources present within a species' stomach contents, which would have led to extremely informative priors. Using very strong priors essentially eliminates the utility of a mixing model, as the posterior distributions will simply reflect the priors (B. X. Semmens et al. unpubl.). Furthermore, the stomach contents were collected from January to April and therefore are representative of the mobulids' diets during only a third of the year. Muscle tissue represents the integrated diet over a much longer period (Table 1) and is therefore useful in determining longer-term integration of diet contributions. For these reasons, we qualitatively

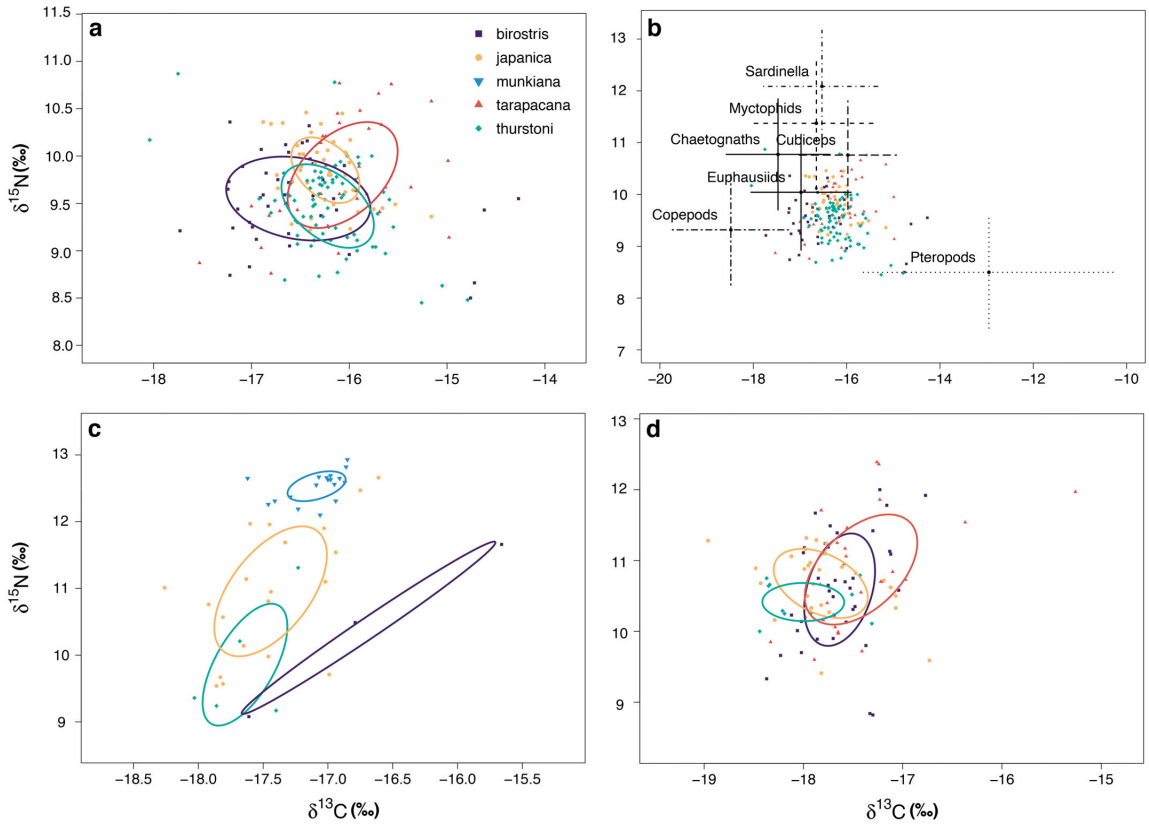

Fig. 2. Isotope data with SIBER ellipses and sources (Philippines). (a) Philippines, (b) Philippines with sources, (c) Peru, (d) Sri Lanka. Ellipses in (a), (c), and (d) represent maximum likelihood standard ellipses for each species, while analyses presented in 'Materials and methods' and 'Results' were performed on Bayesian estimates of standard ellipses (not shown). Bars in (b) represent mean ± SD for each dietary source in the Philippines included in the mixing models. Sources in (b) are corrected for trophic discrimination, including the additional uncertainty in trophic discrimination factors that was incorporated into the mixing models. Legend for species colors and shapes in all regions is listed in (a). See Table 1 for full species names

level relationships and significance values are reported in Figs. S2 & S3 in the Supplement.

Mixing models

The mixing model results from the Philippines support the data from the isotopic niche ellipses indicating that the diets of mobulids in the region are largely overlapping (Fig. 5). Using lipid- and carbonate-corrected prey sources had a minor impact on aggregated posterior distributions, typically reducing the diet contribution from pteropods and slightly increasing the contribution from fish or zooplankton (Table 2, Table S4). All 4 species of *Mobula* appeared to consume similar proportions of the 3 aggregated prey groups (Fig. 5, Table 2): model outputs suggest that diets were dominated by zooplankton, had a substantial input from the pteropod source, and included a smaller but still notable proportion of fish. In many cases, the discrete (non-aggregated) sources were confounded, evidenced by the influence of prior specifications on posterior distributions (e.g. euphausiids in *M. birostris* and *M. tarapacana*, *Cubiceps* in *M. japanica*) (Fig. S1 & Table S5). Aggregated posterior distributions for fish and zooplankton groups, however, were robust to prior specifications (Fig. 5, Table 2). Using a semi-informative prior did not substantially impact median estimates of diet proportions but did substantially reduce credible intervals and the

relaxed the stomach content-informed priors so that the model had a reasonable chance of including any of the possible prey sources, while at the same time providing some weight to the diet preferences implied by stomach content data. Prior distributions for each source are presented in Fig. S1 & Table S1 in the Supplement at www.int-res.com/articles/suppl/m580p131_supp.pdf, and *a posteriori* aggregated priors are presented in 'Results: Mixing models' (see Fig. 5). We ran all mixing models with 3 chains of 300 000 iterations, a burn-in of 200 000, and thinning of 100. We assessed convergence of all Bayesian analyses using visual inspection of chain convergence and autocorrelation plots as well as Gelman-Rubin diagnostics (Gelman & Rubin 1992).

To assess relationships between trophic characteristics and body size, we used Bayesian linear mixed effects models. To do this, we set up models with isotope values ($\delta^{15}N$ and $\delta^{13}C$) as the response (normally distributed), disc width and regions as fixed effects, and species as a random effect. We used a multivariate ANOVA to examine isotopic differences between lipid-extracted liver samples and muscle samples in *M. birostris* and *M. tarapacana*. Because MANOVAs do not provide significance levels for each variable, we used paired *t*-tests to examine within-individual differences in $\delta^{15}N$ and $\delta^{13}C$ values between liver and muscle of individuals from which we collected both tissue types. We applied Bonferroni corrections for repeated measures and report corrected p-values.

Environmental data

We used the xtractomatic package (Mendelssohn 2015) in R to obtain monthly chl *a* values from MODIS satellites for the regions surrounding each of our study sites over the past 10 yr to characterize the long-term patterns and variability in regional productivity. Our bounding boxes were 7.5° S, 85° W to 0° N, 80° W (Peru); 2.5° N, 75° E to 10° N, 85° E (Sri Lanka); and 5° N, 120° E to 12.5° N, 130° E (Philippines) (see Fig. 1). We selected these bounding boxes based on the expected distribution of mobulids in each region, which was supported by bycatch data from the eastern equatorial Pacific (Croll et al. 2016), interviews with fishermen regarding capture locations in Sri Lanka, and records of long-distance movements in several *Mobula* species (Thorrold et al. 2014, Francis & Jones 2017). We averaged chl *a* values over the entire bounding box for a given region and smoothed monthly averages into seasonal (3 mo) averages for plotting purposes.

RESULTS

Isotopic niche areas

The stable isotope values from the 4 mobulid species, and their resulting isotopic niche spaces, largely overlapped among species for those sampled in Sri Lanka and the Philippines, whereas there was a greater separation in isotope values and isotopic niche space among species collected in Peru (Figs. 2 & 3). The mean proportional isotopic niche overlap among species increased from Peru to Sri Lanka to the Philippines (0.10, 0.33, 0.36, respectively), although there was a high degree of overlap between Bayesian credible intervals of these estimates (Fig. 3, Table S2 in the Supplement). Satellite-derived chl *a* values indicate Peru had the greatest mean primary productivity of our 3 study sites, followed by Sri Lanka and the Philippines (1.04, 0.48, 0.19 mg m^{-3}, respectively), while Sri Lanka had the greatest variability (SD) in chl *a* values followed by Peru and the Philippines (SD: 0.38, 0.27, 0.06 mg m^{-3}, respectively) (Fig. 3).

Manta birostris and *Mobula tarapacana*, the largest of the mobulids, had larger isotopic niche areas than *Mobula japanica* and *Mobula thurstoni* in Sri Lanka and the Philippines, while in Peru, *M. japanica* and *M. thurstoni* had much larger isotopic niche areas than *Mobula munkiana* (Fig. 4). We found no pattern between ellipse area and region that was consistent across species. For example, while the median ellipse area of *M. japanica* was largest in Peru and smallest in the Philippines, the median ellipse area of *M. thurstoni* was largest in Peru and smallest in Sri Lanka, and the ellipse area of *M. birostris* was larger than *M. tarapacana* in the Philippines but smaller in Sri Lanka (Fig. 4). We report pairwise comparisons of isotopic niche area credible intervals and median values of isotopic niche areas in Table S3.

Size-based differences in isotopic signatures

Our mixed effects models demonstrated significant but weak relationships between body size (disc width) and isotope values. The median slope across all mobulids demonstrated an increase in the $\delta^{15}N$ value of 0.21‰ per meter increase in disc width and an 89.2% probability of a slope greater than 0. Conversely, mobulids displayed a negative slope in $\delta^{13}C$ values, with a median decrease of 0.23‰ per meter increase in disc width across all species and a 97.47% posterior probability of a slope less than 0. Species-

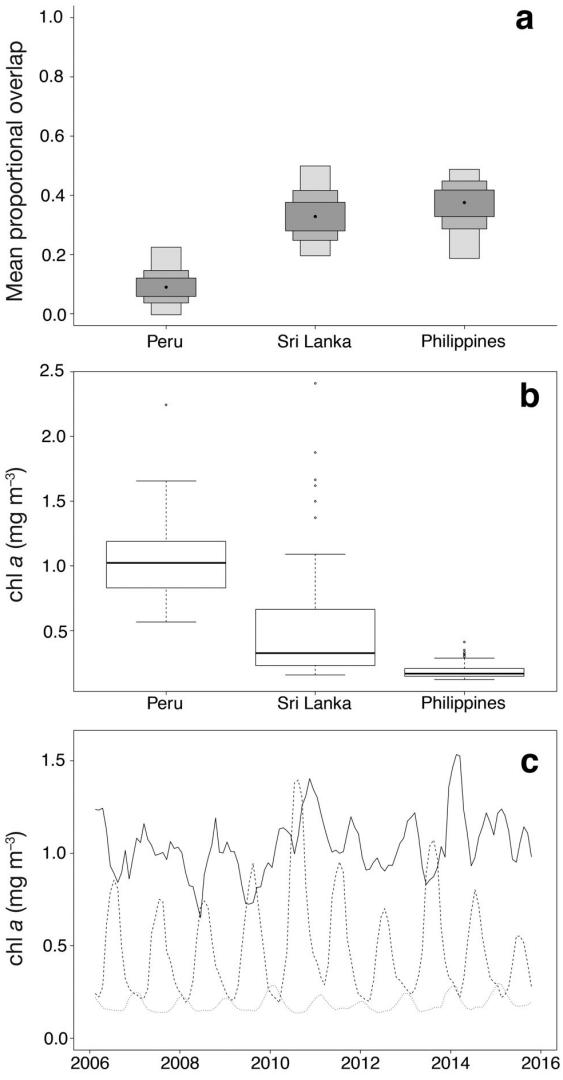

Fig. 3. Niche overlap and environmental data from Peru, Sri Lanka, and the Philippines. (a) Mean proportional overlap between species' isotopic niche areas. Rectangles represent the 50, 75, and 95% credible intervals (dark to light shading, respectively), and black dots represent the mode values. (b) Boxplots of monthly mean chl *a* values for each of the 3 study regions (boundaries defined in 'Materials and methods') across a 10 yr period from 2006 to 2016. (c) Smoothed 3 mo averages of chl *a* values across the same 10 yr period as in (b) for Peru (solid line), Sri Lanka (dashed), and the Philippines (dotted)

skewedness and non-normality of posterior distributions. The 2 exceptions to this were the proportion of fish in the diet of *M. japanica*, which shifted from 0.33 to 0.15 (median) from the uninformative to semi-informative prior, and the normality of the posterior distribution of the proportion of pteropods in the diet of *M. thurstoni*. At the discrete source level, both pteropods and copepods tended to be robust to changes in prior specification across species (Fig. S1). There was more variability in diet contributions from the epipelagic and mesopelagic aggregated sources across species than from the fish and zooplankton groups (Table 2). However, epipelagic and mesopelagic groupings were less robust to prior specifications. There was no seasonal trend in isotope values for euphausiid prey samples, which were collected across multiple months and years. Variability in euphausiid isotope values was similar to the variability in prey samples collected in a single plankton tow (Table 1), suggesting that prey samples from the single plankton tow adequately capture the variability in prey sources for the purpose of diet reconstruction.

Liver samples

The mean effects of lipid extraction on the isotope values from liver samples were an increase of 2.79‰ on $\delta^{13}C$ and a decrease of 0.11‰ on $\delta^{15}N$ (Table 1). In all analyses and discussion of liver samples, we used the $\delta^{13}C$ values from lipid-extracted samples and the $\delta^{15}N$ values from corresponding bulk (non-lipid-extracted) samples unless otherwise specified. Despite repeatedly sonicating liver samples in petroleum ether until the solution was clear instead of a dark orange color (indicating that lipids had been successfully removed), the C:N ratios of liver samples remained high (5.6 to 10.3; Table 1). There was a significant relationship between the bulk C:N ratio and the change in $\delta^{13}C$ between lipid-extracted and bulk liver samples ($p = 0.015$; Fig. S6). The linear regression equation for both species combined was:

$$\delta^{13}C_{\text{lipid-extracted}} - \delta^{13}C_{\text{bulk}} = 0.089 \times C{:}N_{\text{bulk}} + 1.328$$

However, the fit of this relationship was poor ($R^2 = 0.137$). Muscle tissue isotope values from individuals paired with liver samples were no different from the overall muscle tissue isotope values for either *M. birostris* ($\delta^{15}N$: 9.6 ± 0.5; $\delta^{13}C$: −16.6 ± 0.8) or *M. tarapacana* ($\delta^{15}N$: 9.8 ± 0.6; $\delta^{13}C$: −16.2 ± 0.6), indicating that the subsample of individuals with both muscle and liver tissue was representative of the full set of samples.

The multivariate ANOVA indicated that liver samples were significantly different from muscle samples in both *M. birostris* ($p < 0.001$) and *M. tarapacana* ($p < 0.001$). Paired *t*-tests indicated that the $\delta^{15}N$ values were significantly different between muscle and liver in *M. birostris* ($p = 0.049$) but not *M. tarapacana*

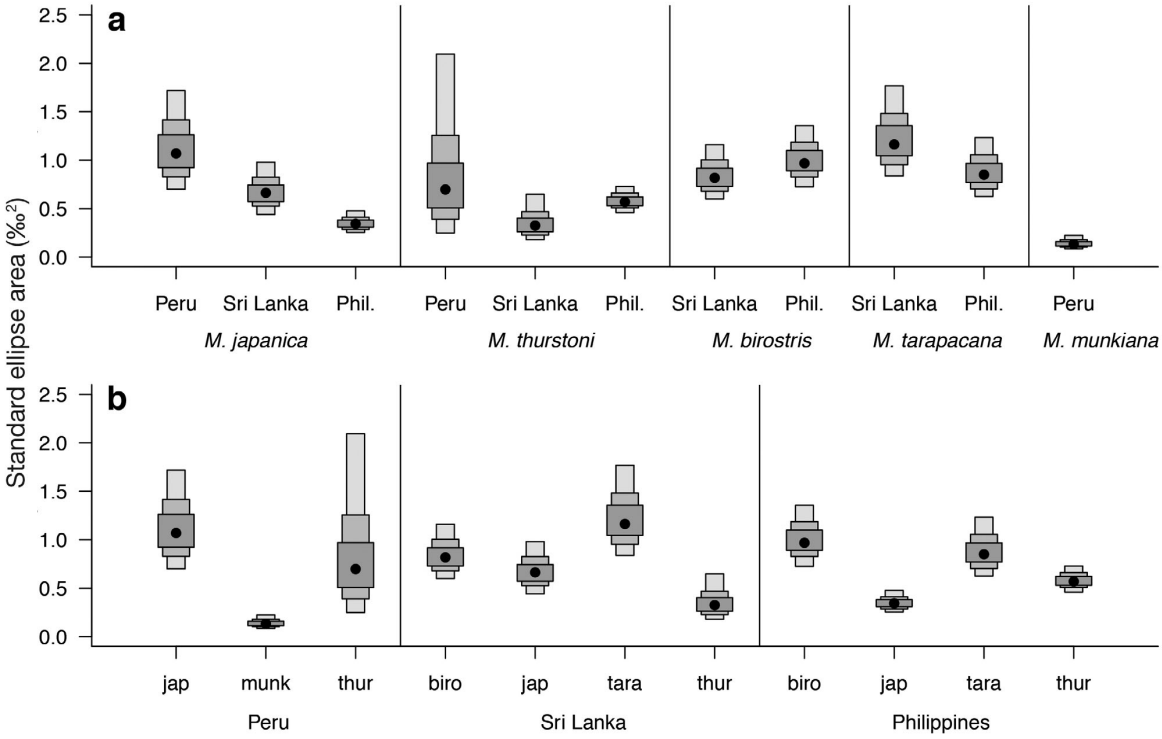

Fig. 4. Niche area by species and region. (a) Between-region comparisons for each species and (b) between-species comparisons for each region. Rectangles represent the 50, 75 and 95% credible intervals (dark to light shading, respectively), and black dots represent the mode values. We excluded *Manta birostris* collected in Peru due to large credible intervals that resulted from small sample size (n = 3). See Table 1 for full species names

($p = 0.53$). The $\delta^{13}C$ values were significantly different between muscle and liver in both species ($p < 0.001$).

DISCUSSION

Niche overlap

Trophic niche partitioning according to body size is commonly observed in nature and is a fundamental theory explaining coexistence of similar species in habitats with limited resources (Hutchinson 1957). For example, in marine fishes, body size frequently correlates with mouth gape, which in turn determines the maximum prey size a consumer can target (Scharf et al. 2000). In filter-feeders, the mechanism that would facilitate trophic niche partitioning is less clearly linked to body size, as prey items are typically orders of magnitude smaller than a filter-feeder's mouth gape. Nevertheless, sympatric rorqual whales demonstrate resource partitioning across a range of body sizes despite morphological similarities, most likely a function of behavioral differences (Santora et al. 2010, Gavrilchuk et al. 2014). Like rorqual whales, mobulid rays are morphologically similar but span a range of body sizes across species. However, despite the wide range of body sizes sampled in our study, we observed a high degree of isotopic overlap for most species within each region. Previous studies found trophic niche overlap between several mobulids in the Gulf of California, Mexico (Notarbartolo di Sciara 1988, Sampson et al. 2010), and our results demonstrate a similar pattern for 5 mobulid species at 3 separate locations across the Indo-Pacific. Additionally, we observed only weak and most likely ecologically irrelevant relationships between body size and $\delta^{13}C$ and $\delta^{15}N$ values in mobulids, further demonstrating inter- and intraspecific trophic similarities regardless of body size.

Niche overlap theory posits that overlap decreases as interspecific competition increases, for example when resources are scarce and species are forced to specialize to outcompete sympatric competitors

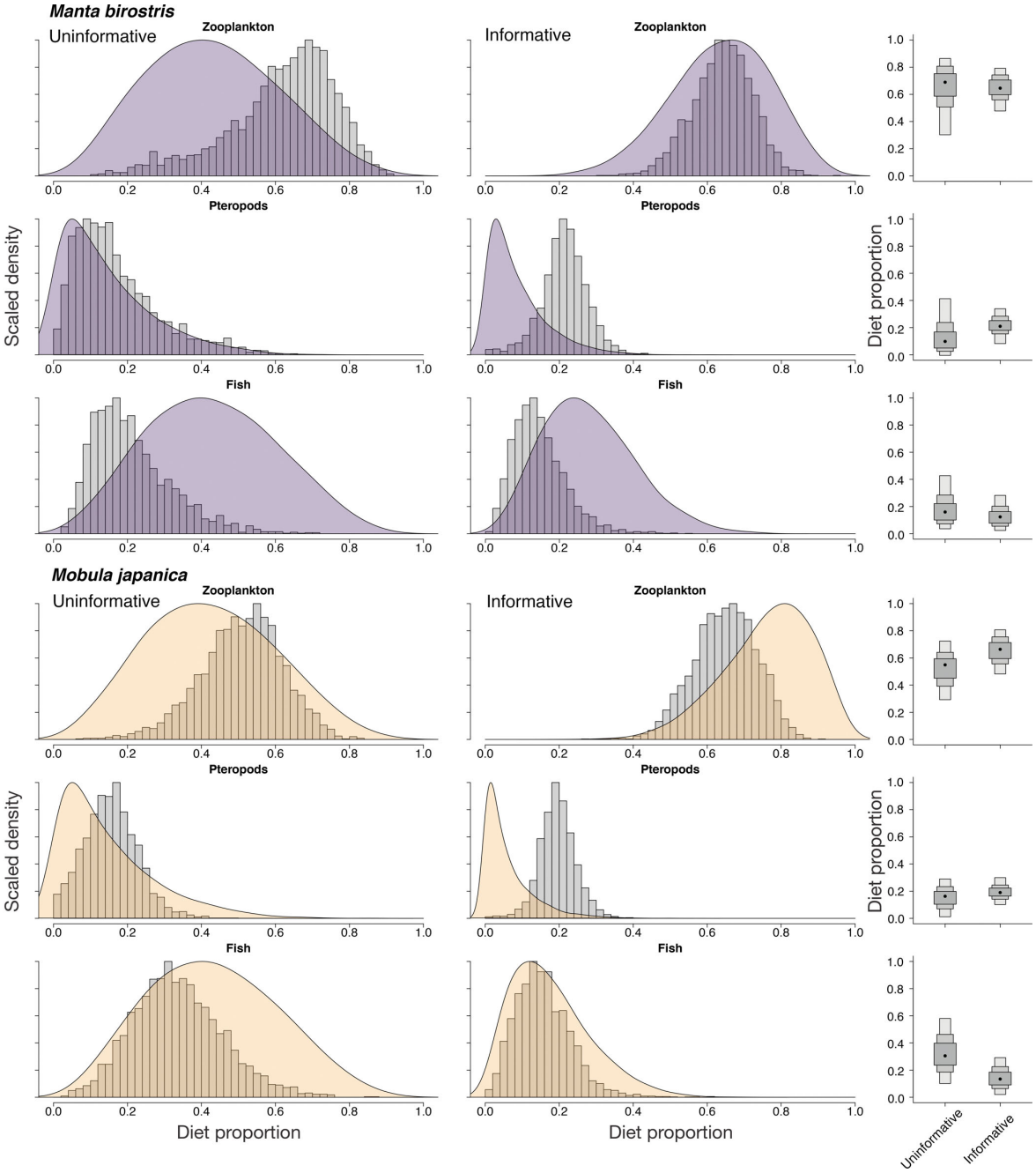

Fig. 5. Mixing model estimates of diet contributions for *a posteriori* aggregated sources. Colored density distributions represent *a posteriori* aggregated prior specifications and grey histograms represent posterior distributions in either the uninformative (left) or informative (right) model runs. The far right panel compares posterior distributions between the uninformative and informative model runs. Rectangles represent the 50, 75 and 95% credible intervals (dark to light shading, respectively), and black dots represent the mode values (Fig. S1 in the Supplement at www.int-res.com/articles/suppl/m580p131_supp.pdf shows the prior distributions that were specified for each source in the model as well as source-specific posterior distributions before *a posteriori* aggregation)

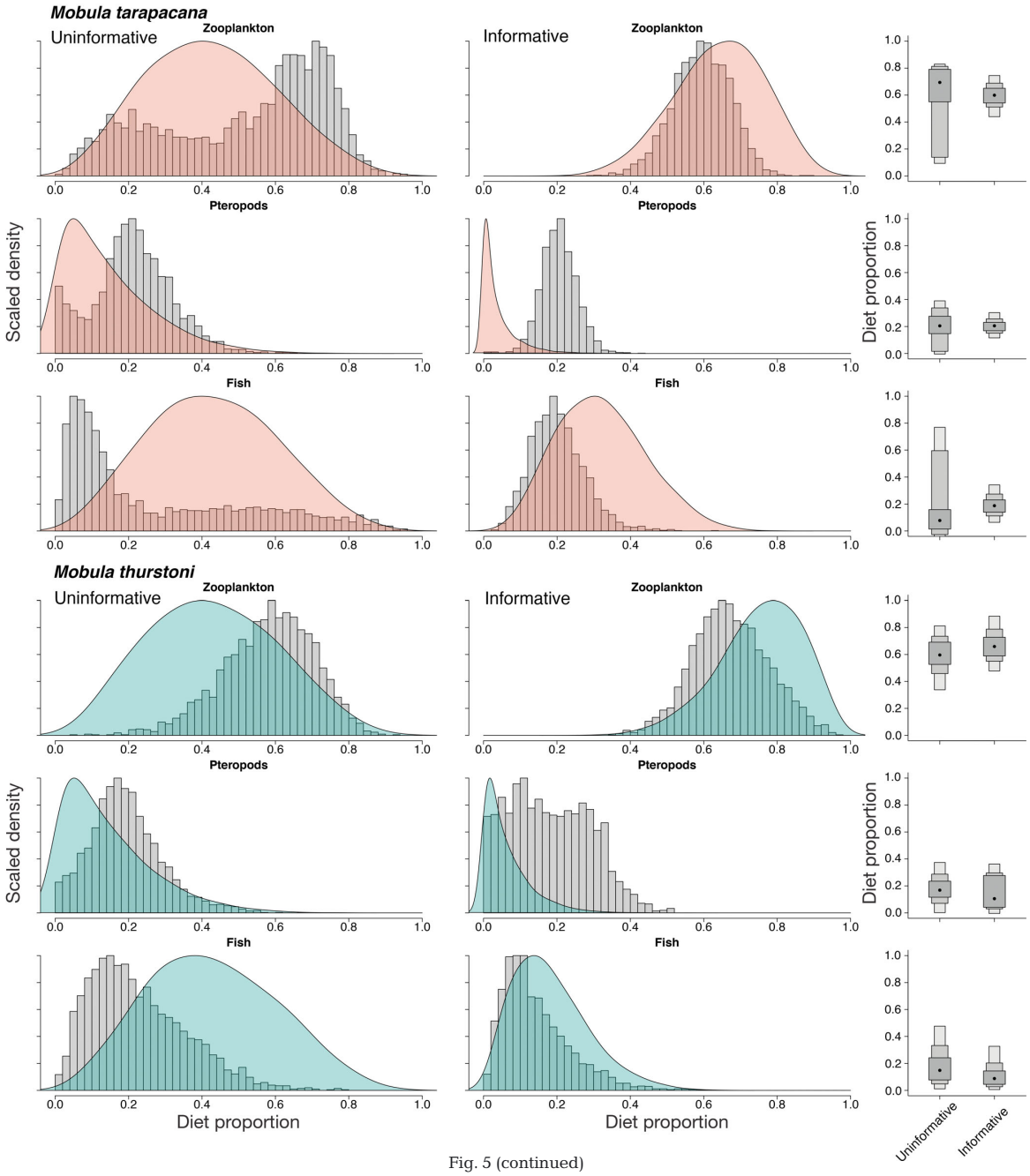

Fig. 5 (continued)

(Pianka 1974, 1981). However, this niche overlap theory (Pianka 1974) has not been definitively supported in observational studies (Porter & Dueser 1982). An alternate explanation for our results is that trophic niche overlap in mobulid rays follows an inverse pattern, where overlap increases as resources become more scarce (e.g. Porter & Dueser 1982). A mechanism for this increasing overlap in nutrient-poor regions may

Table 2. Median diet contributions of *a posteriori* aggregated prey groups from the MixSIAR Bayesian mixing model. Note that epipelagic/mesopelagic groups are different combinations of the same sources in zooplankton/fish groups. Pteropods were kept separate from both grouping scenarios. The groupings and specification of uninformative and semi-informative priors are explained in 'Materials and methods'

Species/source	Uninformative median (95% CI)	Semi-informative median (95% CI)
Manta birostris		
Zooplankton	0.64 (0.26–0.84)	0.64 (0.47–0.79)
Fish	0.19 (0.06–0.48)	0.14 (0.04–0.32)
Pteropods	0.14 (0.03–0.47)	0.21 (0.08–0.33)
Epipelagic	0.55 (0.21–0.78)	0.33 (0.16–0.51)
Mesopelagic	0.28 (0.11–0.56)	0.45 (0.27–0.67)
Mobula japanica		
Zooplankton	0.52 (0.27–0.70)	0.65 (0.48–0.80)
Fish	0.33 (0.12–0.61)	0.15 (0.04–0.32)
Pteropods	0.15 (0.03–0.31)	0.19 (0.10–0.30)
Epipelagic	0.37 (0.15–0.61)	0.21 (0.06–0.41)
Mesopelagic	0.48 (0.21–0.72)	0.60 (0.37–0.78)
Mobula tarapacana		
Zooplankton	0.59 (0.08–0.82)	0.60 (0.43–0.74)
Fish	0.15 (0.02–0.83)	0.19 (0.08–0.36)
Pteropods	0.21 (0.01–0.43)	0.20 (0.12–0.30)
Epipelagic	0.28 (0.04–0.77)	0.19 (0.06–0.40)
Mesopelagic	0.52 (0.04–0.85)	0.60 (0.37–0.78)
Mobula thurstoni		
Zooplankton	0.59 (0.31–0.79)	0.67 (0.48–0.88)
Fish	0.20 (0.04–0.52)	0.12 (0.03–0.37)
Pteropods	0.18 (0.02–0.43)	0.17 (0.01–0.40)
Epipelagic	0.43 (0.19–0.67)	0.32 (0.14– 0.54)
Mesopelagic	0.37 (0.13–0.64)	0.48 (0.28–0.75)

be an increased reliance on high-biomass prey patches that are sparsely distributed and often dominated by 1 or a few prey species (e.g. Rohner et al. 2015, Armstrong et al. 2016). For example, in Peru, where strong equatorial upwelling leads to overall high surface primary productivity, zooplankton prey is likely to be abundant. The density of vertically migrating zooplankton and fish is influenced by surface productivity (Croll et al. 2005, Hazen & Johnston 2010), and therefore an overall increase in zooplankton abundance (surface-associated and deep scattering layers) is expected in a highly productive region such as Peru. Under these conditions, different mobulid species may be able to take advantage of their evolutionarily distinct traits (e.g. size, maximum depth tolerance, thermal inertia) to maximize foraging success by feeding on their preferred zooplankton prey, resulting in greater trophic separation. In contrast, in oligotrophic tropical waters such as our study site in the Philippines, zooplankton should be lower in abundance and more patchily distributed. Numerous studies demonstrate trophic niche separation and resource partitioning in both pelagic and benthic predators in similar oligotrophic regions (e.g. Young et al. 2010, Heithaus et al. 2013, Pardo et al. 2015). However, filter-feeding elasmobranchs such as mobulids appear to require prey densities to exceed a threshold level to make feeding energetically profitable (Armstrong et al. 2016). Consequently, as regional productivity declines, there may be fewer prey patches of adequate density, resulting in multiple sympatric species converging on the same high-density prey sources and therefore greater trophic overlap such as that observed in the present study. This is also supported by observations of mobulid captures in the Philippines. Multiple mobulid species are frequently captured in the same gill nets, which are set at night over deep water in the Bohol Sea when euphausiids are abundant near the surface. Between 2013 and 2014, 25% of 790 recorded fishing trips captured more than 1 species of mobulid in a single net (J. M. Rambahiniarison unpubl.). Whale sharks, another filter-feeding elasmobranch, also rely on dense and often monospecific prey patches to survive in oligotrophic regions (Rohner et al. 2013, 2015), while sympatric rorqual whales exhibit trophic niche separation in highly productive polar foraging grounds (Santora et al. 2010, Gavrilchuk et al. 2014). It is possible that prevalent theories of niche overlap (May & MacArthur 1972, Pianka 1974, 1981) do not adequately describe the trophic dynamics of sympatric marine filter-feeders due to the prey density thresholds they require to meet energetic demands. It may also be the case that large, long-lived, mobile animals are able to escape bottlenecks in resource availability that would otherwise lead to persistent trophic niche differentiation in less productive environments. Importantly, isotopic overlap does not translate directly to trophic overlap, as consumers may feed on mixtures of taxonomically distinct but isotopically similar prey items that would lead to similar consumer isotope signatures. However, analysis of stomach contents in the Philippines verified that the mobulids' diets converge for at least 6 mo of the year (Rohner et al. 2017), effectively ground truthing our inferences from isotope data. This demonstrates the benefits of combining these 2 approaches in dietary studies, and future analysis of mobulid stomach contents in Sri Lanka and Peru would help validate the inferences made here. Our observations of these relationships between trophic dynamics and regional productivity are limited because we have observations from only 3 locations.

Nevertheless, this topic warrants further study in mobulids and perhaps filter-feeders more broadly.

Mobula munkiana appears to be an exception to the pattern of trophic overlap as the only mobulid in our study with an isotopic niche that is almost entirely non-overlapping with other mobulids in the same region. *M. munkiana* had no overlap with *Manta birostris* or *Mobula thurstoni* and only a 6% median isotopic niche overlap with *Mobula japanica* (Table S2 in the Supplement). Notarbartolo di Sciara (1988) found a similar pattern in the Gulf of California, with *M. munkiana* stomach contents dominated by mysids, as compared with the euphausiid prey found in *M. japanica* and *M. thurstoni*. Our results suggest that this trophic niche separation may be consistent for the species throughout its range and that *M. munkiana* may be feeding on an entirely different prey source and/or in an entirely different region from other mobulids in Peru. This is supported in part by differences in landing seasons between *M. munkiana* and other mobulids in Peru (K. Forsberg unpubl.), suggesting that *M. munkiana* may be present along the coast during a different time of year than other mobulids, perhaps due to differences in foraging patterns.

$\delta^{13}C$ and $\delta^{15}N$ values can provide insights into feeding locations and prey types due to predictable changes in $\delta^{13}C$ across marine habitats (France 1995) and increases in $\delta^{15}N$ at higher trophic levels (Owens 1987). In predatory elasmobranchs, changes in isotopic values are common as individuals grow and either change habitats, in the case of an ontogenetic shift, or access larger prey items at higher trophic levels (Estrada et al. 2006, Hussey et al. 2011). Borrell et al. (2011) found a positive relationship between both $\delta^{13}C$ and $\delta^{15}N$ and body size in whale sharks from the northwestern Indian Ocean, suggesting that ontogenetic shifts may also occur in elasmobranch filter-feeders. We found weak relationships between disc width and isotope tracers across all mobulid species. The observed decrease in $\delta^{13}C$ and increase in $\delta^{15}N$ with increasing disc width could indicate a shift to higher trophic level, offshore prey sources in older and larger individuals within species. However, the magnitude of the relationship we found (~0.2‰ per meter disc width) is minimal in comparison to the observed variability in isotope values within a given size class, which often exceeded 2‰ for individuals less than 10 cm apart in size. This suggests that mobulids likely do not experience an ontogenetic shift in feeding behavior and trophic level ($\delta^{15}N$) nor in habitat ($\delta^{13}C$), although there may be some weak overall effect of disc width on trophic dynamics or isotopic fractionation. Notarbartolo di Sciara (1988) found differences in stomach contents between juvenile and adult *M. thurstoni* in the Gulf of California but suggested this was more likely due to the season when either size class was sampled as opposed to a true ontogenetic dietary shift. The individuals sampled in our study spanned a range of disc widths from juveniles to mature adults in all regions and species with the exception of *M. thurstoni* in Peru. This suggests that both juvenile and adult mobulids may occupy the same habitats and target the same prey, as proposed for *M. birostris* by Stewart et al. (2016a). This is further supported by captures of both mature and juvenile mobulids in the same nets in the Philippines (J. M. Rambahiniarison pers. obs.).

The overlap we observed between species' isotopic niches is surprising given the diversity of vertical habitat use and foraging behaviors recorded in mobulids through observational studies and archival tag deployments. *M. japanica* and closely related *Mobula mobular* appear to spend the majority of their time in near-surface habitats, shallower than 50 m depth (Canese et al. 2011, Croll et al. 2012, Francis & Jones 2017). *M. birostris* makes deeper foraging dives and appears to spend substantial amounts of time below 100 m (Stewart et al. 2016b). *Mobula tarapacana* routinely undertakes deep dives below 800 m — in some cases over 1800 m — for periods of 1 to 4 h, presumably to access bathypelagic scattering layers of fishes (Thorrold et al. 2014). These vertical movements are generally linked to observed or inferred foraging behavior and represent a high degree of vertical segregation that could in turn lead to differing trophic niches. However, all of these observations were made in different regions, and our results suggest that the variability in observed behaviors may be a result of regional differences in the location of high-density zooplankton prey as opposed to consistent differences in feeding behavior between species. The few studies that examine multiple mobulid species within a single region support this conclusion. Notarbartolo di Sciara (1988) observed similarities in the euphausiid-dominated stomach contents of adult *M. japanica* and *M. thurstoni* in the Gulf of California, Mexico, which Sampson et al. (2010) later confirmed using isotope analysis. While the majority of stomachs collected from *M. tarapacana* in Notarbartolo di Sciara (1988) were empty, there were traces of euphausiids, among other crustaceans, and 1 stomach contained numerous remains of fishes. Paired with our mixing model results, this suggests that *M. tarapacana* is more piscivorous than the other mobulids. However, the increased proportion of fish

in the diet of *M. tarapacana* is minor in our results, and it is unlikely that the extreme energy expenditure of deep dives to the bathypelagic zone (Thorrold et al. 2014) would justify such a modest dietary contribution. We again posit that such behaviors are likely region-specific, and that *M. tarapacana* from the Philippines may not undertake these types of foraging excursions. Archival tag deployments on *M. tarapacana* in the Philippines could provide insights into vertical habitat use and differences between this region and previous studies in the eastern Atlantic.

Mixing models

Stomach content collections from mobulids landed in the Philippines allowed us to examine dietary overlap in greater detail. Diet contributions from the fish and zooplankton aggregated source groups were similar across species, with the majority of the diet coming from the zooplankton group and lower diet contributions coming from pteropods and the fish group. Our aggregated posterior distributions were robust to our choice of priors, and median values of diet contributions from fish, zooplankton, and pteropods were similar regardless of our use of uninformative or semi-informative priors. The most notable exception to this was *M. japanica*. *M. japanica* muscle tissue had the highest mean δ^{15}N value of all mobulids in the Philippines, placing them closest to the fish sources we identified from *M. birostris* and *M. tarapacana* stomach contents. In our model using an uninformative prior, *M. japanica* appeared to exceed all other species in their consumption of fish. Even when using semi-informative priors with a lower expected contribution of fish in the diet, our model results still indicated that *M. japanica* consumes a greater proportion of fish than *M. thurstoni* and *M. birostris* and a similar proportion to *M. tarapacana*, despite *M. tarapacana* and *M. birostris* being the only mobulids with stomach content samples that contained fish. There are several possible explanations for the discrepancy between stomach contents and mixing model results for *M. japanica*. The first possibility is that *M. japanica* is more piscivorous during the rainy season, and the landings and stomach content sampling during the dry season did not reflect the overall diet. While telemetry data suggest that *M. japanica* is restricted mainly to near-surface waters (Croll et al. 2012), at least some individuals make regular dives to depths of 200 to 300 m (Francis & Jones 2017). Myctophids and *Cubiceps* sp. such as those found in the stomach contents of *M. birostris* and *M. tarapacana*, migrate vertically to depths that are easily within the recorded diving depths of *M. japanica,* while *Sardinella* sp. typically inhabit near-surface waters. Smaller mobulids have been recorded actively feeding on schools of fish in the western Pacific (Heinrichs 2009), and it is possible that *M. japanica* engages in the same behavior in the Philippines. An alternative explanation is that our trophic discrimination factors are incorrect, given the variability in published discrimination factors for elasmobranchs and the lack of experimentally derived discrimination factors for mobulids. There is some evidence to suggest that trophic discrimination factors may vary with body size and compelling evidence to suggest a relationship between trophic enrichment and dietary protein content (Newsome et al. 2010). However, given the similarity in both the stomach content samples and body sizes of *M. japanica* and *M. thurstoni*, we would expect a similar shift for both species in our model. Given the differences between the 2 species' isotopic signatures, we find it more likely that there is a true dietary difference and a greater contribution from an enriched δ^{15}N source — fish or possibly an unsampled source — to *M. japanica* in the rainy season. Diet contributions from our epipelagic and mesopelagic source aggregations tended to be more variable across species than fish and zooplankton groups. However, we found epipelagic and mesopelagic groups to be less informative; first, because they tended to be more sensitive to prior specifications than the fish and zooplankton groups (Table 2) and, second, because they provide fewer insights into habitat use, as both the epipelagic prey and the vertically migrating mesopelagic prey can be accessed by mobulids at the surface at night.

The non-aggregated source contributions from our model outputs provide additional information on dietary sources and possible differences between species. However, our mixing model results on specific prey sources should be interpreted with caution, both because the number of sources (7) is far greater than the number of tracers we used (2) and because of the apparent sensitivity of the sources to prior specifications (Fig. S1). Several sources stand out for their consistency across priors and species. In all cases, our mixing models estimated a higher proportion of pteropods in the diets of mobulids than expected based on their presence in stomach contents. Their prevalence in the estimated diet proportions is undoubtedly due to the geometry of the source and consumer isotope values: without pteropods, the consumers would not be contained within the sources in bivariate isotope space, and therefore pteropods must be included in a sufficient proportion

for the mixing model to come to a mathematical solution. Our mixing model runs with carbonate corrections for pteropod shells led to reductions in pteropod diet contributions, illustrating this concept. It is possible that mobulids are feeding heavily on pteropods in the rainy season, when they are not landed by fishers and sampled, explaining the paucity of pteropods in stomach content samples. Alternatively, there may be an additional, unknown prey source that is isotopically similar to pteropods (either bulk or carbonate corrected) but not included in our mixing models. Burgess et al. (2016) hypothesized that *M. birostris* in Ecuador may be relying heavily on mesopelagic prey sources, which are higher in $\delta^{13}C$ and lower in $\delta^{15}N$ as compared with surface zooplankton, similar to the pteropod source in the present study. It is possible that our pteropod source is isotopically similar to unsampled mesopelagic prey sources in the Philippines and that all mobulid species rely heavily on these prey items. However, the pteropod source (with or without carbonate corrections) was isotopically distinct from both mesopelagic fishes and vertically migrating euphausiids that were sampled from stomach contents, suggesting that pteropods may in fact be an important diet item for these species in the Philippines.

Importantly, our aggregated posterior distributions may artificially inflate the proportion of fish included in the diet due to our inclusion of 3 fish sources. In the discrete source posteriors, the proportion of each fish in the diet of *M. japanica* and *M. thurstoni* abuts zero under the semi-informative prior, suggesting that the proportion of the diet coming from each fish species is negligible — very different from the posterior distributions for fish in *M. tarapacana* and *M. birostris* (Fig. S1). However, when these posterior distributions are summed for the *a posteriori* aggregated fish group, the resulting diet proportion is inflated.

Diet-switching

We analyzed multiple tissue types in mobulids from the Philippines to directly examine the possible diet-switching that our mixing model results suggested. Liver is a metabolically more active tissue than muscle and therefore has a faster turnover rate (Tieszen et al. 1983, Hobson & Clark 1992). Previous studies have used liver and muscle tissue to examine dietary stability in elasmobranchs, with isotopic differences between the 2 tissue types interpreted as evidence of seasonal diet switching (MacNeil et al. 2005). The isotopic signatures of the liver samples we collected in the Philippines were significantly different from the paired muscle samples from the same individuals. The greatest difference between tissues was in $\delta^{13}C$ for both *M. birostris* and *M. tarapacana*. However, liver and muscle tissues are expected to fractionate $\delta^{13}C$ differently, with lower $\delta^{13}C$ values in liver samples even after lipid extraction (Pinnegar & Polunin 1999, MacNeil et al. 2005). Controlled experiments and studies of wild populations of teleost and elasmobranch fishes suggest that this difference in $\delta^{13}C$ fractionation between liver and muscle tissue may range from 0.5 to 2‰ (Pinnegar & Polunin 1999, MacNeil et al. 2005, Hussey et al. 2010a), while the shift in $\delta^{13}C$ between our muscle and liver samples was, on average, 2.8‰. It is therefore likely that some portion of the difference in $\delta^{13}C$ is due to variable fractionation rates between the 2 tissues, while some portion is due to true dietary shifts. This may explain the discrepancies between the frequency of some prey sources in stomach contents and the mixing model outputs of diet proportions for *M. birostris* and *M. tarapacana* and possibly the other mobulid species for which liver samples were not collected (Fig. S1). If liver and muscle tissue isotope values were equal, it would suggest a stable diet throughout the tissue integration period of the metabolically slower tissue, while differences suggest diet-switching (MacNeil et al. 2005). However, the C:N ratios of lipid-extracted liver tissues remained higher than corresponding muscle tissues, which may indicate that lipid extraction was not successful, confounding the interpretation of these results.

We found small but significant differences in $\delta^{15}N$ between tissues in *M. birostris* and no significant difference in $\delta^{15}N$ between tissues in *M. tarapacana*. However, $\delta^{15}N$ may also fractionate differently between tissue types, although with a smaller effect than $\delta^{13}C$. Hussey et al. (2010a) found $\delta^{15}N$ values to be 0.37 to 0.89‰ higher in bulk muscle tissue than in bulk livers of 3 captive sharks and 0.11 to 1.18‰ higher in lipid-extracted muscle than in lipid-extracted livers. Similarly, MacNeil et al. (2005) found $\delta^{15}N$ values to be, on average, 0.03 and 0.57‰ higher in lipid-extracted muscle tissue than in lipid-extracted livers of 2 species of non-captive sharks that they concluded had relatively stable diets. While our comparison of $\delta^{15}N$ in bulk muscle and bulk liver tissue seems to suggest that *M. birostris* may switch its diet seasonally in the Philippines, adding a correction factor of 0.5‰ to liver $\delta^{15}N$ values to account for possible fractionation differences between tissues inverts these results, with $\delta^{15}N$ becoming significantly different between tissues in *M. tarapacana* and not signif-

icant in *M. birostris*. These findings illustrate how even small uncertainties in stable isotope ecology, especially in fractionation factors, can have substantial impacts on the interpretation of results, and they highlight the frequently repeated need for species-specific laboratory validation of parameters that are used in isotope analysis.

CONCLUSIONS

Our findings contribute to a limited but growing body of knowledge on the habitat use and ecology of mobulid rays, which are highly vulnerable to exploitation due to their demographic characteristics (Dulvy et al. 2014, Pardo et al. 2016). Both bycatch and targeted fisheries appear to contribute to global declines in mobulid abundance (Ward-Paige et al. 2013, White et al. 2015, Croll et al. 2016). Targeted fisheries can be managed with legislation banning the capture of mobulids, but bycatch remains a more challenging and persistent threat due to the ubiquity of mobulid bycatch in artisanal and commercial fisheries of all types (Croll et al. 2016). The apparent similarity in diets and overlapping isotopic niches between mobulids in this study are consistent with the spatial overlap in bycatch of the various mobulid species (Croll et al. 2016). Identifying the spatial and temporal patterns of mobulids' primary zooplankton prey (for example euphausiids in the Philippines) could aid in predicting their occurrence and relative vulnerability to bycatch-prone fisheries. Our results further indicate that both adults and juveniles are targeting similar prey and are thus overlapping with and susceptible to the same fisheries pressures, which has implications for the catchability of different life stages and consequently the development of age- or size-based fisheries management strategies. Further research is necessary to corroborate many of the patterns observed here over larger spatial and temporal scales and will aid in our understanding of habitat use by mobulids and the development of fisheries bycatch mitigation strategies.

Acknowledgements. Funding for fieldwork in the Philippines was provided by the Ocean Park Conservation Foundation Hong Kong and the PADI Foundation. Fieldwork in the Philippines was approved by the local government of Jagna and the Sangguniáng Bayan of Jagna (Bohol), and samples were collected under a memorandum of agreement with the Department of Agriculture, Bureau of Fisheries and Aquatic Resources (DA-BFAR) Region 7 for the project 'Visayas Marine Megafauna Research, Conservation and Education project'. C.A.R. was supported by 2 private trusts. J.A. and K.F. were supported by the Marine Conservation Action Fund at the New England Aquarium, the Disney Conservation Fund, the abc* Foundation, WildAid, and Shark Savers. Funding for fieldwork in Sri Lanka was provided by the Save Our Seas Foundation and the Marine Conservation and Action Fund at the New England Aquarium. Funding for isotope analysis was provided by the Center for the Advancement of Population Assessment Methodology. J.D.S. was supported by NOAA ONMS Nancy Foster Scholarship NA15NOS4290068 and a fellowship from the Robert & Patricia Switzer Foundation. We thank all the volunteers of Large Marine Vertebrates Research Institute Philippines for data collection and Maita Verdote and Dr. Jo Marie Acebes (Balyena.org) for the support, advice, and information shared during the mobulid fishery monitoring project in Bohol. We are grateful for the support of the fishers from Jagna; DA-BFAR Region 7; the Department of Environment and Natural Resources Region 7; and the local government unit of Jagna (Bohol). We thank Michelle Robbins, Courtney Pinns, Ana Mendoza, Taylor Smith, and Kara Reynolds for their assistance with sample preparation for isotope analysis and Elena Duke and the Burton Lab at Scripps Institution of Oceanography for their assistance with genetic barcoding of unidentifiable stomach contents. Robert Rubin provided insightful discussion on niche partitioning and body size. We thank Wilmer Purizaca Ayala, Planeta Océano volunteers, local fishermen, and community members for their support in data collection in Peru. We thank Anthony Richardson and the zooplankton lab at CSIRO, Brisbane, for their help with sorting stomach contents prior to isotope analysis.

LITERATURE CITED

Anderson RC, Adam MS, Goes JI (2011) From monsoons to mantas: seasonal distribution of *Manta alfredi* in the Maldives. Fish Oceanogr 20:104–113

Armstrong AO, Armstrong AJ, Jaine FRA, Couturier LIE and others (2016) Prey density threshold and tidal influence on reef manta ray foraging at an aggregation site on the Great Barrier Reef. PLOS ONE 11:e0153393

Barrow LM, Bjorndal KA, Reich KJ (2008) Effects of preservation method on stable carbon and nitrogen isotope values. Physiol Biochem Zool 81:688–693

Ben-David M, Flynn W, Schell M (1997) Annual and seasonal changes in diets of martens: evidence from stable isotope analysis. Oecologia 111:280–291

Borrell A, Aguilar A, Gazo M, Kumarran RP, Cardona L (2011) Stable isotope profiles in whale shark (*Rhincodon typus*) suggest segregation and dissimilarities in the diet depending on sex and size. Environ Biol Fishes 92: 559–567

Braun CD, Skomal GB, Thorrold SR, Berumen ML (2014) Diving behavior of the reef manta ray links coral reefs with adjacent deep pelagic habitats. PLOS ONE 9: e88170

Burgess KB, Bennett MB (2017) Effects of ethanol storage and lipid and urea extraction on δ15N and δ13C isotope ratios in a benthic elasmobranch, the bluespotted maskray *Neotrygon kuhlii*. J Fish Biol 90:417–423

Burgess KB, Couturier LIE, Marshall AD, Richardson AJ, Weeks S, Bennett MB (2016) *Manta birostris*, predator of the deep? Insight into the diet of the giant manta ray through stable isotope analysis. R Soc Open Sci 3:160717

Canese S, Cardinali A, Romeo T, Giusti M, Salvati E, Angiolillo M, Greco S (2011) Diving behavior of the giant devil ray in the Mediterranean Sea. Endang Species Res 14: 171–176

Caut S, Angulo E, Courchamp F (2008) Caution on isotopic model use for analyses of consumer diet. Can J Zool 86: 438–445

Cherel Y, Hobson KA, Guinet C, Vanpe C (2007) Stable isotopes document seasonal changes in trophic niches and winter foraging individual specialization in diving predators from the Southern Ocean. J Anim Ecol 76:826–836

Couturier LIE, Marshall AD, Jaine FRA, Kashiwagi T and others (2012) Biology, ecology and conservation of the Mobulidae. J Fish Biol 80:1075–1119

Couturier LIE, Rohner CA, Richardson AJ, Marshall AD and others (2013) Stable isotope and signature fatty acid analyses suggest reef manta rays feed on demersal zooplankton. PLOS ONE 8:e77152

Croll DA, Marinovic B, Benson S, Chavez FP, Black N, Ternullo R, Tershy BR (2005) From wind to whales: trophic links in a coastal upwelling system. Mar Ecol Prog Ser 289:117–130

Croll DA, Newton KM, Weng K, Galván-Magaña F, O'Sullivan J, Dewar H (2012) Movement and habitat use by the spine-tail devil ray in the Eastern Pacific Ocean. Mar Ecol Prog Ser 465:193–200

Croll DA, Dewer H, Dulvy NK, Fernando D and others (2016) Vulnerabilities and fisheries impacts: the uncertain future of manta and devil rays. Aquat Conserv Mar Freshw Ecosyst 26:562–57

Dobush GR, Ankney CD, Krementz DG (1985) The effect of apparatus, extraction time, and solvent type on lipid extractions of snow geese. Can J Zool 63:1917–1920

Dulvy NK, Pardo SA, Simpfendorfer CA, Carlson JK (2014) Diagnosing the dangerous demography of manta rays using life history theory. PeerJ 2:e400

Estrada JA, Rice AN, Natanson LJ, Skomal GB (2006) Use of isotopic analysis of vertebrae in reconstructing ontogenetic feeding ecology in white sharks. Ecology 87:829–834

Foley CJ, Bowen GJ, Nalepa TF, Sepúlveda MS, Höök TO, Ramcharan C (2014) Stable isotope patterns of benthic organisms from the Great Lakes region indicate variable dietary overlap of *Diporeia* spp. and dreissenid mussels. Can J Fish Aquat Sci 71:1784–1795

France RL (1995) Carbon-13 enrichment in benthic compared to planktonic algae: foodweb implications. Mar Ecol Prog Ser 124:307–312

Francis MP, Jones EG (2017) Movement, depth distribution and survival of spinetail devilrays (*Mobula japanica*) tagged and released from purse-seine catches in New Zealand. Aquat Conserv Mar Freshw Ecosyst 27:219–236

Gannes LZ, O'Brien DM, Martinez del Rio C (1997) Stable isotopes in animal ecology: assumptions, caveats, and a call for more laboratory experiments. Ecology 78:1271–1276

Gavrilchuk K, Lesage V, Ramp C, Sears R, Bérubé M, Bearhop S, Beauplet G (2014) Trophic niche partitioning among sympatric baleen whale species following the collapse of groundfish stocks in the Northwest Atlantic. Mar Ecol Prog Ser 497:285–301

Gelman A, Rubin DB (1992) Inference from iterative simulation using multiple sequences. Stat Sci 7:457–472

Hazen EL, Johnston DW (2010) Meridional patterns in the deep scattering layers and top predator distribution in the central equatorial Pacific. Fish Oceanogr 19:427–433

Heinrichs S (2009) Hunting mobulas of Misool. www.bluespheremedia.com/2009/10/hunting-mobulas-of-misool/ (accessed on 23 January 2017)

Heithaus MR, Vaudo JJ, Kreicker S, Layman CA and others (2013) Apparent resource partitioning and trophic structure of large-bodied marine predators in a relatively pristine seagrass ecosystem. Mar Ecol Prog Ser 481:225–237

Hobson KA, Clark RG (1992) Assessing avian diets using stable isotopes I: turnover of ^{13}C in tissues. Condor 94: 181–188

Hobson KA, Gloutney ML, Gibbs HL (1997) Preservation of blood and tissue samples for stable-carbon and stable-nitrogen isotope analysis. Can J Zool 75:1720–1723

Hussey NE, Brush J, McCarthy ID, Fisk AT (2010a) $\delta^{15}N$ and $\delta^{13}C$ diet–tissue discrimination factors for large sharks under semi-controlled conditions. Comp Biochem Physiol A Mol Integr Physiol 155:445–453

Hussey NE, MacNeil MA, Fisk AT (2010b) The requirement for accurate diet–tissue discrimination factors for interpreting stable isotopes in sharks. Hydrobiologia 654:1–5

Hussey NE, Dudley SFJ, McCarthy ID, Cliff G, Fisk AT (2011) Stable isotope profiles of large marine predators: viable indicators of trophic position, diet, and movement in sharks? Can J Fish Aquat Sci 68:2029–2045

Hutchinson GE (1957) Concluding remarks. Cold Spring Harb Symp Quant Biol 22:417–427

Jackson AL, Inger R, Parnell AC, Bearhop S (2011) Comparing isotopic niche widths among and within communities: SIBER — Stable Isotope Bayesian Ellipses in R. J Anim Ecol 80:595–602

Jackson MC, Woodford DJ, Bellingan TA, Weyl OLF and others (2016) Trophic overlap between fish and riparian spiders: potential impacts of an invasive fish on terrestrial consumers. Ecol Evol 6:1745–1752

Jaine FRA, Rohner CA, Weeks SJ, Couturier LIE, Bennett MB, Townsend KA, Richardson AJ (2014) Movements and habitat use of reef manta rays off eastern Australia: offshore excursions, deep diving and eddy affinity revealed by satellite telemetry. Mar Ecol Prog Ser 510:73–86

Jaine FRA, Couturier LIE, Weeks SJ, Townsend KA, Bennett MB, Fiora K, Richardson AJ (2012) When giants turn up: sighting trends, environmental influences and habitat use of the manta ray *Manta alfredi* at a coral reef. PLOS ONE 7:e46170

Kaehler S, Pakhomov EA (2001) Effects of storage and preservation on the $d^{13}C$ and $d^{15}N$ signatures of selected marine organisms. Mar Ecol Prog Ser 219:299–304

Kashiwagi T, Marshall AD, Bennett MB, Ovenden JR (2011) Habitat segregation and mosaic sympatry of the two species of manta ray in the Indian and Pacific Oceans: *Manta alfredi* and *M. birostris*. Mar Biodivers Rec 4:e53

Kashiwagi T, Marshall AD, Bennett MB, Ovenden JR (2012) The genetic signature of recent speciation in manta rays (*Manta alfredi* and *M. birostris*). Mol Phylogenet Evol 64: 212–218

Kelly B, Dempson JB, Power M (2006) The effects of preservation on fish tissue stable isotope signatures. J Fish Biol 69:1595–1611

Kim SL, Koch PL (2012) Methods to collect, preserve, and prepare elasmobranch tissues for stable isotope analysis. Environ Biol Fishes 95:53–63

Kim SL, Casper DR, Galván-Magaña F, Ochoa-Díaz R, Hernández-Aguilar SB, Koch PL (2012a) Carbon and nitrogen discrimination factors for elasmobranch soft tissues based on a long-term controlled feeding study. Environ Biol Fishes 95:37–52

Kim SL, del Rio CM, Casper D, Koch PL (2012b) Isotopic incorporation rates for shark tissues from a long-term captive feeding study. J Exp Biol 215:2495–2500

Lesage V, Morin Y, Rioux E, Pomerleau C, Ferguson SH, Pelletier E (2010) Stable isotopes and trace elements as indicators of diet and habitat use in cetaceans: predicting errors related to preservation, lipid extraction, and lipid normalization. Mar Ecol Prog Ser 419:249–265

Logan JM, Lutcavage ME (2010) Stable isotope dynamics in elasmobranch fishes. Hydrobiologia 644:231–244

Logan JM, Jardine TD, Miller TJ, Bunn SE, Cunjak RA, Lutcavage ME (2008) Lipid corrections in carbon and nitrogen stable isotope analyses: comparison of chemical extraction and modelling methods. J Anim Ecol 77: 838–846

MacNeil MA, Skomal GB, Fisk AT (2005) Stable isotopes from multiple tissues reveal diet switching in sharks. Mar Ecol Prog Ser 302:199–206

MacNeil MA, Drouillard KG, Fisk AT (2006) Variable uptake and elimination of stable nitrogen isotopes between tissues in fish. Can J Fish Aquat Sci 63:345–353

Madden T (2002) The BLAST sequence analysis tool. In: McEntyre J, Ostell J (eds) The NCBI handbook. National Center for Biotechnology Information, Bethesda, MD

Malpica-Cruz L, Herzka SZ, Sosa-Nishizaki O, Lazo JP, Trudel M (2012) Tissue-specific isotope trophic discrimination factors and turnover rates in a marine elasmobranch: empirical and modeling results. Can J Fish Aquat Sci 69:551–564

Mateo MA, Serrano O, Serrano L, Michener RH (2008) Effects of sample preparation on stable isotope ratios of carbon and nitrogen in marine invertebrates: implications for food web studies using stable isotopes. Oecologia 157:105–115

May RM, MacArthur RH (1972) Niche overlap as a function of environmental variability. Proc Natl Acad Sci USA 69: 1109–1113

Mendelssohn R (2015) xtractomatic: extracts environmental data from ERD's ERDDAP web service. http://coastwatch.pfel.noaa.gov/xtracto/

Moore JW, Semmens BX (2008) Incorporating uncertainty and prior information into stable isotope mixing models. Ecol Lett 11:470–480

Newsome SD, Clementz MT, Koch PL (2010) Using stable isotope biogeochemistry to study marine mammal ecology. Mar Mamm Sci 26:509–572

Notarbartolo di Sciara G (1988) Natural history of the rays of the genus *Mobula* in the Gulf of California. Fish Bull 86: 45–66

Owens NJP (1987) Natural variation in ^{15}N in the marine environment. Adv Mar Biol 24:389–451

Pardo SA, Burgess KB, Teixeira D, Bennett MB (2015) Local-scale resource partitioning by stingrays on an intertidal flat. Mar Ecol Prog Ser 533:205–218

Pardo SA, Kindsvater HK, Cuevas-Zimbrón E, Sosa-Nishizaki O, Pérez-Jiménez JC, Dulvy NK (2016) Growth, productivity, and extinction risk of a data-sparse devil ray. Sci Rep 6:33745

Parng E, Crumpacker A, Kurle CM (2014) Variation in the stable carbon and nitrogen isotope discrimination factors from diet to fur in four felid species held on different diets. J Mammal 95:151–159

Pianka ER (1974) Niche overlap and diffuse competition. Proc Natl Acad Sci USA 71:2141–2145

Pianka ER (1981). Competition and niche theory. In: May RM (ed) Theoretical ecology: principles and applications, 2nd edn. Sinauer Associates, Sunderland, MA, p 167–196

Pinnegar JK, Polunin NVC (1999) Differential fractionation of $\delta^{13}C$ and $\delta^{15}N$ among fish tissues: implications for the study of trophic interactions. Funct Ecol 13:225–231

Plass-Johnson JG, McQuaid CD, Hill JM (2013) Stable isotope analysis indicates a lack of inter- and intra-specific dietary redundancy among ecologically important coral reef fishes. Coral Reefs 32:429–440

Poortvliet M, Olsen JL, Croll DA, Bernardi G and others (2015) A dated molecular phylogeny of manta and devil rays (Mobulidae) based on mitogenome and nuclear sequences. Mol Phylogenet Evol 83:72–85

Porter JH, Dueser RD (1982) Niche overlap and competition in an insular small mammal fauna: a test of the niche overlap hypothesis. Oikos 39:228–236

Post DM, Layman CA, Arrington DA, Takimoto G, Quattrochi J, Montaña CG (2007) Getting to the fat of the matter: models, methods and assumptions for dealing with lipids in stable isotope analyses. Oecologia 152:179–189

R Core Team (2016) R: a language and environment for statistical computing. R Foundation for Statistical Computing, Vienna

Rohner CA, Couturier LIE, Richardson AJ, Pierce SJ, Prebble CEM, Gibbons MJ, Nichols PD (2013) Diet of whale sharks *Rhincodon typus* inferred from stomach content and signature fatty acid analyses. Mar Ecol Prog Ser 493: 219–235

Rohner CA, Armstrong AJ, Pierce SJ, Prebble CEM and others (2015) Whale sharks target dense prey patches of sergestid shrimp off Tanzania. J Plankton Res 37: 352–362

Rohner CA, Burgess KB, Rambahiniarison JM, Stewart JD, Ponzo A, Richardson AJ (2017) Mobulid rays feed on euphausiids in the Bohol Sea. R Soc Open Sci 4:161060

Sampson L, Galván–Magaña F, De Silva-Dávila R, Aguiniga-Garcia S, O'Sullivan JB (2010) Diet and trophic position of the devil rays *Mobula thurstoni* and *Mobula japanica* as inferred from stable isotope analysis. J Mar Biol Assoc UK 90:969–976

Santora JA, Reiss CS, Loeb VJ, Veit RR (2010) Spatial association between hotspots of baleen whales and demographic patterns of Antarctic krill *Euphausia superba* suggests size-dependent predation. Mar Ecol Prog Ser 405:255–269

Sarakinos HC, Johnson ML, Vander Zanden MJ (2002) A synthesis of tissue-preservation effects on carbon and nitrogen stable isotope signatures. Can J Zool 80: 381–387

Scharf FS, Juanes F, Rountree RA (2000) Predator size-prey size relationships of marine fish predators: interspecific variation and effects of ontogeny and body size on trophic-niche breadth. Mar Ecol Prog Ser 208: 229–248

Semmens BX, Ward EJ, Moore JW, Darimont CT (2009) Quantifying inter-and intra-population niche variability using hierarchical Bayesian stable isotope mixing models. PLOS ONE 4:e61871–9

Stallings CD, Nelson JA, Rozar KL, Adams CS, Wall KR, Switzer TS, Winner BL, Hollander DJ (2015) Effects of preservation methods of muscle tissue from upper-trophic level reef fishes on stable isotope values ($\delta^{13}C$ and $\delta^{15}N$). PeerJ 3:e874

Stevens GMW (2014) Field guide to the identification of mobulid rays (Mobulidae): Indo-West Pacific. Manta Trust, Dorchester

Stewart JD, Beale CS, Fernando D, Sianipar AB, Burton RS, Semmens BX, Aburto-Oropeza O (2016a) Spatial ecology and conservation of *Manta birostris* in the Indo-Pacific. Biol Conserv 200:178–183

Stewart JD, Hoyos-Padilla EM, Kumli KR, Rubin RD (2016b) Deep-water feeding and behavioral plasticity in *Manta birostris* revealed by archival tags and submersible observations. Zoology 119:406–413

Stock BC, Semmens BX (2016) Unifying error structures in commonly used biotracer mixing models. Ecology 97: 2562–2569

Thorrold SR, Afonso P, Fontes J, Braun CD, Santos RS, Skomal GB, Berumen ML (2014) Extreme diving behaviour in devil rays links surface waters and the deep ocean. Nat Commun 5:4274

Tieszen LL, Boutton TW, Tesdahl KG, Slade NA (1983) Fractionation and turnover of stable carbon isotopes in animal tissues: implications for $\delta^{13}C$ analysis of diet. Oecologia 57:32–37

Vizza C, Sanderson BL, Burrows DG, Coe HJ (2013) The effects of ethanol preservation on fish fin stable isotopes: Does variation in C:N ratio and body size matter? Trans Am Fish Soc 142:1469–1476

Walter RP, Kessel ST, Alhasan N, Fisk AT and others (2014) First record of living *Manta alfredi* × *Manta birostris* hybrid. Mar Biodivers 44:1–2

Ward-Paige CA, Davis B, Worm B (2013) Global population trends and human use patterns of *Manta* and *Mobula* rays. PLOS ONE 8:e74835

White ER, Myers MC, Flemming JM, Baum JK (2015) Shifting elasmobranch community assemblage at Cocos Island — an isolated marine protected area. Conserv Biol 29:1186–1197

Young JW, Lansdell MJ, Campbell RA, Cooper SP, Juanes F, Guest MA (2010) Feeding ecology and niche segregation in oceanic top predators off eastern Australia. Mar Biol 157:2347–2368

Editorial responsibility: Stephen Wing, Dunedin, New Zealand

Submitted: March 1, 2017; Accepted: August 11, 2017
Proofs received from author(s): September 25, 2017

The following supplement accompanies the article

Trophic overlap in mobulid rays: insights from stable isotope analysis

Joshua D. Stewart*, Christoph A. Rohner, Gonzalo Araujo, Jose Avila, Daniel Fernando, Kerstin Forsberg, Alessandro Ponzo, Joshua M. Rambahiniarison, Carolyn M. Kurle, Brice X. Semmens

*Corresponding author: j8stewart@ucsd.edu

Marine Ecology Progress Series 580: 131–151 (2017)

Table S1: Semi-informative prior specifications for prey sources from the Philippines. α values are probabilities for a Dirichlet distribution. Uninformative prior specifications were $\alpha = 1/(\text{n sources})$ for all species. Prior specifications are explained in detail in section 2.4 Statistics and Mixing Models.

Prey source	*M. birostris* α	*M. japanica* α	*M. tarapacana* α	*M. thurstoni* α
Chaetognaths	0.7	0.7	1.0	0.8
Copepods	2.0	1.5	1.0	2.0
Pteropods	1.0	0.7	0.5	0.8
Euphausiids	5.0	7.0	7.0	7.0
Sardinella	0.7	0.7	2.0	0.8
Myctophids	2.0	0.7	0.5	0.8
Cubiceps	0.7	0.7	2.0	0.8

Table S2 Pairwise Comparisons of Niche Overlap

A. Median values of niche overlap, pairwise by species for each region

Values represent the overlapping proportion of the total, combined niche area of the two species.

Peru	birostris	japanica	munkiana	thurstoni
birostris	-	0.13	0	0.12
japanica		-	0.06	0.2
munkiana			-	0
thurstoni				-

Sri Lanka	birostris	japanica	tarapacana	thurstoni
birostris	-	0.4	0.46	0.26
japanica		-	0.36	0.32
tarapacana			-	0.22
thurstoni				-

Philippines	birostris	japanica	tarapacana	thurstoni
birostris	-	0.27	0.38	0.44
japanica		-	0.31	0.34
tarapacana			-	0.38
thurstoni				-

B. Pairwise comparison of Bayesian credible intervals for region-specific mean niche overlap proportions

Values represent the proportional overlap between Bayesian credible intervals, not to be confused with niche overlap

	Peru	Sri Lanka	Philippines
Peru	-	0.5	0.83
Sri Lanka	0.99	-	0.99
Philippines	1	0.99	-

Table S3. Pairwise Comparisons of Niche Area Posterior Distributions

A. Niche areas by species and region

Values represent the proportion of the posterior distribution of the species in each ROW that is overlapping with the posterior distribution of the species in each COLUMN

Example: The posterior distribution for the size of M. japanica's niche area is 100% overlapping with the posterior distribution for the size of M. thurstoni's niche area, while the posterior distribution for the size of M. thurstoni's niche area is 81% overlapping with the posterior distribution for the size of M. japanica's niche area.

Not to be confused with actual overlap of niche areas (Table S3)

Peru	japanica	munkiana	thurstoni
japanica	-	0	1
munkiana	0	-	0.03
thurstoni	0.81	0.02	-

Sri Lanka	birostris	japanica	tarapacana	thurstoni
birostris	-	0.99	0.98	0.94
japanica	0.93	-	0.74	0.99
tarapacana	0.86	0.82	-	0.3
thurstoni	0.13	0.39	0.06	-

Philippines	birostris	japanica	tarapacana	thurstoni
birostris	-	0	0.99	0.2
japanica	0	-	0.14	0.31
tarapacana	0.99	0.1	-	0.48
thurstoni	0.4	0.69	0.89	-

B. Median values of niche areas by species and region

Median species niche areas:		
Peru	japanica	1.14
	munkiana	0.14
	thurstoni	0.87
Sri Lanka	birostris	0.85
	japanica	0.69
	tarapacana	1.24
	thurstoni	0.36
Philippines	birostris	1.01
	japanica	0.35
	tarapacana	0.9
	thurstoni	0.58

Table S4: Median diet contributions of *a posteriori* aggregated prey groups from the MixSIAR Bayesian mixing model, run with lipid- and carbonate-corrected sources. Note that Epipelagic / Mesopelagic groups are different combinations of the same sources in Zooplankton / Fish groups. Pteropods were kept separate from both grouping scenarios. The groupings and specification of uninformative and semi-informative priors are explained in Methods.

Species	Source	Uninformative median (95% CI)	Semi-Informative median (95% CI)
M. birostris	Zooplankton	0.45 (0.19 – 0.73)	0.67 (0.43 – 0.87)
	Fish	0.27 (0.10 – 0.48)	0.15 (0.04 – 0.33)
	Pteropods	0.26 (0.10 – 0.52)	0.16 (0.01 – 0.38)
	Epipelagic	0.30 (0.12 – 0.59)	0.32 (0.11 – 0.55)
	Mesopelagic	0.41 (0.16 – 0.64)	0.51 (0.32 – 0.71)
M. japanica	Zooplankton	0.57 (0.32 – 0.77)	0.73 (0.49 – 0.92)
	Fish	0.33 (0.16 – 0.51)	0.15 (0.03 – 0.34)
	Pteropods	0.08 (0.01 – 0.29)	0.11 (0.00 – 0.27)
	Epipelagic	0.39 (0.14 – 0.66)	0.20 (0.05 – 0.45)
	Mesopelagic	0.51 (0.25 – 0.74)	0.68 (0.43 – 0.87)
M. tarapacana	Zooplankton	0.50 (0.06 – 0.93)	0.65 (0.43 – 0.83)
	Fish	0.32 (0.03 – 0.77)	0.27 (0.10 – 0.51)
	Pteropods	0.13 (0.01 – 0.46)	0.06 (0.00 – 0.27)
	Epipelagic	0.12 (0.02 – 0.69)	0.22 (0.06 – 0.45)
	Mesopelagic	0.70 (0.11 – 0.94)	0.70 (0.45 – 0.89)
M. thurstoni	Zooplankton	0.58 (0.28 – 0.82)	0.74 (0.46 – 0.92)
	Fish	0.29 (0.08 – 0.50)	0.16 (0.03 – 0.35)
	Pteropods	0.11 (0.02 – 0.41)	0.06 (0.00 – 0.39)
	Epipelagic	0.43 (0.12 – 0.72)	0.36 (0.13 – 0.58)
	Mesopelagic	0.44 (0.16 – 0.68)	0.54 (0.33 – 0.74)

Table S5 Median diet contributions from all sources

Bulk Prey Sources

Uninformative Prior	Chaetognaths	Copepods	Pteropods	Euphausiids	Sardinella	Myctophids	Cubiceps
M. birostris	0.09	0.39	0.14	0.1	0.03	0.04	0.09
M. japanica	0.09	0.2	0.15	0.19	0.04	0.07	0.18
M. tarapacana	0.06	0.09	0.21	0.06	0.01	0.02	0.06
M. thurstoni	0.06	0.32	0.18	0.16	0.02	0.03	0.11

Informative Prior	Chaetognaths	Copepods	Pteropods	Euphausiids	Sardinella	Myctophids	Cubiceps
M. birostris	0.02	0.27	0.22	0.33	0.01	0.07	0.03
M. japanica	0.04	0.11	0.2	0.47	0.03	0.04	0.04
M. tarapacana	0.04	0.07	0.2	0.46	0.06	0.01	0.11
M. thurstoni	0.04	0.23	0.17	0.38	0.02	0.03	0.04

M. birostris	Chaetognaths	Copepods	Pteropods	Euphausiids	Sardinella	Myctophids	Cubiceps
Uninformative Prior	0.09	0.39	0.14	0.1	0.03	0.04	0.09
Informative Prior	0.02	0.27	0.22	0.33	0.01	0.07	0.03

M. japanica	Chaetognaths	Copepods	Pteropods	Euphausiids	Sardinella	Myctophids	Cubiceps
Uninformative Prior	0.09	0.2	0.15	0.19	0.04	0.07	0.18
Informative Prior	0.04	0.11	0.2	0.47	0.03	0.04	0.04

M. tarapacana	Chaetognaths	Copepods	Pteropods	Euphausiids	Sardinella	Myctophids	Cubiceps
Uninformative Prior	0.06	0.09	0.21	0.06	0.01	0.02	0.06
Informative Prior	0.04	0.07	0.2	0.46	0.06	0.01	0.11

M. thurstoni	Chaetognaths	Copepods	Pteropods	Euphausiids	Sardinella	Myctophids	Cubiceps
Uninformative Prior	0.06	0.32	0.18	0.16	0.02	0.03	0.11
Informative Prior	0.04	0.23	0.17	0.38	0.02	0.03	0.04

Lipid and Carbonate Corrected Prey Sources

Uninformative Prior	Chaetognaths	Copepods	Pteropods	Euphausiids	Sardinella	Myctophids	Cubiceps
M. birostris	0.068	0.163	0.264	0.156	0.041	0.049	0.142
M. japanica	0.095	0.213	0.082	0.241	0.06	0.071	0.171
M. tarapacana	0.021	0.054	0.125	0.169	0.017	0.019	0.153
M. thurstoni	0.046	0.315	0.109	0.169	0.03	0.034	0.19

Informative Prior	Chaetognaths	Copepods	Pteropods	Euphausiids	Sardinella	Myctophids	Cubiceps
M. birostris	0.021	0.258	0.164	0.368	0.016	0.078	0.031
M. japanica	0.023	0.128	0.112	0.541	0.023	0.026	0.063
M. tarapacana	0.032	0.09	0.06	0.491	0.069	0.011	0.16
M. thurstoni	0.033	0.266	0.056	0.411	0.03	0.03	0.055

M. birostris	Chaetognaths	Copepods	Pteropods	Euphausiids	Sardinella	Myctophids	Cubiceps
Uninformative Prior	0.068	0.163	0.264	0.156	0.03	0.049	0.142
Informative Prior	0.021	0.258	0.164	0.368	0.016	0.078	0.031

M. japanica	Chaetognaths	Copepods	Pteropods	Euphausiids	Sardinella	Myctophids	Cubiceps
Uninformative Prior	0.095	0.213	0.082	0.241	0.04	0.071	0.171
Informative Prior	0.023	0.128	0.112	0.541	0.023	0.026	0.063

M. tarapacana	Chaetognaths	Copepods	Pteropods	Euphausiids	Sardinella	Myctophids	Cubiceps
Uninformative Prior	0.021	0.054	0.125	0.169	0.01	0.019	0.153
Informative Prior	0.032	0.09	0.06	0.491	0.069	0.011	0.16

M. thurstoni	Chaetognaths	Copepods	Pteropods	Euphausiids	Sardinella	Myctophids	Cubiceps
Uninformative Prior	0.046	0.315	0.109	0.169	0.02	0.034	0.19
Informative Prior	0.033	0.266	0.056	0.411	0.03	0.03	0.055

Figure S1: Mixing model estimates of diet contributions for non-aggregated sources. Colored density distributions represent prior specifications and grey histograms represent posterior distributions in either the Uninformative (left) or Informative (right) model runs.

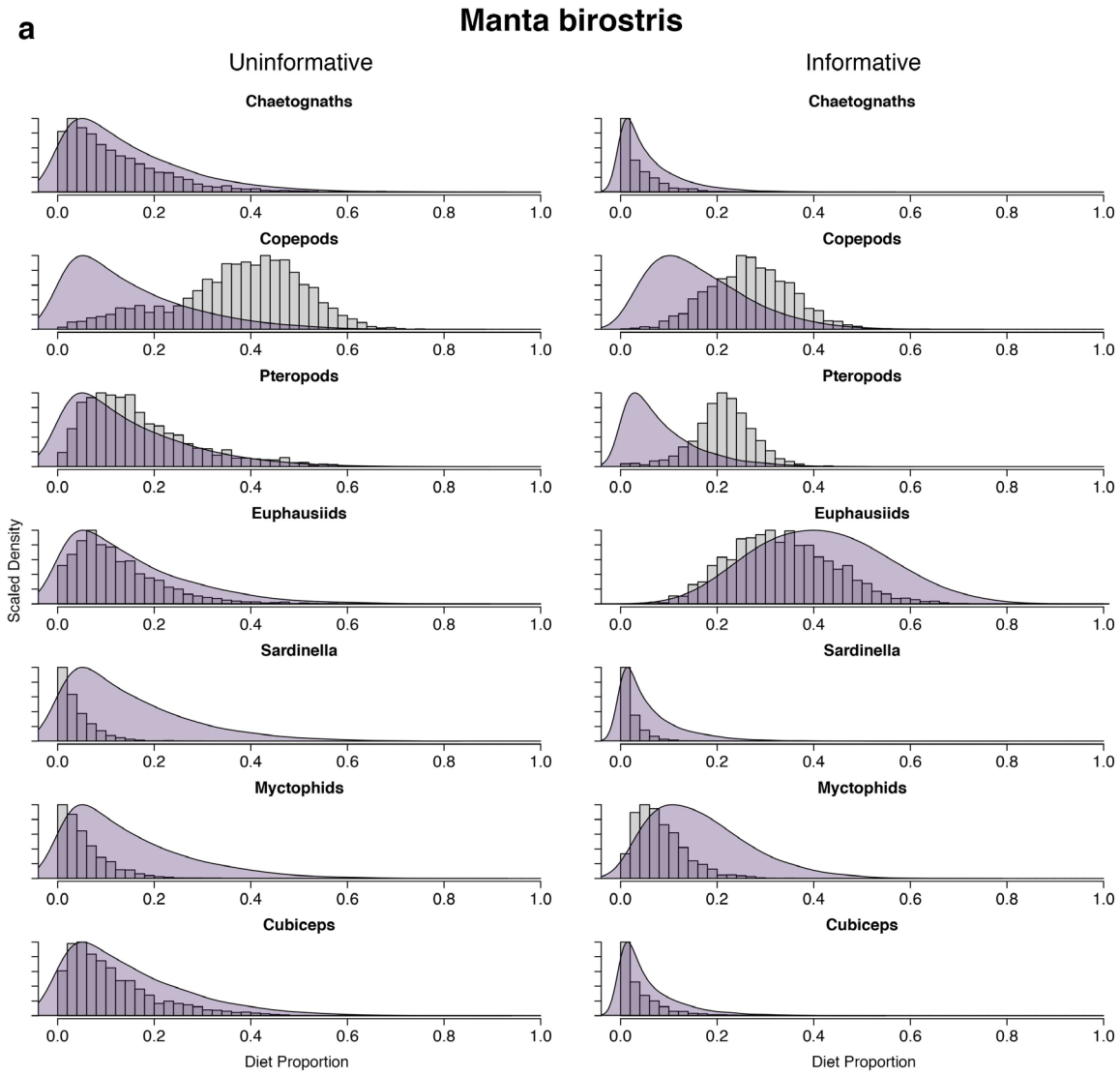

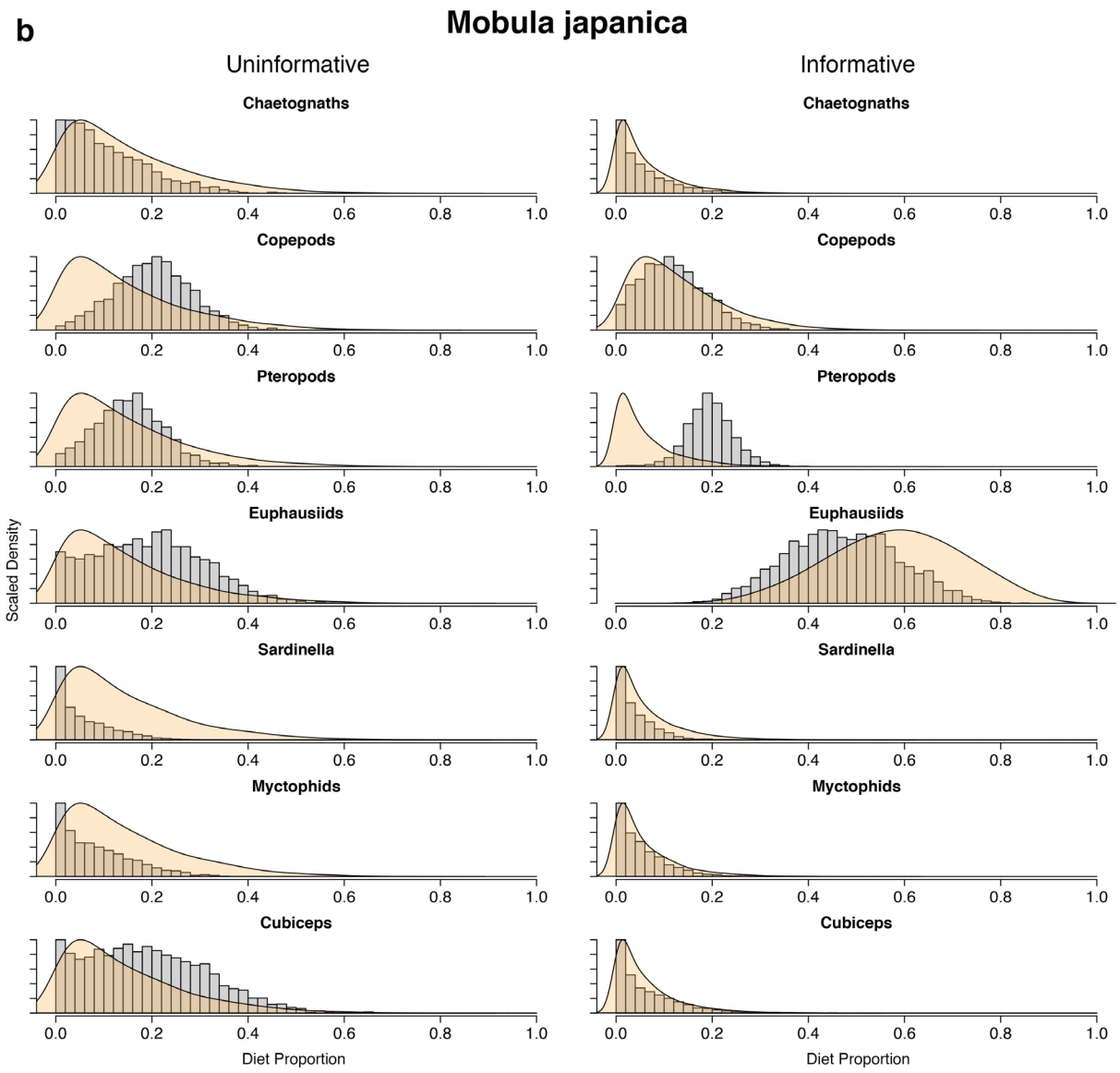
b
Mobula japanica
Uninformative
Informative
Chaetognaths
Copepods
Pteropods
Euphausiids
Sardinella
Myctophids
Cubiceps
Scaled Density
Diet Proportion
0.0
0.2
0.4
0.6
0.8
1.0

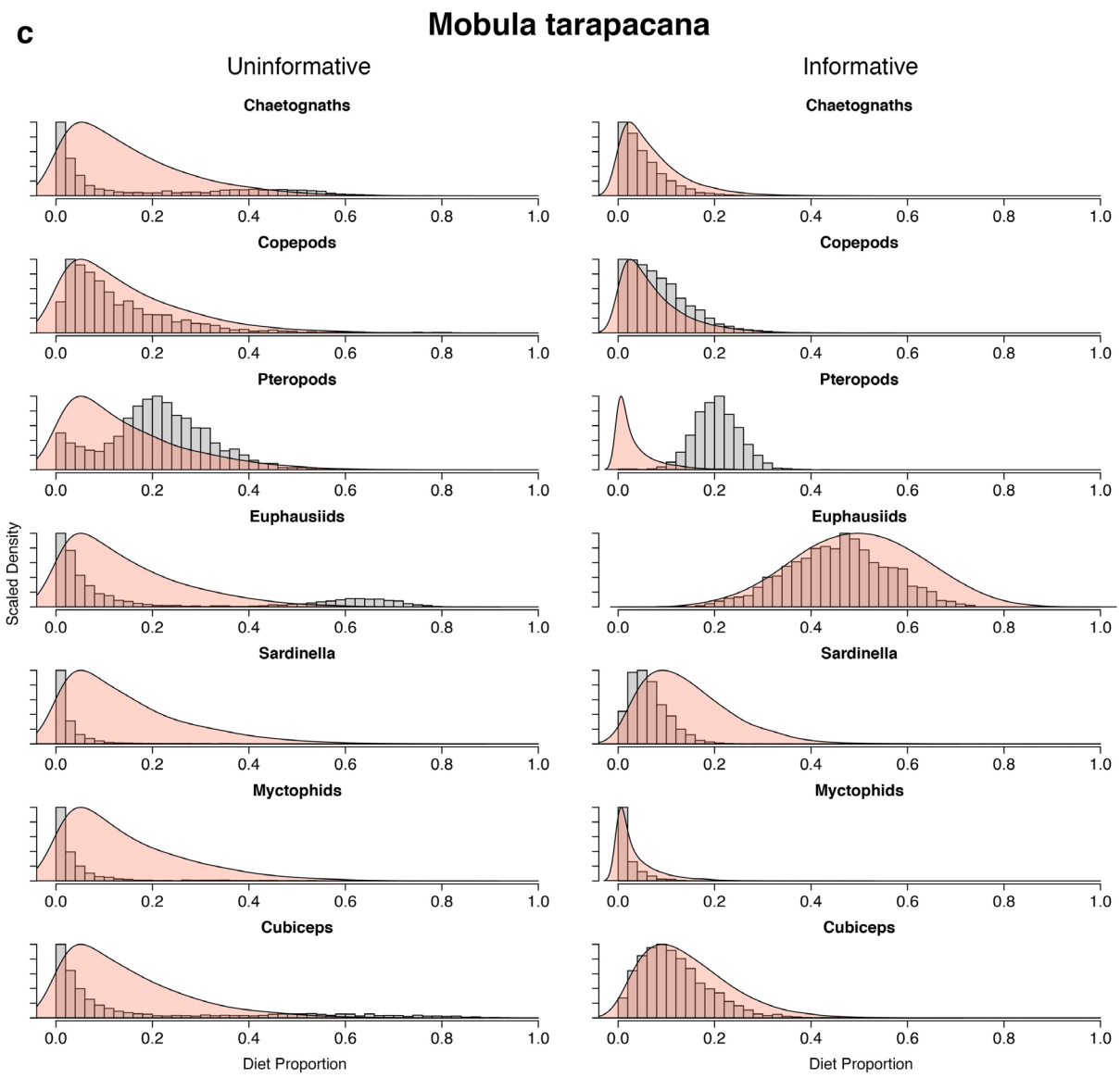
c
Mobula tarapacana
Uninformative
Informative
Chaetognaths
Copepods
Pteropods
Euphausiids
Sardinella
Myctophids
Cubiceps
Scaled Density
Diet Proportion
0.0
0.2
0.4
0.6
0.8
1.0

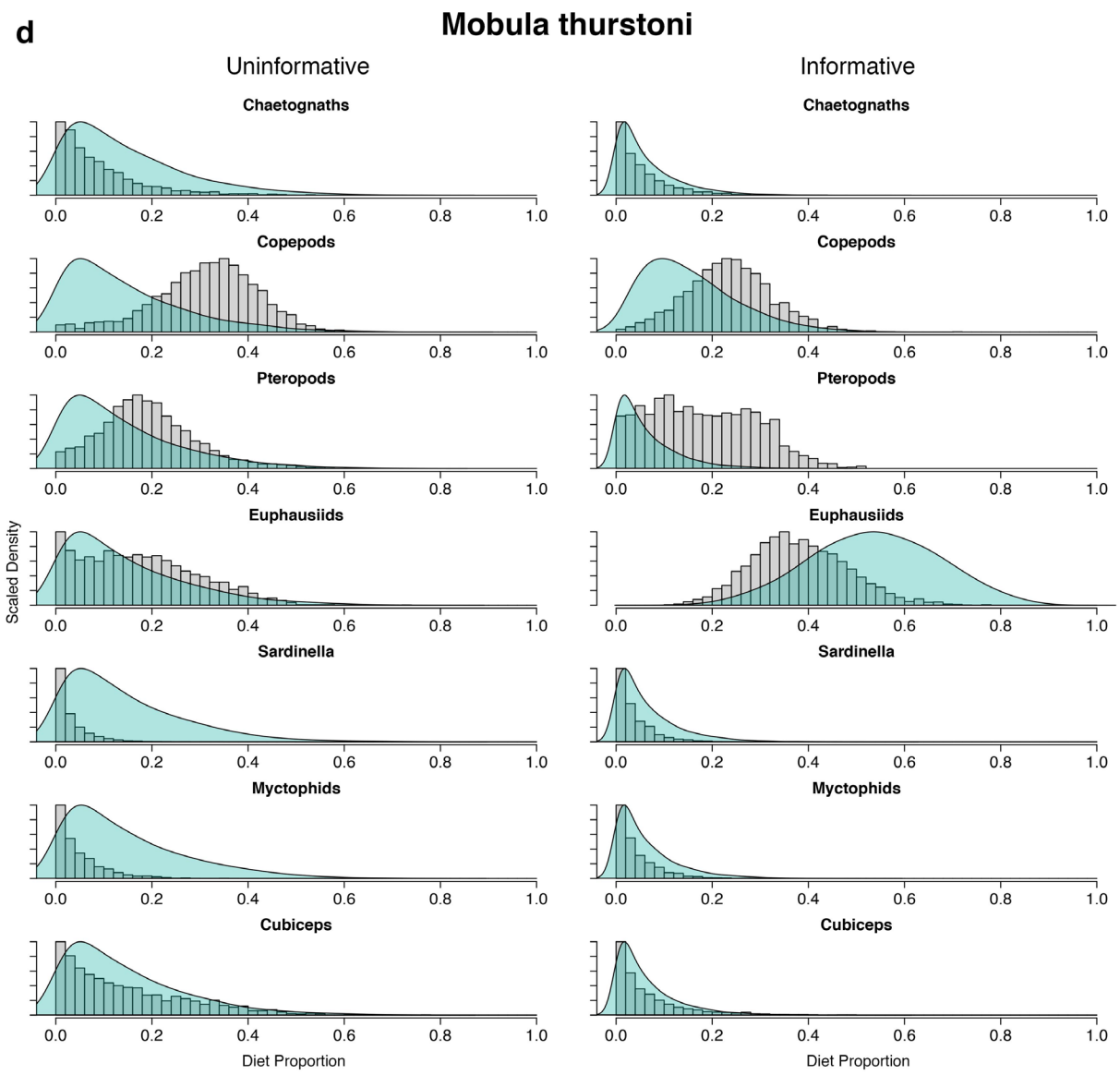
d
Mobula thurstoni
Uninformative
Informative
Chaetognaths
Copepods
Pteropods
Euphausiids
Sardinella
Myctophids
Cubiceps
Scaled Density
Diet Proportion
0.0
0.2
0.4
0.6
0.8
1.0

Figure S2: Bayesian mixed effects model output for δ^{15}N. Histograms represent the posterior distributions of the slope for the relationship between disc width and δ^{15}N for each species (random effects) and the mean slope across all species (final histogram). In this figure, slopes represent the change in δ^{15}N per centimeter change in disc width.

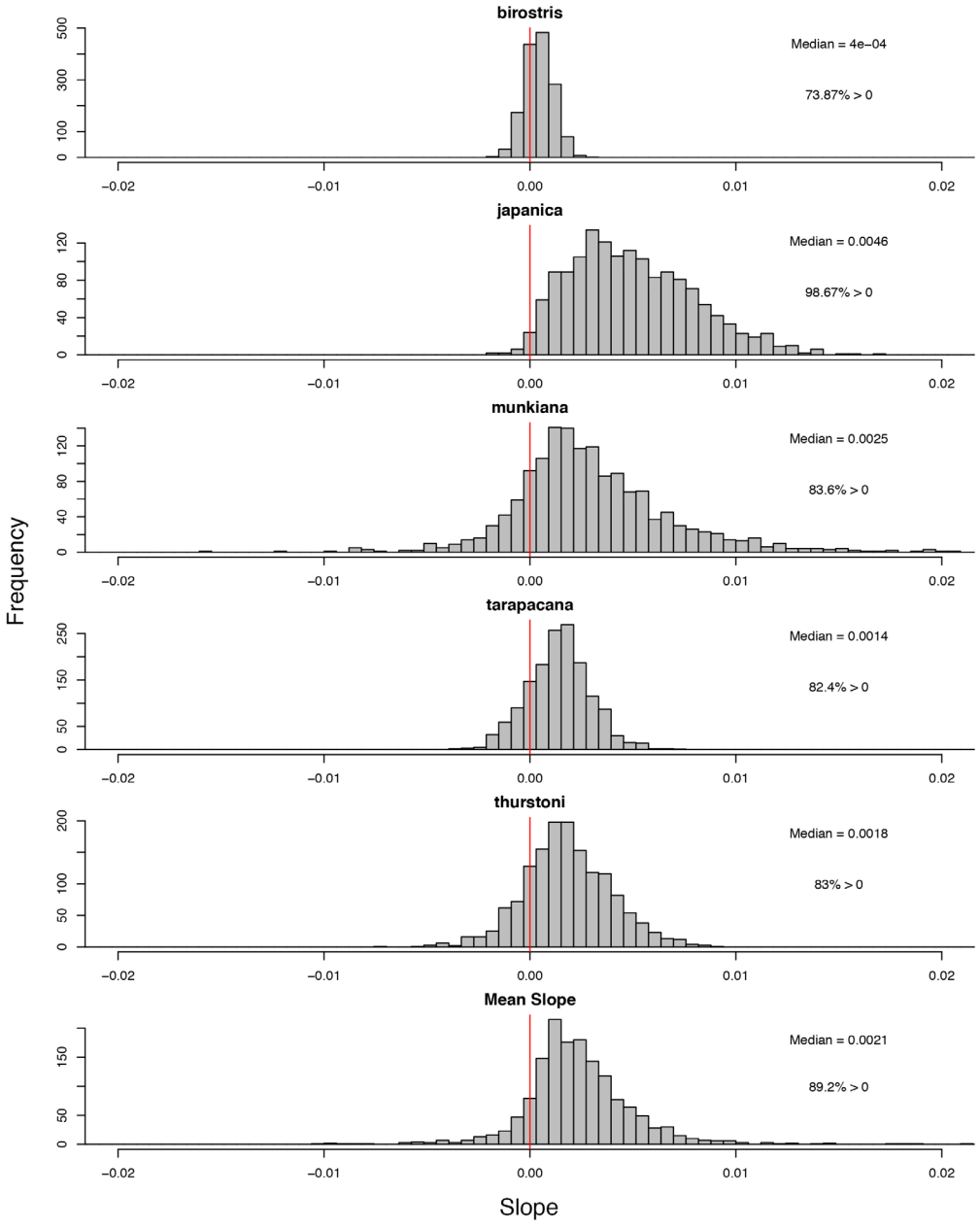

Figure S3: Bayesian mixed effects model output for $\delta^{13}C$. Histograms represent the posterior distributions of the slope for the relationship between disc width and $\delta^{13}C$ for each species (random effects) and the mean slope across all species (final histogram). In this figure, slopes represent the change in $\delta^{13}C$ per centimeter change in disc width.

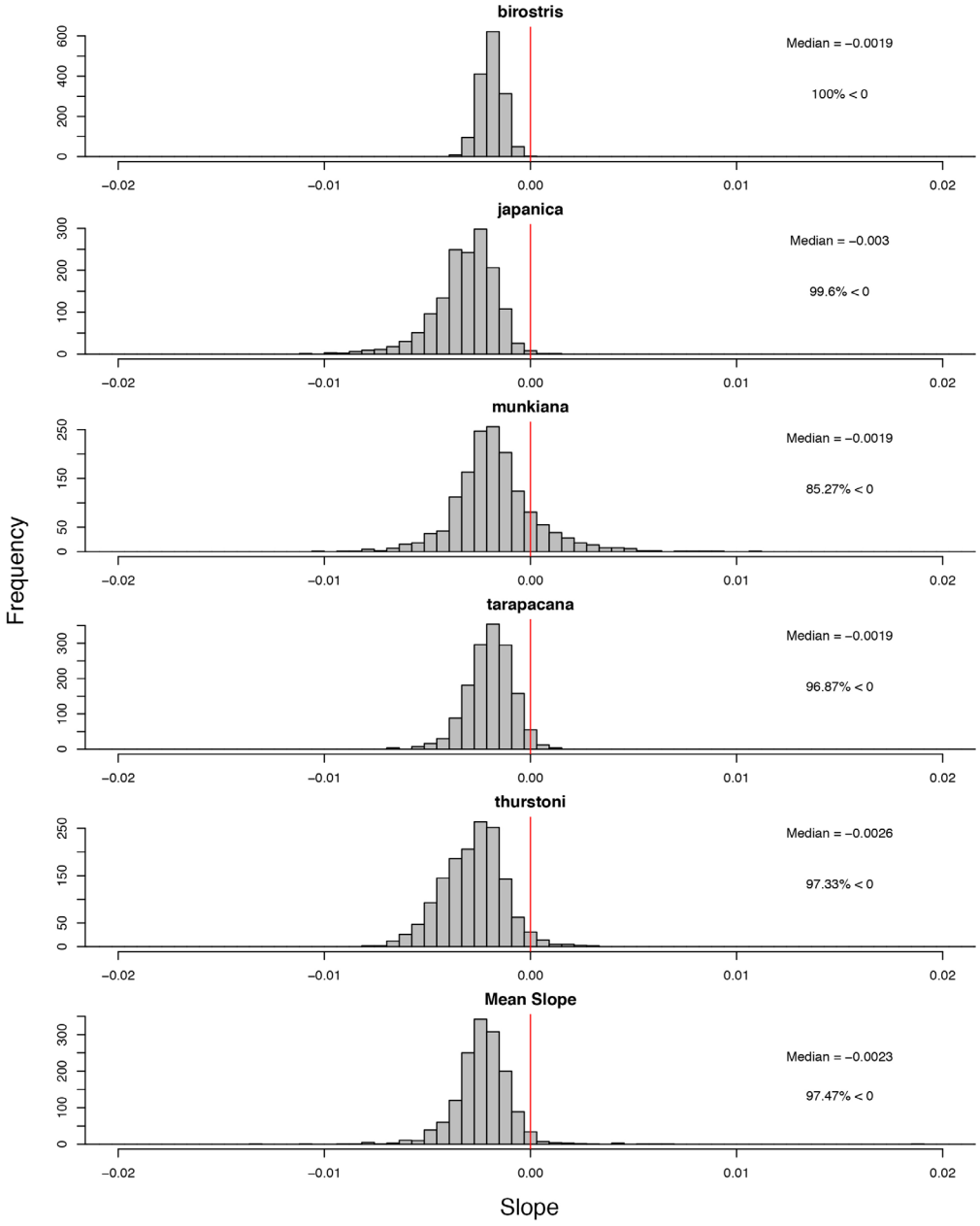

Figure S4: *Manta birostris* muscle samples (red) and lipid-extracted liver samples (blue) from the Philippines plotted alongside prey sources that have been corrected for muscle tissue diet-discrimination factors. Lines connect muscle and liver samples from the same individual.

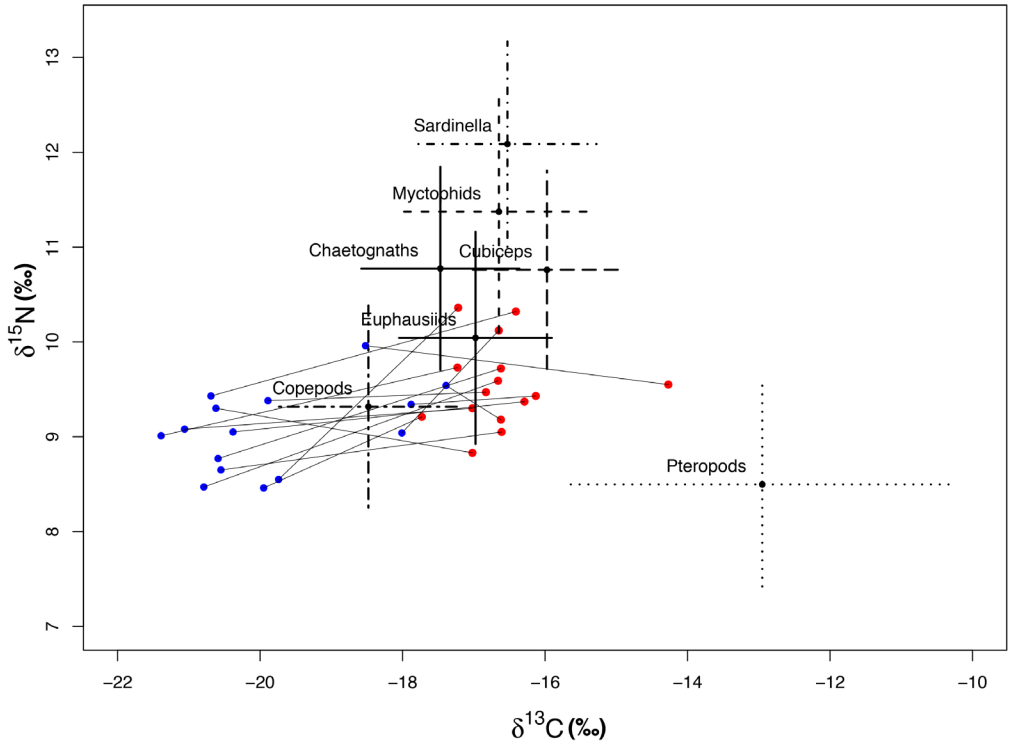

Figure S5: *Mobula tarapacana* muscle samples (red) and lipid-extracted liver samples (blue) from the Philippines plotted alongside prey sources that have been corrected for muscle tissue diet-discrimination factors. Lines connect muscle and liver samples from the same individual.

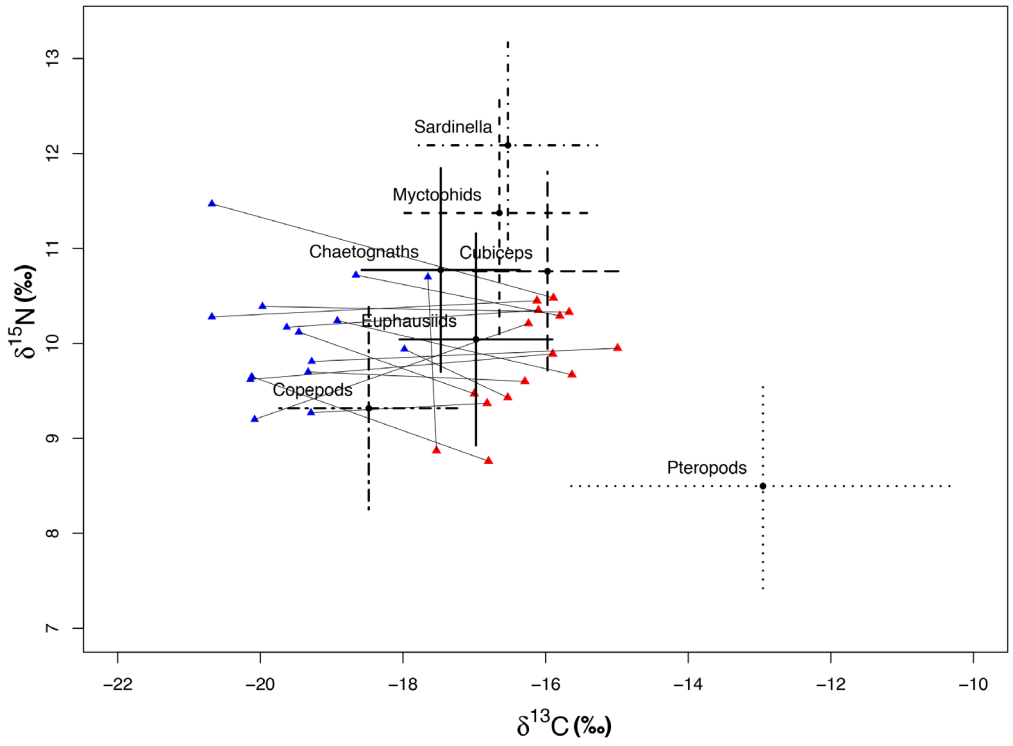

Figure S6: Effects of lipid extraction in petroleum ether on the $\delta^{13}C$ values of *M. birostris* (circles) and *M. tarapacana* (triangles). The red line is the regression equation fit to all data combined.

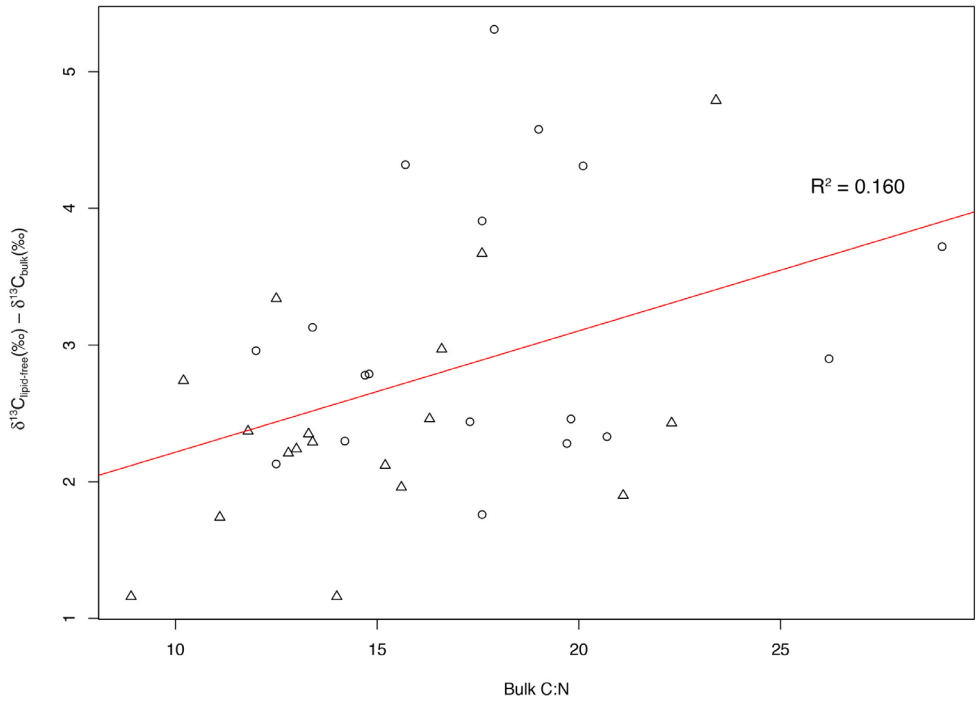

Chapter 3, in full, is a reprint of the material as it appears in Marine Ecology Progress Series 2017. Stewart, J.D., Rohner, C.A., Araujo, G., Avila, J., Fernando, D., Forsberg, K., Ponzo, A., Rambahiniarison, J.M., Kurle, C.A., Semmens, B.X. The dissertation author was the primary investigator and author of this material.